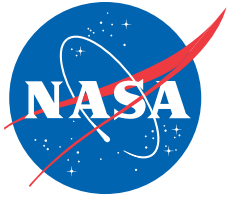


NASA/TP-2011-215971



Milestones in Rotorcraft Aeromechanics

*Wayne Johnson
Ames Research Center
Moffett Field, California*

May 2011

The NASA STI Program Office . . . in Profile

Since its founding, NASA has been dedicated to the advancement of aeronautics and space science. The NASA Scientific and Technical Information (STI) Program Office plays a key part in helping NASA maintain this important role.

The NASA STI Program Office is operated by Langley Research Center, the Lead Center for NASA's scientific and technical information. The NASA STI Program Office provides access to the NASA STI Database, the largest collection of aeronautical and space science STI in the world. The Program Office is also NASA's institutional mechanism for disseminating the results of its research and development activities. These results are published by NASA in the NASA STI Report Series, which includes the following report types:

- **TECHNICAL PUBLICATION.** Reports of completed research or a major significant phase of research that present the results of NASA programs and include extensive data or theoretical analysis. Includes compilations of significant scientific and technical data and information deemed to be of continuing reference value. NASA's counterpart of peer-reviewed formal professional papers but has less stringent limitations on manuscript length and extent of graphic presentations.
- **TECHNICAL MEMORANDUM.** Scientific and technical findings that are preliminary or of specialized interest, e.g., quick release reports, working papers, and bibliographies that contain minimal annotation. Does not contain extensive analysis.
- **CONTRACTOR REPORT.** Scientific and technical findings by NASA-sponsored contractors and grantees.

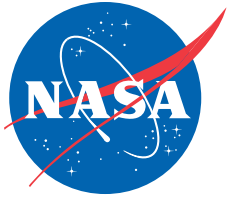
- **CONFERENCE PUBLICATION.** Collected papers from scientific and technical conferences, symposia, seminars, or other meetings sponsored or cosponsored by NASA.
- **SPECIAL PUBLICATION.** Scientific, technical, or historical information from NASA programs, projects, and missions, often concerned with subjects having substantial public interest.
- **TECHNICAL TRANSLATION.** English-language translations of foreign scientific and technical material pertinent to NASA's mission.

Specialized services that complement the STI Program Office's diverse offerings include creating custom thesauri, building customized databases, organizing and publishing research results . . . even providing videos.

For more information about the NASA STI Program Office, see the following:

- Access the NASA STI Program Home Page at <http://www.sti.nasa.gov>
- E-mail your question via the Internet to help@sti.nasa.gov
- Fax your question to the NASA Access Help Desk at (301) 621-0134
- Telephone the NASA Access Help Desk at (301) 621-0390
- Write to:
NASA Access Help Desk
NASA Center for AeroSpace Information
7115 Standard Drive
Hanover, MD 21076-1320

NASA/TP-2011-215971



Milestones in Rotorcraft Aeromechanics

*Wayne Johnson
Ames Research Center
Moffett Field, California*

National Aeronautics and
Space Administration

Ames Research Center
Moffett Field, California 94035-1000

May 2011

Acknowledgments

This report was the basis for the AHS International 2010 Alexander A. Nikolsky Honorary Lecture, presented at the American Helicopter Society 66th Annual Forum, Phoenix, Arizona, May 2010.

The assistance of Eduardo Solis, Susan O, Manikandan Ramasamy, Douglas Boyd, Neal Chaderjian, William Warmbrodt, Barry Lakinsmith, Susan Gorton, David Lundy, and Juliet Johnson in preparing the lecture and this paper is much appreciated.

Discussions with Richard Bennett, William Bousman, Francis Caradonna, Earl Dowell, Franklin Harris, Dewey Hodges, Robert Loewy, Robert Ormiston, David Peters, Raymond Piziali, Michael Scully, Chee Tung, Berend van der Wall, and Gloria Yamauchi contributed many important details to this history of rotorcraft aeromechanics.

Available from:

NASA Center for AeroSpace Information
7115 Standard Drive
Hanover, MD 21076-1320
(301) 621-0390

National Technical Information Service
5285 Port Royal Road
Springfield, VA 22161
(703) 487-4650

TABLE OF CONTENTS

LIST OF FIGURES	iv
LIST OF TABLES	vi
NOMENCLATURE	vii
SUMMARY	1
INTRODUCTION	1
THE BEGINNING OF AEROMECHANICS	2
Induced velocity	3
Flapping and hub forces	3
Longitudinal inflow gradient	4
Energy losses	4
Profile power	4
Rotor lift-to-drag ratio	5
The innovation	5
The conflict	6
Inflow curve	8
Profile power function	8
After Glauert	9
GROUND RESONANCE	10
AEROMECHANICS BOOKS	13
UNSTEADY AERODYNAMICS	14
DIGITAL COMPUTERS	17
AIRLOADS AND WAKES	17
Miller	18
Piziali and DuWaldt	20
Parallels	23
HOVER WAKE GEOMETRY	24
LATERAL FLAPPING	27
DYNAMIC INFLOW	28
ROTOR AERODYNAMIC STATE	31
BEAM THEORY	33
Houbolt and Brooks	33
Hingeless rotors	34
Ames Directorate, USAAMRDL	37
Hodges and Dowell	37
After Hodges and Dowell	39
Finite elements	39
And multibody dynamics	40
MULTIBLADE COORDINATES	40
Floquet theory	43
COMPREHENSIVE ANALYSIS	44
COMPUTATIONAL FLUID DYNAMICS	46
CFD/CSD LOOSE COUPLING	49
HOVER AIRLOADS	53
ROTOR AIRLOADS TESTS	53
H-34 flight test	54
UH-60A Airloads Program	55
HART wind tunnel tests	57
CONCLUSION	58
REFERENCES	59

LIST OF FIGURES

Figure 1.	H. Glauert of the Royal Aircraft Establishment.	2
Figure 2.	C.6A autogyro at Farnborough.	2
Figure 3.	Axial inflow curve, RAE's form (ref. 14).	8
Figure 4.	Axial inflow curve, Hafner's form (ref. 15).	8
Figure 5.	Axial inflow curve, Lock's form (ref. 16).	8
Figure 6.	Profile power function.	9
Figure 7.	Simplified mechanical system representing rotor (ref. 27).	12
Figure 8.	Coleman diagram: whirl frequency for neutral stability as a function of rotor speed, zero damping (ref. 38).	12
Figure 9.	Solution of real and imaginary equations of ground resonance, for articulated rotor (lag frequency $\nu_{\zeta}^2 = 0.22 + (0.265\Omega)^2$) on symmetric support; frequency (in fixed system) as a function of rotor speed, both normalized by the support frequency (ref. 27).	12
Figure 10.	Rotor head and blade oscillation frequency diagram (ref. 40).	13
Figure 11.	Loewy's development of two-dimensional model for influence of returning shed wake (ref. 45).	15
Figure 12.	Bending mode damping (ref. 51).	16
Figure 13.	Pitch-flap flutter (ref. 51).	16
Figure 14.	Flap response to vertical hub excitation (ref. 52).	16
Figure 15.	Damping of second (top) and third (bottom) flap bending modes (ref. 53).	16
Figure 16.	Wake geometry showing trailing tip vortex and element of shed wake (ref. 58).	20
Figure 17.	Comparison of computed and experimental air loads; H-34 flight test at $\mu = 0.2$ (ref. 58).	20
Figure 18.	Finite straight-line approximation (refs. 61–62).	20
Figure 19.	Pictorial example of the initial portion of the wake of a two-bladed rotor divided into four radial segments (ref. 63).	21
Figure 20.	Example of wake configuration (ref. 67).	22
Figure 21.	Near shed-wake models (refs. 67–68).	23
Figure 22.	Azimuthal variation of airloads for NASA model rotor, $\mu = 0.15$ (ref. 64).	23
Figure 23.	Azimuthal variation of airloads for HU-1A, $\mu = 0.26$ (ref. 64).	23
Figure 24.	Measured and computed lift for H-34 at $\mu = 0.18$, mean removed; dashed line measured, solid line computed (ref. 67).	24
Figure 25.	Fully developed wake. White dots are the tip vortex; the dashed lines show the approximate position of the vortex sheet (ref. 77).	24
Figure 26.	The vortex pattern in the wake of a single-bladed hovering helicopter rotor as obtained from smoke studies (ref. 78).	25
Figure 27.	Nondimensional radial and vertical displacement of tip vortex as a function of azimuth position from blade (ref. 77).	25
Figure 28.	Landgrebe: sample flow visualization photograph (ref. 80).	26
Figure 29.	Kocurek and Tangler: single and multiple exposure schlieren photographs (ref. 82).	26
Figure 30.	A rotor-wake system with an embedded finite-difference grid (ref. 83).	26
Figure 31.	PIV measurement of hover wake geometry for untwisted blades (courtesy M. Ramasamy, ref. 84).	26
Figure 32.	Vertol Division universal helicopter model (ref. 85).	27
Figure 33.	Measured rotor lateral flapping angle, compared with calculations using various wake models (ref. 85).	27
Figure 34.	Calculation of lateral flapping angle using Scully's free-wake geometry (ref. 86).	28
Figure 35.	Flap response to cyclic stick stir, amplitude, and phase as a function of frequency ratio (ref. 98).	29
Figure 36.	Ellipsoidal coordinate system (ref. 87).	30
Figure 37.	Overall view of model (ref. 113).	32
Figure 38.	Modal frequencies as a function of rotor speed for configuration 4, matched stiffness: comparison of measurements (points) and CAMRAD calculations without inflow dynamics (ref. 115).	32

LIST OF FIGURES (cont.)

Figure 39.	Modal frequencies as a function of rotor speed for configuration 4, matched stiffness: comparison of measurements (points) and CAMRAD calculations with inflow dynamics (ref. 115).	33
Figure 40.	Case of coupled bending-torsion of twisted rotating beam (ref. 116).	33
Figure 41.	Hingeless rotor helicopters.	35
Figure 42.	Flap-lag-torsion coupling on rotor blades (ref. 135).	36
Figure 43.	Undeformed coordinate systems, elastic displacements, and resultant forces and moments (ref. 117).	38
Figure 44.	A finite element showing nodal degrees of freedom (ref. 172).	40
Figure 45.	Detailed multibody representation of a rotor system (ref. 181).	40
Figure 46.	Rotor blade stability diagram (ref. 190).	43
Figure 47.	Regions of destabilization (ref. 194).	43
Figure 48.	Rotor blade stability diagram (ref. 196).	43
Figure 49.	Damping levels of free-flapping blade (ref. 200).	44
Figure 50.	U.S. Army helicopters in 1972.	45
Figure 51.	Rotor in S2 Chalais-ONERA wind tunnel for non-lifting tests (ref. 234).	47
Figure 52.	Comparison between calculation and experiment for straight tip, non-lifting rotor at $\mu = 0.55$ (ref. 237).	48
Figure 53.	Three-bladed rotor in S2 Chalais-Meudon wind tunnel for lifting tests (ref. 238).	48
Figure 54.	Comparison of measured and computed chordwise pressure distribution at different azimuth angles; $\mu = 0.39$, $C_T / \sigma = 0.0665$, $r/R = 0.90$ (ref. 229).	48
Figure 55.	Publications on rotor CFD by year.	49
Figure 56.	Matching of integral and differential rotor flow methods (ref. 243).	50
Figure 57.	A comparison of computed and experimental upper surface pressures, $\mu = 0.298$ and $r/R = 0.95$ (ref. 243).	50
Figure 58.	UH-60A Airloads Program level flight operating conditions.	52
Figure 59.	The model and experimental set up (ref. 261).	53
Figure 60.	Comparison of measured and calculated surface pressure results for hovering rotor, $M_{tip} = 0.877$ and 8-degree collective pitch (ref. 263).	53
Figure 61.	H-34 flight test aircraft (ref. 74).	55
Figure 62.	Blade planform and instrumentation for the H-34 flight test (ref. 74).	55
Figure 63.	H-34 airloads rotor in the 40- by 80-Foot Wind Tunnel.	55
Figure 64.	Blade planform and instrumentation for the H-34 wind tunnel test (ref. 268).	55
Figure 65.	Rotating scissors geometry for the H-34 wind tunnel model (John L. McCloud III).	55
Figure 66.	UH-60A Airloads aircraft over the Livermore valley (ref. 269).	56
Figure 67.	UH-60A Airloads Program test conditions.	56
Figure 68.	UH-60A blade planform and instrumentation (ref. 269).	56
Figure 69.	UH-60A Airloads rotor in the 40- by 80-Foot Wind Tunnel.	57
Figure 70.	HART I rotor test in the DNW wind tunnel.	57
Figure 71.	HART II rotor test in the DNW wind tunnel.	57
Figure 72.	Blade planform and instrumentation for the HART wind tunnel tests (ref. 271).	58
Figure 73.	PIV test matrix (ref. 271).	58

LIST OF TABLES

Table 1. Milestones in rotorcraft aeromechanics.....	2
Table 2. Analysis development building on Glauert's achievements.....	10

NOMENCLATURE

a	two-dimensional lift-curve slope
A	rotor disk area, πR^2
c	blade chord
c_d	section drag coefficient
C_L	rotor roll moment coefficient, $L / \rho A (\Omega R)^2 R$
C_M	rotor pitch moment coefficient, $M / \rho A (\Omega R)^2 R$
C_T	rotor thrust coefficient, $T / \rho A (\Omega R)^2$
I_b	blade flap moment of inertia
N	number of blades
r	blade radial station
R	blade radius
t	time
V	rotor flight speed
γ	Lock number, $\rho a c R^4 / I_b$
λ	inflow ratio (induced velocity divided by ΩR)
μ	advance ratio (flight speed divided by ΩR)
ρ	air density
σ	rotor solidity, $Nc / \pi R$
ψ	rotor azimuth angle
Ω	rotor rotational speed

MILESTONES IN ROTORCRAFT AEROMECHANICS

Wayne Johnson

Ames Research Center

SUMMARY

The subject of this paper is milestones in rotorcraft aeromechanics. Aeromechanics covers much of what the engineer needs: performance, loads, vibration, stability, flight dynamics, and noise. These topics cover many of the key performance attributes and many of the often-encountered problems in rotorcraft design. A milestone is a critical achievement, a turning point, or an event marking a significant change or stage in development. The milestones identified and discussed include the beginnings of aeromechanics with autogyro analysis, ground resonance, aeromechanics books, unsteady aerodynamics and airloads, nonuniform inflow and wakes, beams and dynamics, comprehensive analysis, computational fluid dynamics, and rotor airloads tests. The focus on milestones limits the scope of the history but allows the author to acknowledge his choices for key steps in the development of the science and engineering of rotorcraft.

INTRODUCTION

The subject of this paper is an aspect of the history of the engineering and science of our profession: milestones in rotorcraft aeromechanics. A milestone is a critical achievement, a turning point, or an event marking a significant change or stage in development.

Defining “aeromechanics” is more difficult. Today’s dictionaries do not capture what the term means for the rotorcraft community. Typical definitions are not broad enough and do not reflect the multidisciplinary facet of the word as applied to rotorcraft: mechanics that deals with equilibrium and motion of gases and solid bodies immersed in them (Merriam-Webster); branch of mechanics that deals with air in motion or equilibrium (Webster); study of gases in motion and in equilibrium, including study of mechanical effects of gases on objects; mechanics is study of energy and forces (MSN Encarta). I propose the following definition:

Aeromechanics: The branch of aeronautical engineering and science dealing with equilibrium, motion, and control of elastic rotorcraft in air.

This paper covers rotorcraft aeromechanics development, including analysis and test. Invention of rotorcraft is not the subject. The focus is milestones, not the much larger task of presenting a history of aeromechanics. Much progress in aeromechanics development is made that is not marked by events that can be considered milestones, but it is the milestones that produce the interesting stories. The scope is narrowed to topics to which I have paid enough attention that I have an opinion about the critical steps. Table 1 summarizes my choices for milestones.

Inventors do not wait for the analysts. Yet, presented with a new concept, analysis and test are needed to check the performance claims being made. Moreover, the developer needs engineering calculations if designs are to fulfill the potential of the concept. Aeromechanics covers much of what the rotorcraft engineer needs: performance, loads, vibration, stability, flight dynamics, and noise. These topics cover many of the key performance attributes and many of the often-encountered problems in rotorcraft designs. Thus, aeromechanics development is intertwined with the aircraft invention. Aeromechanics technology is pulled by invention and facilitates the aircraft development and evolution, as well as the next generation of invention.

TABLE 1. MILESTONES IN ROTORCRAFT
AEROMECHANICS

1926	The beginning	Glauert
1943	Ground resonance	Coleman
1952	Aeromechanics book	Gessow and Myers
1956	Hover wake geometry	Gray
1957	Unsteady aerodynamics	Loewy
1958	Beams	Houbolt and Brooks
1960	Digital computer	IBM
1962	Rotor airloads tests	H-34
1962	Airloads and wakes	Miller, Piziali
1972	Lateral flapping	Harris
1972	Multiblade coordinates	Coleman, Hohenemser
1974	Beams	Hodges and Dowell
1974	Comprehensive analysis	C81
1981	Dynamic inflow	Pitt and Peters
1981	Rotor aerodynamic state	Bousman
1981	Hover airloads	Caradonna and Tung
1982	Computational fluid dynamics	Caradonna, Tung, and Desopper
1984	CFD/CSD loose coupling	Johnson
1994	Rotor airloads tests	UH-60A, HART

THE BEGINNING OF AEROMECHANICS

Rotorcraft aeromechanics analysis begins with Glauert. In a remarkable November 1926 report for the British Aeronautical Research Council (ref. 1) and a paper read two months later to the Royal Aeronautical Society (RAS) (ref. 2), Hermann Glauert of the Royal Aircraft Establishment (RAE) (fig. 1) gave us the foundations of induced and profile power analysis for rotors, and introduced blade element theory for performance and hub loads of flapping rotors in forward flight.

As described in the RAS lecture, the impetus for this work was the demonstration flights in Britain of the Cierva C.6A autogyro, carried out at Farnborough in October of 1925 (fig. 2), and a lecture by Juan de la Cierva that was read to the RAS on October 22 (ref. 3). The RAE work was motivated by the need to check the claims that Cierva was making for his aircraft. The first general account of



Figure 1. H. Glauert of the Royal Aircraft Establishment.



Figure 2. C.6A autogyro at Farnborough.

Cierva's invention was received in Britain in February 1925 (ref. 4), which led immediately to preliminary wind tunnel tests (reported in May 1925) and a theoretical investigation first reported in November 1925. This initial presentation of the theory gave a maximum L/D that proved to be in good agreement with the results from subsequent wind tunnel tests. Following the C.6A demonstration, wind tunnel tests and model autogyro drop tests were conducted at the National Physical Laboratory (NPL) and the RAE (1926–1927). The more detailed theory (ref. 1) provided a satisfactory estimate of maximum lift, an account of flapping, and a qualitative explanation of the side force (ref. 4). The theory was extended by C.N.H. Lock of the NPL in an Aeronautical Research Council (ARC) report of 1927 (ref. 5).

Induced velocity

Glauert proposed an expression (usually given his name) for the rotor induced velocity based on an argument that has not since been improved. He made the connection between propeller and wing induced power. From reference 2:

“The axial velocity u through the disc of the windmill is less than the undisturbed velocity $V \sin i$ owing to the interference of induced velocity caused by the windmill itself. The determination of this induced velocity or of the relationship between the velocities u and $V \sin i$ is undoubtedly the most fundamental point in the development of the theory of the gyroplane.”

Here i is the disk incidence angle and V is the flight speed.

“Firstly, the momentum equation for an airscrew of radius R giving a thrust T is

$$T = 2\pi R^2 \rho u v$$

where u is the velocity through the airscrew disc and v is the induced velocity at the disc, so that $2v$ is the slipstream velocity.

Secondly, the equation for the normal induced velocity v of an aerofoil of semi-span s with lift L distributed elliptically across the span is

$$L = 2\pi s^2 \rho V v$$

These two expressions may now be written in the general form

$$(\text{Force}) = 2 (\text{Mass affected}) \times (\text{induced velocity})$$

and in each case the mass affected is the product of the density, of the area of the circle on the span as diameter, and of the velocity through this circle. The direction of the induced velocity is always opposite to that of the force. This general expression will therefore be taken to apply also to the case of the inclined windmill of a gyroplane. The induced velocity v will be directed downwards along the shaft and its magnitude will be determined by the equation

$$T = 2\pi R^2 \rho V' v$$

where V' is the resultant of the velocities V and v .”

Glauert (ref. 1) characterized the result $v = T / 2\pi R^2 \rho V'$ as a “logical generalization of the ordinary aerofoil formula,” reducing for small i to the standard formula for the normal induced velocity of an aerofoil of semi-span R , and for i nearly 90 degrees to the ordinary momentum formula for an airscrew. “It is anticipated therefore that the formula will be valid over a wide range of angle of incidence.” The key fact permitting this generalization is that the mass flow affected by a wing is that through a circle around the wing span. Glauert recognized that for a circular wing this circle has the same area as the rotor disk. Because for an autogyro the edgewise velocity is considerably greater than the axial velocity, “the induced velocity due to the system of trailing vortices will correspond more closely to the induced velocity of an aerofoil than to that usually associated with an airscrew and its slipstream.”

Flapping and hub forces

Glauert introduced blade element theory for edgewise-moving rotors. “The autogyro is essentially a windmill of low pitch working in a sidewind, and it is natural to apply to it the modern methods of strip theory combined with the Prandtl theory of interference, which have been so successful in the case of the monoplane wing and the ordinary airscrew” (ref. 5). Glauert developed expressions for the blade section velocities including flight speed, rotation, flapping, and induced velocity. The section analysis was based on two-dimensional airfoil characteristics with a constant lift-curve slope and a mean drag coefficient. “The aerodynamic characteristics of the aerofoil section must be taken to correspond to two dimensional motion or infinite aspect ratio in accordance with modern aerofoil and airscrew theory” (ref. 2). Glauert solved the flapping equation of motion obtained from equilibrium of inertial, centrifugal, aerodynamic, and weight moments about the flap hinge (with no hinge offset).

Glauert neglected squares and higher powers of advance ratio μ . Considering the breakdown of the small angle assumption near reverse flow, he viewed the limit of validity to be $\mu < 0.5$. The maximum speed of the C.6A gave about $\mu = 0.4$, although later autogyros would operate at much higher advance ratios. However, an order μ blade element analysis led to performance estimates more pessimistic than those obtained by energy methods.

Glauert developed equations for the thrust and torque (C_T and C_Q , to first order independent of μ), drag and side force (C_H and C_Y , linear in μ), and first harmonic flapping (linear in μ). The equation $C_Q = 0$ was solved for the inflow ratio.

In a report published the next year (1927) (ref. 5), Lock eliminated the order μ assumption of the blade element analysis, and verified that the blade element analysis and energy method gave identical performance results. He also added cyclic pitch, and solved for the higher harmonics of flap motion.

Longitudinal inflow gradient

Glauert's result for lateral flapping and side force implied a lateral shaft-axis force proportional to thrust and forward speed, the direction being to port (the retreating side) with curved blades and to starboard with straight blades. This did not agree with the observed lateral movement of the shaft on the Cierva autogyro. From reference 1:

“Experimentally the lateral force appears to be to port at high speed and to starboard at low speed. Thus the sense of the variation of the lateral force with speed has been obtained correctly, but there is a discrepancy in the value at low speeds. To explain this divergence it is necessary to abandon the assumption that the axial velocity u is constant over the whole disc and to consider the effect of a varying induced velocity.

At small angles of incidence, when the windmill give rise to a trailing vortex sheet very similar to that of an aerofoil, the induced velocity must increase from the front to rear of the disc, and hence the axial velocity u will decrease from front to rear [ref. 2].”

Glauert introduced an increment of the induced velocity proportional to the distance behind the center of the disk, hence

$$v + v_1 \frac{r}{R} \cos \psi$$

for the total, with an estimate of $v_1 = v$. The resulting correction improved the prediction of the lateral shaft angle, but the correction was not sufficiently large (ref. 1).

Energy losses

In an appendix to reference 1, Glauert considered the energy losses of an autogyro in order to provide an independent check of the blade element results.

“Two main sources of loss of energy are considered, due respectively to the induced

velocity caused by the thrust and to the profile drag of the blades. An additional source of loss of energy is the periodic distribution of thrust over the disc of the windmill but no simple method has been found of estimating its magnitude [ref. 1].”

The drag of the windmill is determined by $DV = E$, where E is the rate of energy loss (power), and the drag-to-lift ratio is then $D/L = E/VT$ (assuming small incidence, so the lift is nearly the rotor thrust).

“The thrust of the windmill causes an induced velocity v and a corresponding loss of energy Tv .” The induced drag term is then $D_i/L = C_T/2\mu^2$.

The profile drag term is written

$$D_o/L = E_o/VT = \frac{\sigma c_d}{8\mu C_T} F_p(\mu)$$

using a mean drag coefficient c_d . The rotor drag-to-lift ratio $D/L = D_i/L + D_o/L$ follows.

Profile power

First considering just the blade section tangential velocity, Glauert wrote the energy loss due to the drag of the blades (ref. 1):

$$E = B \int_0^R \delta c \rho (\Omega r + V \sin \psi)^3 dr$$

where $2\delta = c_d$, and B is the number of blades. Assuming a mean drag coefficient, the integration gives $F_p = 1 + 3\mu^2$. This result ignores the axial velocity and the blade section radial velocity. The effect of the former is small for small disk incidence, but the effect of the radial velocity is quite important. Thus, the profile energy loss is

$$E = B \int_0^R \delta c \rho \{(\Omega r + V \sin \psi)^2 + V^2 \cos^2 \psi\}^{\frac{3}{2}} dr$$

averaged over the azimuth. Glauert evaluated this integral analytically (for $\mu < 1$) at azimuth angles of $\psi = 0, 90, 180,$ and 270 degrees, and the sum of these 4 integrals gave

$$F_p = 1 + n\mu^2 = \frac{1}{2}(1 + 6\mu^2 + \mu^4) + \frac{1}{4}(2 + 5\mu^2)\sqrt{1 + \mu^2} + \frac{3}{8}\mu^4 \ln \left[\frac{\sqrt{1 + \mu^2} + 1}{\sqrt{1 + \mu^2} - 1} \right]$$

Evaluation of this integral gave $n = 4.5$ at low speed, and $n = 6.13$ at $\mu = 1$.

This result for the profile power was developed as a check of the blade element theory result, particularly at low disk incidence and high speed. Since the connection between

the two approaches is complex, the blade element theory form was viewed as the primary result by Glauert. That was unfortunate since the energy form was, in fact, more accurate and predicted better performance for the autogyro.

Rotor lift-to-drag ratio

A principal objective of Glauert's work was to estimate the performance of the autogyro, particularly the rotor lift-to-drag ratio. Glauert's blade element approach predicted a maximum $L/D = 5.9$ (refs. 1–2) for a solidity of $\sigma = 0.2$ and mean drag coefficient $\delta = 0.0060$ ($c_d = 0.0120$); or $L/D = 6.5$ for $\sigma = 0.1$. The energy approach gave a maximum $L/D = 7.9$ for $\sigma = 0.2$, a result found only in the appendix of reference 1 and described as certainly overestimating the merit of the autogyro. Lock's extension of the blade element approach to higher order in advance ratio (ref. 5) resolved this difference in L/D , confirming the energy method result. As summarized in reference 4, flight tests in 1927 implied an L/D of about 5, performance considered comparable with the theory and inferior to an airplane. Wind tunnel tests showed a maximum L/D of 7.5 to 8.0.

Cierva (ref. 6) gave experimental results of rotor-alone L/D of about 10 for $\sigma = 0.1$ (and $L/D = 12$ with a small fixed wing). The RAE results could have been considered consistent with Cierva's L/D values, but Cierva remained focused on the initial blade element predictions of Glauert, and seemed unaware of either the energy method result or the summary provided in reference 4.

The innovation

Glauert's results for the induced velocity and the profile power were very original. Interestingly, neither reference 1 nor 2 cites any other publications. Glauert was perhaps in a unique position to make the connection between wing and propeller induced power, based on his work in both subjects (ref. 7). The profile power equation in the energy method was not derived. Perhaps Glauert saw this as an obvious extension of the axial flow result, but including the radial flow effect was an important insight. His approximate evaluation of the integral was clever.

Between them, Glauert and Lock established many of the key concepts and even the notation of rotor aeromechanics. Glauert (ref. 1) introduced the concept of the tip-path plane and derived the expression for the mean lift coefficient: $\bar{k}_L = 3T_c / \sigma$ (or $\bar{c}_l = 6C_T / \sigma$ in modern notation). He used β for the blade flap angle (but not a Fourier series expansion), and $\sigma = Bc / \pi R$ for rotor

solidity. Lock (ref. 5) described the equivalence of flapping and feathering and used a negative Fourier series for the flap motion (to become National Advisory Committee for Aeronautics (NACA) notation). He used $\mu = V \cos i / \Omega R$ for the advance ratio. Lock introduced the parameter representing the ratio of aerodynamic and inertial forces on the blade, $\gamma = \rho a c R^4 / I_1$, which consequently bears his name (though differing by a factor of 2 from the U.S. definition, because of the different convention for lift coefficient).

Cierva (ref. 8) estimated the rotor induced power using the fixed-wing expression, without the connection to a propeller for axial flow. He had the energy expression for profile power but was not able to evaluate the integral accurately.

According to Brooks (ref. 9), Cierva put the first edition of his "Engineering Theory of the Autogyro" into final form with the technical assistance of Paul H. Stanley of Pitcairn. Cierva later (1934–1935) wrote "Theory of Stresses in Autogyro Rotor Blades." While neither document was published, Brooks says they were widely read by rotary-wing designers. In the discussion after Cierva's 1930 RAS lecture (ref. 6), Yeatman said that "he hoped that Senor de la Cierva would publish in the Journal his mathematical theory of the autogyro." At his 1935 RAS lecture (ref. 10), Cierva was "unable to reply definitely to Mr. Relf's question as to whether he would be prepared to publish more of his work." The works remained unpublished at Cierva's death in 1936, although they were later edited by J.A.J. Bennett (ref. 8).

Cierva, in 1930 (ref. 6), described his theory:

"My engineering theories, all based on energy equations since 1924 and very similar in general lines to that developed later by Mr. C.N.H. Lock, and published by the Air Ministry in the R. & M. 1127, in 1927 were not a useful guide to me until, in 1928, I succeeded in finding an analytical method of integrating the frictional losses of energy. ... The present results check with amazing accuracy the simple assumptions which form basis of my theory."

Likely reflecting the animosity from 1926, he cites Lock but not Glauert and was unaware, evidently, of Glauert's better approximation for the profile power integral.

The conflict

Glauert concluded the main text of reference 1 with:

“Thus the principal merit of a gyroplane, its low landing speed, inevitably disappears when high speed of level flight is required, and there remains only the absence of a sudden stall to counter-balance the very poor efficiency as compared with an aeroplane.”

After a consideration of the maximum design speed, he states in reference 2:

“So it appears that for high speed aircraft a gyroplane will not land much slower than the corresponding aeroplane, while owing to its greater drag the top speed will be from 10 to 20 m.p.h. lower.

In light of these results, that a high speed gyroplane is slower than the corresponding aeroplane and is incapable of carrying out the characteristic slow landing associated with this type of aircraft, it would appear that the useful field of the gyroplane is confined to those cases where extreme high speed is not required. There are undoubtedly many cases where it is advantageous to sacrifice some degree of top speed and general efficiency in order to obtain ease of landing and safety from the danger of stalling, and it is in these cases that the autogyro system will find its most useful application.”

And concludes the lecture with:

“Improvement in the design of the windmill may lead to better results, but I believe that the gyroplane will always be slightly inferior to the aeroplane for top speed. On the other hand, the gyroplane has the very important advantages of a slower landing speed and of the absence of a sudden and violent stall.”

Cierva sent a letter as his contribution to the discussion of Glauert’s 1927 RAS lecture, excusing “himself from coming to speak in person on the grounds of his difficulty in speaking English” (ref. 2). In this letter, Cierva objected strongly to Glauert’s results and conclusions. Early in the discussion, Handley Page remarked on the “extraordinary divergence of opinion among the experts,” and expressed the desire for “some actual measured data.” He also said: “When that next paper comes I hope it will be a paper from Senor de la Cierva, but I suppose it will be replied to by a letter from Mr. Glauert, who will be unable to be present.”

Respect for the autogyro and its inventor was not diminished by the conflict, and the RAS invited Cierva to present lectures in 1930 and 1935. Neither Glauert nor Lock, however, were present at the 1930 lecture. Glauert was no longer working on autogyros or airscrews at that time—his last papers on the subjects appearing in 1928—perhaps because he became Head of the Aerodynamics Department at Farnborough. Lock though continued publishing in the field into the late 1940s.

Cierva’s letter said:

“In the first place I must, with respect, record my protest against the manner in which Mr. Glauert has made assertions in an almost axiomatic form, from which the evident conclusion must be drawn that the autogyro is, in effect, useless. Such assertions are based only on very incomplete and uncertain calculations which I am able to state are not at all in agreement with the experimental results.

I disagree with almost every point contained in Mr. Glauert’s developments, which in any case are wrong both in principle and in conclusions, and also in many details. This observation does not involve any personal criticism of such an eminent mathematician, whose mistake is, I believe, that he has tried to treat in too simple and theoretical a manner, a most complicated and novel aerodynamical problem, and that he has considered his conclusions as proved when he might well have waited for the shortly forthcoming tests to tell us the truth.”

Glauert replied to the discussion: “I hope, however, that I have not given the impression that the autogyro is “useless.” I believe that it is less economical than an aeroplane, but that it has very considerable advantages as regards safety and ease of landing.” And there would seem to be common ground with Cierva’s remark: “The autogyro will have performance at least as good as, and possibly better than, the aeroplane, since lift/drag is not the sole criterion of performance.” However, there was direct disagreement regarding the values of lift-to-drag ratio and vertical rate of descent, Glauert’s estimate of the performance being significantly less than Cierva’s statements, and Cierva could not have appreciated the treatment of maximum speed capability.

At the time, Glauert had wind tunnel and drop test data to support his analysis, while Cierva had not yet produced quantitative flight test results. From today’s perspective,

Glauert's analysis is considered optimistic. Cierva was likely most concerned about the possible impact of Glauert's results on his continued development of the autogyro, for he concluded his letter with a remark on "the risk of mistake which is necessarily involved in trying to limit from the beginning the possibilities and improvements of any new system."

When Cierva returned to the RAS in February 1930 (ref. 6), he described the autogyro in terms very similar to Glauert's:

"The autogiros lately produced have not better performance than the equivalent conventional aeroplanes. In fact, they have a little less speed and a little less climb than the best equivalent aeroplanes. Nevertheless, they are better flying machines. If they fall a little short of the best aeroplanes in that rather vague quality which is called "performances," they have a performance of their own, which is utility and safety."

There should have been common ground with the RAE in both quantitative and qualitative assessment of the autogyro. Their estimates of performance were close by this time. Yet the animosity was still evident in Cierva's remarks regarding the conservative estimate of L/D by "both eminent mathematicians and experimenters" and the inability of "certain theorists" to see any physical possibility of the vertical rate of descent being significantly less than that of a parachute. In a brief description of his theory, Cierva cited only Lock, not Glauert. Based on reference 8, Cierva apparently remained unaware of Glauert's elegant expressions for induced and profile power.

Exacerbating the animosity was the disagreement regarding vertical descent rate in autorotation. In this case, the Englishmen started the argument. They were right, but the topic was not central to a discussion of autogyro performance. Evidently the subject had come up during the demonstration flights, so following Cierva's October 1925 lecture (ref. 3) Lock opened the discussion with:

"What would be the actual velocity of descent in a very steep glide? Would it be possible for machine to descend absolutely vertically at a safe speed? ... Whether you anticipate that the resistance of the Autogyro, in falling vertically, would be very much greater than that of a parachute of area equal to the disc area of the Autogyro, since a simple calculation indicates that a parachute having the same area and loading

as the Autogyro would fall at a velocity of between 30 and 40 feet per second."

Phrased as questions, this stated a position based on the experience since 1922 of Lock, Glauert, and others at the RAE and NPL, with propellers in axial flow, including autorotation. In reply, Cierva stated that the vertical descent rate of the C.6A was 3–4 m/sec (10–13 ft/sec) for a disk loading of about 9.5 kg/m² (1.9 lb/ft²). Glauert finished his 1927 paper with a paragraph on "the possibility of vertical descent of a gyroplane." Based on empirical results (wind tunnel experiments and dropping tests) he gave $25\sqrt{T/A}$ as the velocity of steady descent of a windmill, which means a rate of descent of 35 ft/sec for $T/A = 2$ lb/ft² (a modern result is $26.2\sqrt{T/A}$; see reference 11). Thus, Glauert concluded: "I see no reason for believing that the rate of descent of a full scale windmill can be appreciably less than this value, and so I do not believe that it would be safe for a gyroplane to descend vertically to the ground for any considerable height in still air." Cierva's contribution to the discussion of the paper included: "The rate of descent in a practically vertical path from some 500 feet was found in repeated official tests to be some 50 per cent of that allowed by Mr. Glauert." Glauert, in reply to the discussion, allowed that an exaggerated importance had been attached to the question but only after reiterating, "I cannot reconcile this slow rate of descent with the fundamental laws of motion, nor can I believe in so tremendous a scale effect as would be required to increase the drag coefficient of the windmill four times." In their 1928 summary of autogyro work (ref. 4), Glauert and Lock stated that "the only point which remains uncertain is the capacity of a gyroplane to descend vertically at a low speed, but the practical importance of this question should not be exaggerated." Drop tests were consistent with results for airscrews, so the vertical rate of descent was expected to be double that recorded. Cierva devoted a large part of his 1930 lecture (ref. 6) to vertical descent. He stated that 13–15 ft/sec was "obtained now and again in free descent," compared to 12–13 ft/sec descent at 45 degrees. He attributed the discrepancy between full-scale results and models to stall on the inboard part of the blades, and described a theory that expansion of the wake could explain how the rotor could actuate on a much greater mass of air. In the discussion (ref. 6), McKinnon Wood of RAE stated that the apparent parachutal coefficient was improbable and disagreed with the wake explanation presented.

Inflow curve

One thing the RAE group did not get right was the presentation of inflow curve—the momentum theory solution for the induced power as a function of axial velocity—and its extension into the vortex ring and turbulent brake states. Writing the loading distribution as $dT/dr = 4\pi\rho(V+v)^2 F = 4\pi\rho V^2 f$, they plotted $1/f = (V/v_h)^2$ as a function of $1/F = ((V+v)/v_h)^2$ (refs. 12–13), as shown in figure 3. This form is unfavorable because using squares hides the sign of V and $(V+v)$, and hides the slope of the curve at hover. The more useful forms were introduced in 1947: v as a function of V from Hafner (fig. 4, ref. 15) and $(V+v)$ as a function of V from Lock (fig. 5, ref. 16). As Lock described (ref. 16):

“On reading Dr. Hislop's paper on experiments on a Hoverfly I aircraft which reproduces the ‘characteristic’ curve of an airscrew as given in R. & M. 1026, and on re-reading the latter report and R. & M. 1014 after an interval of twenty years, it occurred to me that a modification of the method of plotting adopted in these reports would have certain advantages.

The change of variable has three advantages,

1. The three principal working states now correspond to three different quadrants. ...
2. The representation in the neighbourhood of the x-axis (static condition) and the y-axis (ideal gyroplane descending) is more definite since the curve has a finite slope at both these points.
3. The formulae of the 'Vortex theory' take the simple form ...”

Although his report was dated earlier, Lock cited Hafner's conference paper.

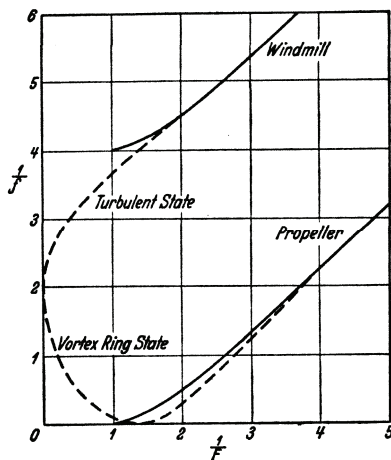


Figure 3. Axial inflow curve, RAE's form (ref. 14).

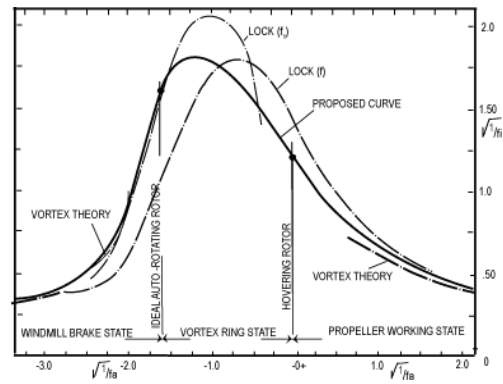


Figure 4. Axial inflow curve, Hafner's form (ref. 15).

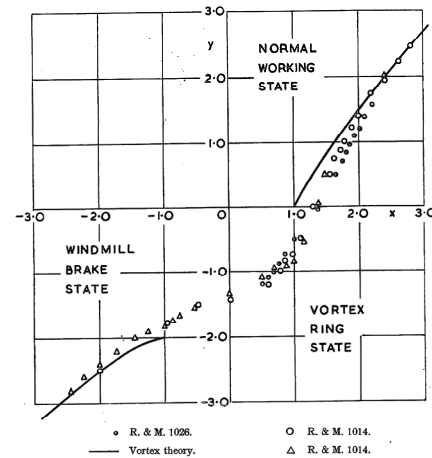


Figure 5. Axial inflow curve, Lock's form (ref. 16).

Profile power function

The profile power function $F_p(\mu, \mu_z)$ has an interesting history. This function accounts for the influence of edgewise and axial rotor velocity on the profile power coefficient: $C_{P_o} = (\sigma c_d / 8) F_p$. Including radial flow, axial flow, and reverse flow, the function is

$$F_p = 4 \int_0^1 (u_T^2 + u_R^2 + u_P^2)^{3/2} dr$$

(an average over the azimuth is also performed). Glauert's approximate expression for $F_p(\mu)$ (axial flow excluded) has an error of less than 1% up to $\mu = 1.9$, but this result has been largely ignored—even by Lock and those who built on the work of Glauert and Lock. Glauert suggested the form $F_p = 1 + n\mu^2$, but then showed that to match the exact result, the coefficient varies from $n = 4.5$ at $\mu = 0$ to $n = 6.13$ at $\mu = 1$. Cierva, by an approximate integration, obtained $F_p = 1 + 4\mu^2 + \mu^4$ (ref. 8), which has an error less than 1% only up to $\mu = 0.15$, and 4% up to $\mu = 0.3$. The work that followed Glauert built on blade element theory rather than the energy method, and hence omitted the radial flow effects. Without either radial flow or reverse flow,

$$F_p = 4 \int u_T^3 dr = 1 + 3\mu^2.$$

Including reverse flow gives $F_p = 1 + 3\mu^2 + \frac{3}{8}\mu^4$.

What I first encountered in class was $F_p = 1 + 4.6\mu^2$, which has its origin in Bennett's work (ref. 17). Bennett, who was the chief engineer at the Cierva Autogyro Company in 1940, developed an expansion of F_p for small μ , and found that the expansion was fit well by $n = 4.65$; but the expansion is not accurate for large μ , having an error less than 1% up to $\mu = 0.35$, and 4% up to $\mu = 0.5$. Bennett cites Glauert (ref. 1), but like Cierva (ref. 6) prefers Lock's work (ref. 5). Lock reconciled the blade element and energy results, but with the assumptions that lead to $F_p = 1 + 3\mu^2$. Bennett evidently obtained

$$F_p = 4 \int (u_T^2 + u_R^2)^{3/2} dr$$

from Cierva and did not look at the Appendix of reference 1 that gave Glauert's approximate integration.

For reference 11, I fit numerically integrated results to $F_p = 1 + 4.5\mu^2 + 1.61\mu^{3.7}$, which has an error of less than 1% up to $\mu = 1.4$. Harris worked on the problem for nearly 45 years (ref. 18). With the help of mathematics software, Harris developed an approximation valid to 1% over the full range of μ and μ_z :

$$F_p \cong \sqrt{1 + V^2} \left(1 + \frac{5}{2} V^2 + \frac{3}{8} \mu^2 \frac{4 + 7V^2 + 4V^4}{(1 + V^2)^2} - \frac{9}{16} \frac{\mu^4}{1 + V^2} \right) + \left(\frac{3}{2} \mu_z^4 + \frac{3}{2} \mu_z^2 \mu^2 + \frac{9}{16} \mu^4 \right) \ln \left[\frac{\sqrt{1 + V^2} + 1}{V} \right]$$

with $V^2 = \mu^2 + \mu_z^2$ (ref. 19). This expression is exact for axial flow ($\mu = 0$). Figure 6 compares the various expressions for $F_p(\mu)$. At the scale shown, the approximations of Glauert and Harris are indistinguishable from the numerical integration line.

After Glauert

In the decades following Glauert's work, development of the basic analysis of autogyro and helicopter rotors progressed in a series of steps built on the foundation provided by Glauert. Glauert considered a flapping rotor with no twist, constant chord, no hinge offset, and no cyclic pitch; small angle aerodynamics with constant lift-curve slope and mean drag coefficient. The rotor loads and flapping (coning and first harmonic) were obtained with only first order terms in advance ratio retained.

Lock (1927, ref. 5) extended Glauert's analysis by including higher powers of advance ratio, second harmonic flapping, and cyclic pitch. He showed the equivalence of no-feathering plane and tip-path plane analyses, and the equivalence of the blade element theory and energy method results for power (though neglecting radial flow and reverse flow).

Wheatley (1934, ref. 20) extended the theory of Glauert and Lock and evaluated the accuracy of the theory by comparing it with test results. He considered a flapping rotor with no hinge offset; linear twist, constant chord blades; the tip loss factor and linear induced velocity variation. Wheatley included reverse flow (accounting for the sign of lift and drag in the reverse flow region) but still with small angle aerodynamics, and he neglected radial flow and radial drag effects in the profile losses. The calculations were compared with test data for the Pitcairn autogyro. The comparison was generally good up to about $\mu = 0.5$. A significant discrepancy occurred in the calculation of lateral flapping, which was typically 1.5 degrees low in magnitude. Including an estimate of the longitudinal inflow gradient reduced the error to about 1.0 degree. Wheatley considered the likely source of this discrepancy to be the simple induced velocity variation used.

Sissingh (1939, ref. 21) extended Wheatley's analysis, considering a flap hinge offset and eliminating the assumption of a constant (mean) drag coefficient by using a general drag polar of the form $c_d = \delta_0 + \delta_1\alpha + \delta_2\alpha^2$.

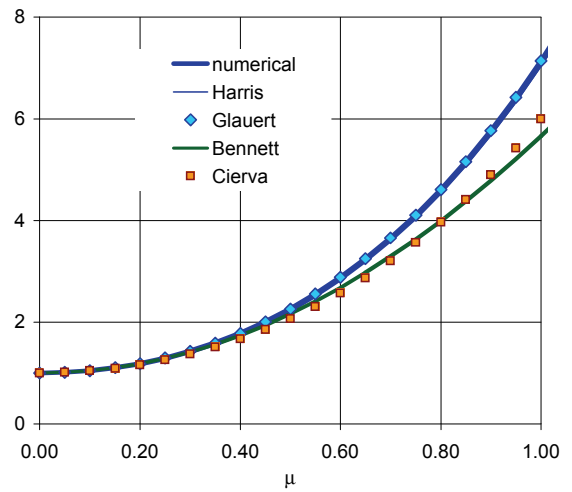


Figure 6. Profile power function.

Bailey (1941, ref. 22) put Wheatley's analysis in practical form for routine use by expressing all quantities as direct functions of the blade collective pitch, twist, and no-feathering-plane inflow ratio. The coefficients of these expressions are a function of advance ratio, the Lock number, and the tip loss factor. Bailey considered a flapping rotor with linearly twisted, constant chord blades, and a drag polar $c_d = \delta_0 + \delta_1\alpha + \delta_2\alpha^2$. The aerodynamic model still neglected the radial drag, assumed small angles to evaluate the angle of attack, and used a constant lift-curve slope, $c_l = a\alpha$. Bailey presented a solution procedure for the rotor performance (iterative for helicopter rotors, but for autogyros, solving $C_Q = 0$ directly for the inflow ratio).

Castles and New (1952, ref. 23) extended the theory of Wheatley and Bailey to large angles of pitch and inflow. They represented the section aerodynamic coefficients as $c_l = a \sin \alpha$ and $c_d = \varepsilon_0 + \varepsilon_1 \sin \alpha + \varepsilon_2 \cos \alpha$; substituted trigonometric expansions of $\sin \alpha = \sin(\theta - \phi)$ and $\cos \alpha = \cos(\theta - \phi)$; and used large angle expressions for $\sin \phi$ and $\cos \phi$. They considered an articulated blade with arbitrary twist and chord distributions, and root cutout. A linear inflow distribution was used.

Gessow and Crim (1952, ref. 24) also extended the theory of Wheatley and Bailey to large pitch and inflow angles, for a linearly twisted, constant chord blade. The angle of attack $\alpha = \theta - \phi$ was still assumed to be small. Reverse flow aerodynamics were approximated by using stalled values of lift and drag coefficients.

Gessow and Crim (1955, ref. 25) developed the equations and a solution procedure for the numerical integration of the transient flap motion. They considered an articulated rotor with offset flapping hinge (or a teetering rotor); large angles of flapping, inflow, and pitch; and general airfoil characteristics (lift and drag coefficients as function of angle of attack and Mach number). The solution was obtained by numerical integration using a digital computer. The analysis was developed for investigations of the flap dynamic stability (from the transient motion) and rotor performance (from the converged periodic solution). By using numerical integration, general aerodynamic characteristics could be considered, including stall, compressibility, and reverse flow (assuming that the required airfoil characteristics were available).

Gessow (1956, ref. 26) further developed the equations for numerical calculation of the aerodynamic characteristics of rotors in a form intended for digital computer applications. The model included arbitrary blade twist, chord, and mass distribution; general two-

dimensional aerodynamic coefficients for the blade airfoil; and large angles of pitch and inflow. The blade flap angle was assumed to be small and radial flow effects were still neglected. The solution procedure solved the flap equation of motion directly for the harmonics of the blade motion.

Table 2 summarizes the key developments after Glauert. This series of analytical developments was accompanied by a shift of the work from Britain (RAE and NPL) to the United States (NACA), and from autogyros to helicopters. The progression from Glauert was clear up to the introduction of the digital computer, which changed the way problems would be formulated and solved.

TABLE 2. ANALYSIS DEVELOPMENT BUILDING ON GLAUERT'S ACHIEVEMENTS

1927	Lock (ref. 5)	higher powers μ , cyclic pitch
1934	Wheatley (ref. 20)	twist, tip loss, reverse flow, compare with test
1939	Sissingh (ref. 21)	$c_d = \delta_0 + \delta_1\alpha + \delta_2\alpha^2$
1941	Bailey (ref. 22)	$c_d = \delta_0 + \delta_1\alpha + \delta_2\alpha^2$, tabulated coefficients
1952	Castles and New (ref. 23)	large pitch and inflow, arbitrary twist and chord
1952	Gessow and Crim (ref. 24)	large pitch and inflow angles, reverse flow, stall
1955	Gessow and Crim (ref. 25)	DIGITAL COMPUTER offset hinge, airfoil tables, large angles
1956	Gessow (ref. 26)	DIGITAL COMPUTER arbitrary twist and chord, large pitch and inflow, 2D airfoil characteristics

GROUND RESONANCE

The analysis of ground resonance was developed by Coleman of NACA (ref. 27). According to the forward of reference 28:

“During the early part of World War II, some of the helicopters designed for military use were observed during ground tests to exhibit a violent oscillatory rotor instability which endangered the safety of the aircraft. This instability was at first attributed to rotor-blade flutter, but a careful analysis indicated it to be caused by a hitherto unknown phenomenon in which the rotational energy of the rotor was converted into oscillatory

energy of the blades. This phenomenon was usually critical when the helicopter was operating on or near the ground and, hence, was called ground resonance. An oscillatory instability of such magnitude as resulted from this phenomenon would generate forces that could quickly destroy a helicopter. The research efforts of the National Advisory Committee for Aeronautics were therefore enlisted to investigate the difficulties introduced by this phenomenon. During the interval between 1942 and 1947, a theory of the self-excited instability of hinged rotor blades was worked out by Robert P. Coleman and Arnold M. Feingold at the Langley Aeronautic Laboratory. This theory defined the important parameters and provided design information which made it possible to eliminate this type of instability.”

The original reports (refs. 27, 29, 30) were combined into a single volume (ref. 31) by George W. Brooks, who also contributed an appendix. The combined volume was reissued as a NACA Report (ref. 28).

Ground resonance involves the coupled airframe inplane hub motion and blade lag motion, specifically the regressive lag mode of an articulated or soft-inplane rotor (lag frequency less than 1/rev). Insufficient damping of either the airframe motion or the lag motion can lead to a mechanical instability at rotor speeds near the resonance of an airframe mode and the regressive lag mode frequencies. For articulated rotors the physics of the instability are simple, typically involving neither aerodynamics nor other blade degrees of freedom. For soft-inplane hingeless or bearingless rotors (with higher lag frequency than articulated rotors), the flap motion can be important, contributing to both stiffness and damping (through aerodynamics) of the airframe modes; and the phenomenon can occur in flight as well as on the ground, then being called “air resonance.”

Ground resonance was a problem encountered by a number of autogyros (ref. 32). Reference 33, in discussing resonance possibilities, remarks: “An unpleasant, and at times dangerous vibration has been experienced in various rotor aircraft while on the ground with the rotor turning. These disturbances have all been identified as ground resonance.” Gregory (ref. 34) describes several accidents with the Kellett YG-1 autogyro during 1936, clearly ground resonance but at the time attributed to pilot error. When the YG-1 rotor destroyed itself in the NACA Langley full-scale wind tunnel, the problem was recognized as an inherent instability of the aircraft.

Gustafson (ref. 35) mentions the 1937 accident in the NACA wind tunnel, but records that “the studies of [Coleman] were originally inspired by industry test experience for an advanced autogyro” (ref. 36). Brooks (ref. 9) describes the 1941 Kellett XR-2 development:

“The accident to XR-2 proved to be important to the whole development of rotary wings. During one of the first tests of a jump take-off, ground resonance set in at high rotor speed. This built up so rapidly that the aircraft broke up before anything could be done to stop it. In less than five seconds, the rotor pylon support structure collapsed and the fuselage broke in two places, between the engine and pylon and pylon and tail. This dramatic further demonstration of a problem that had recurred repeatedly throughout the development of rotary-wing aircraft had an important effect in influencing the United States Army Air Force, the NACA and Kellett into tackling the basic problem of ground resonance. Bob Wagner of Kellett and Prewitt Coleman of NACA came up independently with mathematical solutions for the proper configuration and for damping to prevent ground resonance. This was a major step in the development of rotary-wing aircraft. Paul Stanley of the Autogyro Company of America had also arrived at mathematical and engineering solutions to the problem with the result that Pitcairn Autogyros are claimed to have largely avoided ground resonance.”

Coleman’s 1943 report (ref. 27) was a corrected version of a July 1942 Advance Restricted Report (ARR) of the same title. Coleman acknowledges Wagner (ref. 27):

“An alternative derivation of the characteristic equation for the whirling speeds of a three-blade rotor has been given by Wagner of the Kellett Autogyro Corporation. By considering only the case of a pylon having equal stiffness in all directions of deflection, Wagner has shortened the analysis by considering directly the equilibrium of forces and moments under conditions of steady circular whirling. Some examples of the dependence of whirling speed upon rotational speed are given, and the formula for the shaft-critical speed is obtained.”

Wagner (ref. 37) cites first Coleman (the ARR of July 1942) and his own 1942 Kellett Autogyro Corp reports, and then credits Coleman (ref. 27) for the general theory.

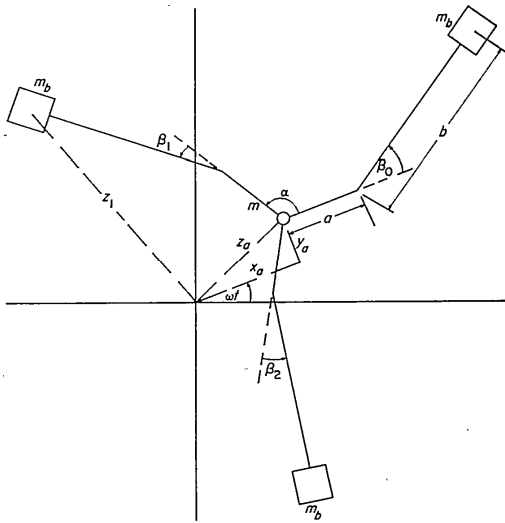


Figure 7. Simplified mechanical system representing rotor (ref. 27).

Coleman (ref. 27) developed the theory of ground resonance stability for rotors with three or more blades (fig. 7), on symmetric or asymmetric support, including the effects of damping. "Of the large number of degrees of freedom of a hinged rotor, the important ones for the present problem have been found to be hinge deflection of the blades in the plane of rotation and horizontal deflections of the pylon. Other degrees of freedom, such as the flapping hinge motion of the blades, the bending or torsion of the blades, and the torsion of the drive shaft, are considered unimportant in the problem of self-excited oscillations." By using "special linear combinations of the hinge deflections" in the fixed-reference frame (equivalent to multiblade coordinates), equations with constant coefficients were obtained, and only the first-harmonic coordinates of the lag motion were coupled with the pylon motion. "The physical meaning of this partial separation of variables is that ... involves a motion of the common center of mass of the blades and, thus, a coupling effect with the pylon." Introducing these new coordinates was a crucial step, enabling a practical mathematical solution for ground resonance stability. Complex combinations of the pylon degrees of freedom and the lag-hinge degrees of freedom reduced the number of equations from four to two. The case of no damping reduces to a single equation that is a quadratic function of the rotor speed, for an assumed value of the whirl frequency (eigenvalue). The resulting plot of lag and body mode frequencies as a function of rotor speed is the Coleman diagram (fig. 8), in which the absence of a solution at a rotor speed indicates instability. Coleman presented a method for finding the stability boundary in the presence of damping, by

assuming purely imaginary eigenvalue and plotting the solutions of the real and imaginary parts of the characteristic equation (fig. 9). The solutions of the real and imaginary parts intersect at the stability boundary.

Feingold and Coleman (refs. 29–30) extended the analysis for two-bladed rotors. In addition to the ground resonance instability, the shaft-critical vibration (1/rev lag frequency resonance, potentially unstable for rotors with only two blades) was examined. For symmetric support, the ground resonance equations for a two-bladed rotor can be analyzed in the rotating frame with constant coefficients. For the case of anisotropic support (ref. 30), "the mathematical treatment of this case is considerably more

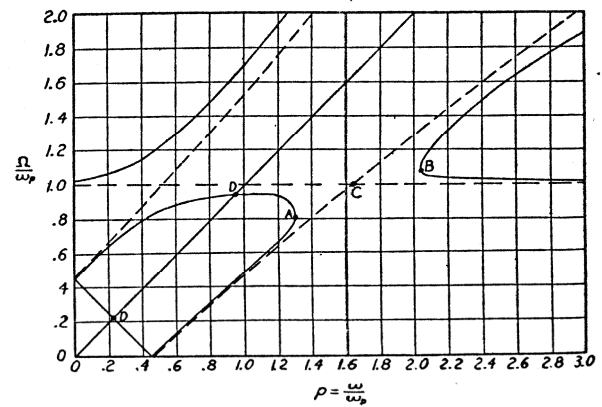


Figure 8. Coleman diagram: whirl frequency for neutral stability as a function of rotor speed, zero damping (ref. 38).

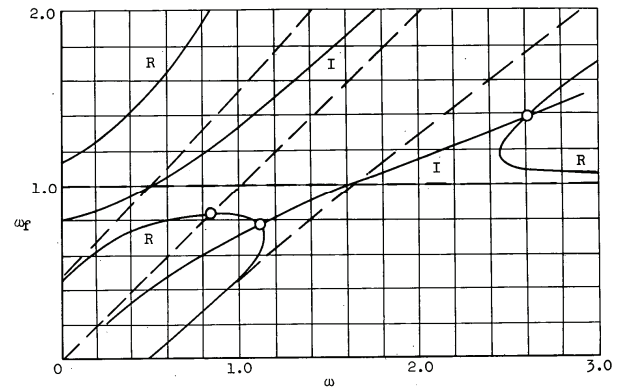


Figure 9. Solution of real and imaginary equations of ground resonance, for articulated rotor (lag frequency $v_{\zeta}^2 = 0.22 + (0.265\Omega)^2$) on symmetric support; frequency (in fixed system) as a function of rotor speed, both normalized by the support frequency (ref. 27).

complicated than the other cases because of the occurrence of differential equations with periodic coefficients. The characteristic frequencies are obtained from an infinite-order determinant." A consequence of the periodic coefficients is "the existence of an infinite number of instability ranges which occurred at low rotor speeds."

Deutsch (ref. 38) discussed ground resonance "with emphasis on practical considerations." This paper was a summary of his work since the early 1940s. He started from Coleman's draft ARR of July 1942, and extended it for anisotropic supports (ref. 39). Based on Coleman's analysis (ref. 27), "the results are stated in terms of simple formulas for the center of the range of instability, the critical speeds for resonance, and the damping required for the elimination of the range of instability." Deutsch obtained the simple result that at the rotor speed for resonance, $\Omega = \omega_x / (1 - \nu_\zeta)$, the damping required for stability is (in modern notation)

$$C_\zeta C_x > \omega_x^2 \frac{N}{2} \frac{1 - \nu_\zeta}{\nu_\zeta} S_\zeta^2$$

for isotropic support, and half that value for anisotropic support. Here C_ζ and C_x are the lag hinge and support damping, respectively; ω_x is the support mode frequency; N is the number of blades; ν_ζ is the lag mode frequency (per rev); and S_ζ is the first moment of inertia of the blade about the lag hinge. Deutsch concluded with a discussion of "practical considerations in the design of the landing gear and blade dampers," including friction, viscous and hydraulic dampers, and recommendations for test procedures.

Henrich Focke (ref. 40) described the phenomenon of ground resonance and discussed dealing with the problem as part of the development of the F61. At Focke's plant, his team investigated the problem analytically and, to prove that the air forces are negligible, conducted a full-scale test with circular steel arms replacing the rotor blades. No theoretical development is presented, but figure 10 (figure 15 of reference 40) makes it clear that the analysis was well developed. Evidently Focke was not aware of other ground resonance incidents and investigations, for reference 40 states: "We asked ourselves, why this oscillation never appeared on any of the numerous rotary-wing vehicles tested worldwide so far and why it was analytically investigated by his team for the first time" (translation by Berend van der Wall). The work by Focke's team on ground resonance must have occurred well before 1943 (the date of reference 40), but the theory was not published then or since. Enigmatically, a sketch similar to figure 10 occurs,

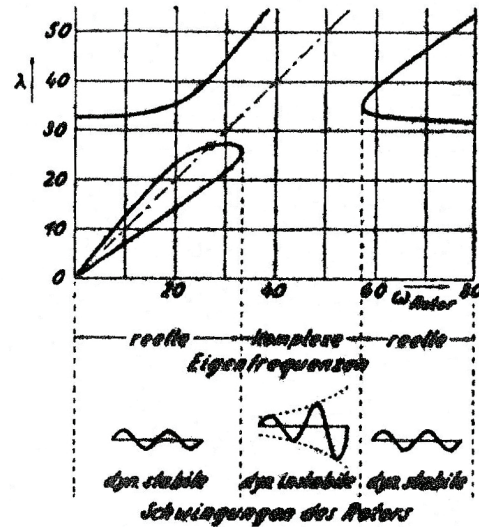


Figure 10. Rotor head and blade oscillation frequency diagram (ref. 40).

without discussion, in the notes of Prewitt's interview of Hohenemser (then with Flettner) in the summer of 1945 (ref. 41). It was Coleman's work that provided the foundation for future engineering treatment of ground resonance on helicopters.

AEROMECHANICS BOOKS

A large number of books on helicopter aeromechanics have been published since the 1940s. The most notable of these is "The Aerodynamics of the Helicopter" by Alfred Gessow and Garry C. Myers, Jr. (ref. 42). It was one of the first expositions of helicopter engineering, although preceded by Nikolsky's book (ref. 43) and a couple of others. As stated in the preface:

"This book was written as a text for senior and graduate engineering students and engineers in the helicopter industry who are interested in obtaining a more thorough understanding of the rudiments of helicopter aerodynamics. ... The vast background of experimental and theoretical rotor work (comprising over seventy published papers) done by the NACA during the past fifteen years, served as a sound basis for the aerodynamic material developed in the book."

There are several reasons for the lasting value of this book by Gessow and Myers: it is a report of the excellent NACA research on autogyros and helicopters; it is a concise introduction to helicopter aerodynamics (343 pages and only 1/2-inch thick in the original format); and

it has been continuously in print, first from The Macmillan Company (1952), then from Frederick Unger Publishing Co. (1967), and today from College Park Press (1999).

In his review of the book upon its publication in England (ref. 44), Bennett wrote:

“The two authors, having had a background of experience in helicopter work at Langley Field, are well qualified to present an abridged version of N.A.C.A. literature on the subject. The physical principles are discussed with the utmost clarity, lengthy mathematical derivations being omitted. ... The textbook is a great contribution to helicopter literature and is recommended to all who are interested in the physical principles of rotary-wing aircraft and in the fundamentals of helicopter aerodynamics.”

UNSTEADY AERODYNAMICS

The extension of wing unsteady aerodynamic theory to a rotor blade was accomplished by Loewy (ref. 45). After blade load problems were encountered on the Hughes XH-17 Sky Crane, the Cornell Aeronautical Laboratory (CAL) conducted a research program involving vibratory rotor blade bending (refs. 46–47). In research at CAL on rotor blade flutter, good predictions of test results were achieved except at low collective, where measured frequency and damping were not predicted using either quasistatic or unsteady airfoil theory. Robert G. Loewy was at CAL during 1949–1952 and 1954–1957. While getting a master’s degree at Massachusetts Institute of Technology (MIT) in 1948, working with Rene Miller, Loewy had taken classes in rotorcraft and in Theodorsen’s unsteady airfoil theory, so he was well prepared to undertake an analysis of rotor blade unsteady aerodynamics.

Loewy chose to focus initially on “taking into consideration the influence of vorticity which has been shed and *blown below the rotor disc* and which must be passed over by succeeding blades and/or in succeeding revolutions,” leaving three-dimensional aspects of the aerodynamics to future work. Thus, (ref. 45):

“A two-dimensionalized model is postulated for the representation of the aerodynamics of an oscillating rotary wing airfoil operating at low inflow; forward speed effects are neglected. The resulting unsteady integral downwash equation leads to an equation for pressure distribution

identical in form to that of classical fixed-wing flutter, but with a modified lift deficiency function. ... Theodorsen’s function of reduced frequency, $C(k)$, is modified to include the effects of the number of blades in the rotor, the ratio of oscillatory frequency to rotational frequency, and the inflow ratio. ... These effects (1) reduce the flap damping significantly at integer values of the ratio of oscillatory frequency to rotational frequency, and (2) make single degree of freedom pitch instability possible.”

The development of the two-dimensional model of the wake of a rotor hovering or in vertical flight is illustrated in figure 11. When the inflow “is very small, all the sheets of shed vorticity tend to pile up on each other, and the effect of that vorticity close to the blade in question (shed by the several previous blades and/or in the several previous revolutions) is of more importance than that which exists beyond a still smaller azimuth angle on either side of the blade” (fig. 11(a) B). This “condition certainly occurs at blade-pitch angles near zero and is of prime importance in ‘wake-flutter.’” Then “in arriving at a model which is mathematically tractable, the assumption has been made that for the case of low inflows, only the vorticity contained within a small double azimuth angle straddling the blade is of real consequence” (fig. 11(b) a), so “the azimuthal angularity of shed vorticity with respect to the blade may be ignored,” and the wake sheets extended to infinity. The result is “a two-dimensional model of unsteady rotor aerodynamics for a single-bladed rotor operating at low inflows” (fig. 11(b) b), extended to multibladed rotors as shown in figure 11(c).

Following classical unsteady aerodynamic analysis of thin airfoils, the sole influence of the returning wake sheets is the Loewy lift deficiency function:

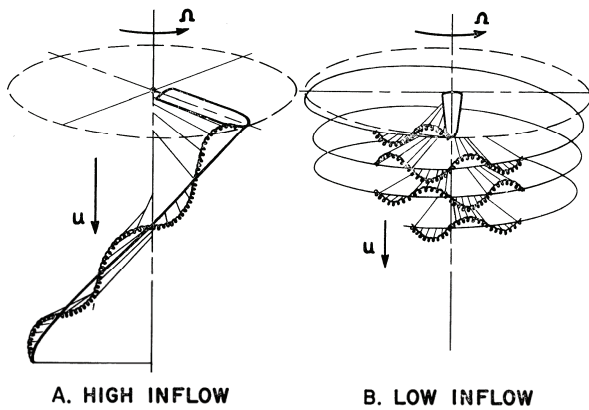
$$C'(k, m, h) = \frac{H_1^{(2)}(k) + 2J_1(k)W(kh, m)}{H_1^{(2)}(k) + iH_0^{(2)}(k) + 2[J_1(k) + iJ_0(k)]W(kh, m)}$$

a very pretty result. Here h is the vertical distance between successive rows of vorticity (fraction semi-chord), k is the reduced frequency, and the frequency ratio is $m = \omega/\Omega$ (fraction rotor speed Ω ; only the non-integer part of m is of consequence).

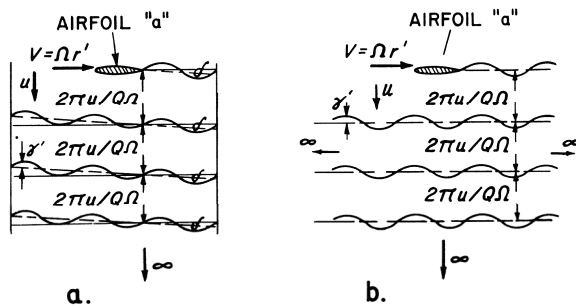
Loewy examined the implications of this lift deficiency function on blade pitch and flap damping. If the pitch axis is not at the quarter chord, “negative damping can exist when the oscillatory frequencies are certain close-to-integer multiples of the rotor speed.” Moreover, “flap-damping can go to very low (but positive) values at

integer values of the frequency ratio,” implying large resonant amplification factors.

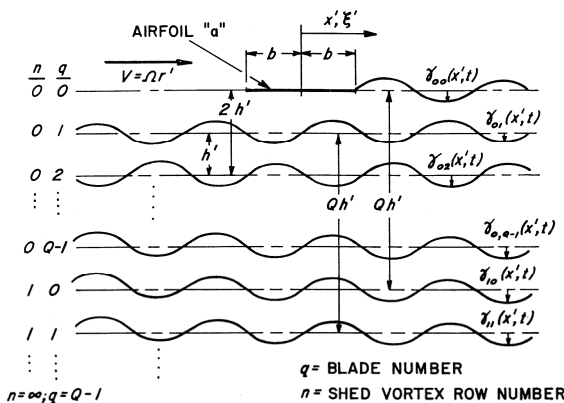
Loewy’s work formed the starting point for further development of unsteady aerodynamic theory for rotor blades, in particular, extensions to include trailed wake as well as shed wake, and forward flight as well as axial flow. With the shift of attention from frequency-domain to time-domain aerodynamic models, Loewy’s function remains a crucial test case for all new theories.



(a) Schematic representation of unsteady rotor flow fields.



(b) Two-dimensional models of unsteady rotor flow.



(c) Aerodynamic model for a multibladed rotor.

Figure 11. Loewy’s development of two-dimensional model for influence of returning shed wake (ref. 45).

Similar unsteady aerodynamic theories were developed by Timmen and van de Vooren (ref. 48), and by Jones (ref. 49). Loewy’s work was conducted during 1955 at CAL and presented at the IAS Annual Meeting in January 1956. The CAL work on rotor flutter was part of the motivation of both references 48 and 49. Timman and van de Vooren (ref. 48) considered the limit of no vertical convection, with all shed sheets in the plane of the airfoil. They performed two degree-of-freedom flutter calculations, including comparisons with experiment. They submitted the paper to the Journal of Aeronautical Sciences in June 1956, citing an Nationaal Luchtvaartlaboratorium of The Netherlands (N.L.L.) report of 1956 by Timman, and remark: “Since this paper was submitted, the authors have become aware of R. G. Loewy’s solution of the same problem by a different analysis [ref. 45]. Loewy’s results for the aerodynamic forces when $h = 0$ (no flow through the rotor plane) agree completely with ours.” In the paper by Jones (ref. 49) “an approximate theory is described which takes into account the influence of the wake on the aerodynamic derivatives of an oscillating rotor blade.” Jones considered the same two-dimensional aerodynamic model as Loewy, but did not quite obtain Loewy’s pretty result for the lift deficiency function. Jones submitted the paper to the Journal of Aeronautical Sciences in October 1957, and remarked: “The material in this paper is based on a report submitted to the Department of Scientific and Industrial Research in June 1954, which was later extended and circulated as A.R.C. Report 18,173, in January 1956.”

Loewy’s aerodynamic theory was verified experimentally through tests at CAL (refs. 50–51), at MIT (ref. 52), and at NACA Langley Research Center (ref. 53).

Daughaday, DuWaldt, and Gates (refs. 50–51) conducted a test of a one-bladed, teetering model rotor, varying the mass characteristics, pitch spring, and pitch-flap coupling. Using excitation through a moment at the flap hinge, forced response was measured and damping obtained from the free decay. For the damping of the first bending mode in hover, a reduction of damping ratio when the frequency was near 3/rev was observed experimentally and predicted using Loewy’s theory (fig. 12). This wake effect was significant at zero collective, but reduced for 4 degrees collective. The second bending mode damping was reduced near 7/rev and 8/rev. Pitch-flap flutter was investigated for a two-bladed rotor with 63.4 degrees of pitch-flap coupling, varying rotor speed and blade chordwise center-of-gravity position. A stabilizing effect of the returning wake was observed for pitch mode frequency near 2/rev, and predicted using Loewy’s theory (fig. 13).

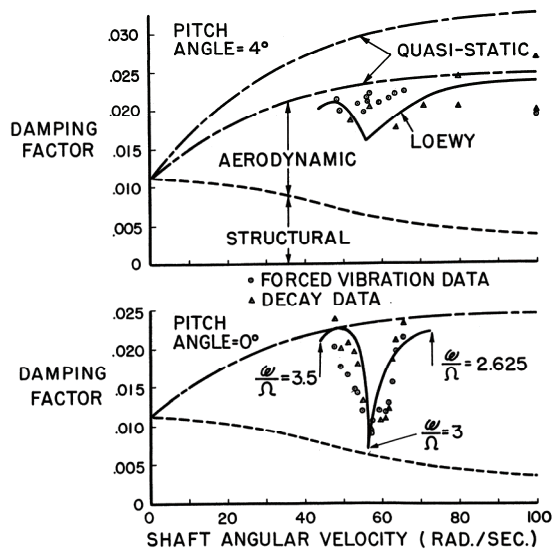


Figure 12. Bending mode damping (ref. 51).

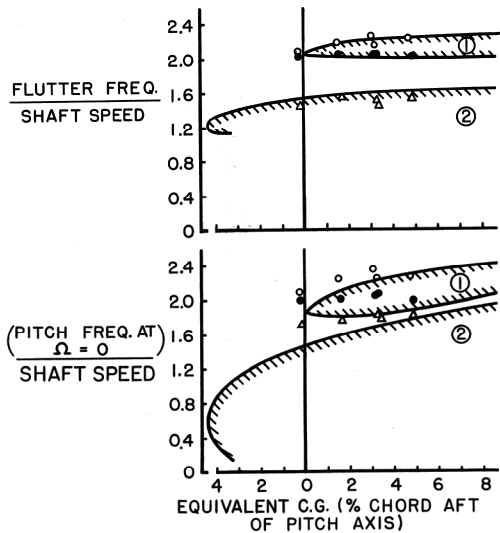


Figure 13. Pitch-flap flutter (ref. 51).

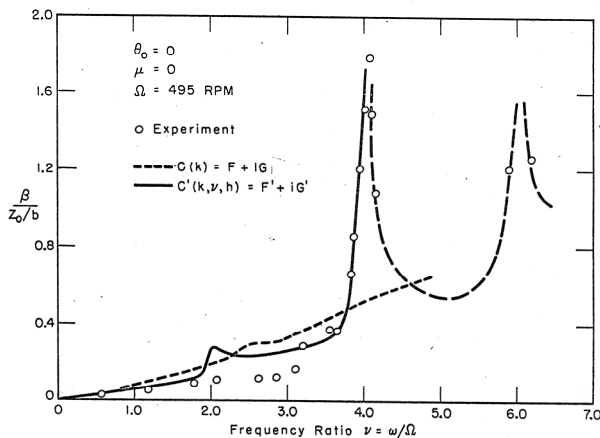


Figure 14. Flap response to vertical hub excitation (ref. 52).

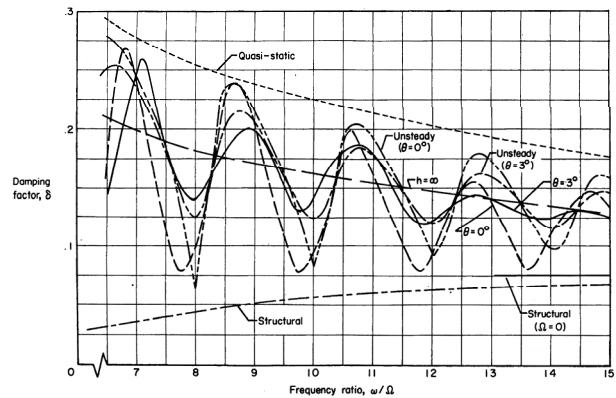
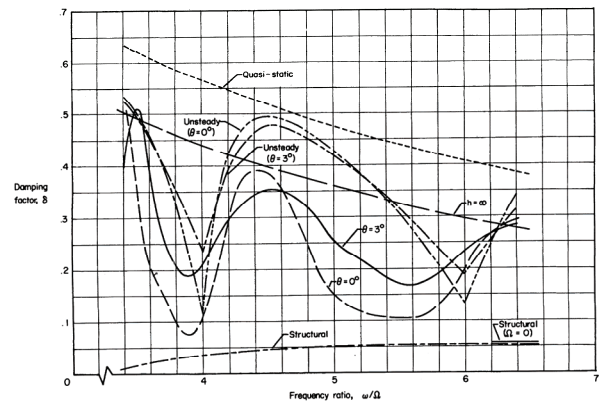


Figure 15. Damping of second (top) and third (bottom) flap bending modes (ref. 53).

Ham, Moser, and Zvara (ref. 52) measured blade flap response to collective pitch and to vertical hub motion on a two-bladed articulated rotor model with rectangular, untwisted blades. At low blade pitch, significant effects of the returning shed wake were observed for excitation frequencies near an integer. In the hover flap response to collective, for zero mean collective, the magnitude of the response was nearly quasistatic (good prediction using $C = 1$) except near $2/\text{rev}$, where the reduced magnitude observed experimentally was predicted using Loewy's C' . The phase was nearly quasistatic at low frequency, with significant phase shift above $1.5/\text{rev}$, predicted using Loewy's function. In the hover flap response to vertical hub motion, for zero collective, a large increase in the magnitude was observed experimentally at frequencies near a multiple of $2/\text{rev}$, predicted using Loewy's C' (fig. 14). At collectives of 5 and 10 degrees in hover, the measured response was reduced. Forward flight ($\mu = 0.1$ and 0.2) produced little effect on the measured response to hub motion for zero collective.

Silveira and Brooks (ref. 53) tested two-bladed teetering and articulated rotors in hover, for collective pitch angles

of 0 and 3 degrees. For the teetering rotor, the flap bending modes were excited by vertical motion of the hub, then the damping obtained from free decay. The measured damping of the second and third elastic flap modes exhibited a reduction in damping at multiples of 2/rev (fig. 15), which was successfully predicting using the real part of Loewy's function, $F'(k,m,h)$.

DIGITAL COMPUTERS

The availability of practical digital computers had a critical impact on the development of rotorcraft aeromechanics, far greater than the impact on the engineering for fixed-wing aircraft. Rotation makes all the problems harder. Important problems that for fixed-wing aircraft can be attacked analytically or with simple numerical methods, cannot be handled successfully for rotary wings.

Wakes are more important for rotor blades, which must fly over the vorticity from preceding blades, and the wake filaments are helices instead of straight lines. Rotorcraft systems are described not by time-invariant equations, but by equations with periodic coefficients and periodic steady-state solutions. Rotor blades move, and even low-frequency models require representation of the rotor states in addition to aircraft states. Blades can be modeled by beam theory but with small, yet important, nonlinearities. All of these difficulties were waiting for the engineer with a digital computer.

The computer changed the way problems would be formulated and solved. Before the computer, there were extensive analytical developments with results in tabular or graphic form. After the computer, detailed theoretical models with numerical solutions for specific cases became possible. Typically, the first applications of the computer were to generate bigger tables and graphs based on more elaborate models, but soon more engineers had access to the machines and dedicated solutions became practical.

For example, the succession of efforts following Glauert's work dealt primarily with refinement of the estimate of profile power, while still using Glauert's momentum theory for the induced power. The work on wakes focused on calculating the flow field using actuator disk models. The digital computer was needed in order to attack induced velocity and induced power calculation using detailed aerodynamic models. Even today, rotary-wing aeromechanics finds immediate use for every advance in computer speed and capacity.

High-speed digital computers first became available to industry and government laboratories for use in engineering calculations during the early 1960s.

AIRLOADS AND WAKES

Computation of harmonic airloading on a helicopter rotor blade in forward flight was accomplished by Rene Miller of MIT (refs. 54–62), and Raymond A. Piziali and Frank A. DuWaldt of CAL (refs. 63–68). Miller (refs. 54–55) described the problem:

“The determination of the air loads acting on rotor blades in forward flight presents an interesting and challenging problem in applied aerodynamics. Of particular importance for design purposes are the oscillatory components of this loading occurring at harmonics of the rotor speed. Unlike a wing, the trailing and shed vortex system of the blade generates a spiral wake that returns close to the blade. Because of its close proximity to the blade, the wake cannot be considered as rigid. Also, since the resulting loads are highly time-dependent, unsteady aerodynamic effects become important. ...

The oscillatory air loads occurring at harmonics of the rotor speed are the primary source of the blade stresses that establish the fatigue life of the structure and of the periodic hub loads that determine the fuselage vibration level. ...

The higher harmonic components of the air loading must, therefore, arise primarily from a nonuniform downwash at the rotor disk generated by the rotor wake. Their analytical determination requires some means of computing this downwash which takes into account both the spiral wake geometry, its effects on the individual blades, and the unsteady aerodynamic effects associated with the blade passage through this variable velocity field.”

With a uniform or linear inflow distribution, the predicted harmonic blade loading is of the order μ^n (where n is the harmonic number), in contrast to the large fifth or sixth harmonics that are measured in certain flight states such as transition or flare. This large harmonic loading is the source of the roughness and noise associated with such flight states, and is due primarily to the wake-induced velocities. The work at MIT and CAL was the extension of nonrotating wing and two-dimensional airfoil unsteady aerodynamic theory to the complicated wake of the

helicopter rotor in forward flight, made possible by the digital computer. Developing wake models for rotor nonuniform inflow calculations continues today, but the work started with Miller.

Miller

Miller relates (ref. 57) that experimental work at MIT in the 1950s (such as references 69–70) made clear the importance of unsteady aerodynamics for rotor blades:

“The tests ... clearly indicated the need for an analytical tool for computing blade downwash velocities which would take into account the individual blade wake geometry and also introduce the effects of unsteady aerodynamics. Attempts to obtain a closed form solution to this problem, or one based on tabulated integrals, were not successful and it was evident that extensive computer facilities would be required to explore this problem and, hopefully, to provide a basis for obtaining simplified solutions suitable for engineering applications. In 1960 the availability of an IBM 709 computer at the MIT Computation Center and funds from a Carnegie grant permitted initiation of such a program.”

Miller’s first publication of this work was a 102-page IAS paper presented in January 1962 (ref. 54), later published as reference 55. The work was supported primarily by the Department of the Navy. In October 1963, Miller delivered the Cierva Memorial Lecture to the RAS; this lecture was the basis for reference 58.

The rotor model consisted of a sheet of distributed vorticity for the blade, and a wake of shed and trailed vorticity. “Obviously the trailing wake does not disappear to infinity but returns underneath the rotor in a spiral form and the very nature of this spiral prevents the development of simple solutions for the downwash w_1 which it induces at the blade” (ref. 56). From reference 58:

“It becomes possible to discuss the physics of rotor aerodynamic loading in fairly simple terms. The primary element is the steady rotor lift generated by the bound circulation on the rotor blades. This bound circulation, as it leaves the blades, generates a spiral vortex system in the wake of constant strength dependent only on mean rotor thrust. The vertical component of induced velocity generated by this vortex system at a point on the blade, when combined with the horizontal velocity at the blade due to the blade rotation and forward speed, determines the induced angle. ... As might be expected, it is far

from uniform over the disc. Consequently the blade is subjected to a constantly varying induced angle as it rotates and this is the primary source of the higher harmonic blade loading. ...

These vortices are swept back relative to the rotor by the forward speed and consequently a blade, as it advances towards the leading edge of the rotor must pass over a series of vortices generated by itself and the other blades [fig. 16]. Similarly in returning towards the trailing edge it must re-pass over this system of vortices. Consequently any point on the blade will experience a fairly abrupt change in downwash on the advancing and retreating sides of the rotor and this is a primary source of rotor vibration.”

The concept of a “semirigid” wake was introduced (ref. 55): “Every element of vorticity will be assumed to retain the instantaneous vertical velocity imparted to it at the moment it was shed or trailed. This establishes a spiral wake descending at every spanwise station with a constant velocity in time but permits different vertical velocities azimuthwise.” The Biot-Savart law gave the induced velocity increment caused by trailed vorticity (from radial change in bound circulation) simplified to the case of a lifting line in which the variation over the chord is neglected. Based on computations that indicated the circulation was substantially constant over at least the outer 50% of the blade span (ref. 58), usually the trailing wake was assumed to consist of a single tip vortex, plus another vortex of equal strength located somewhat inboard of 50% span. It was necessary to integrate from the blade to infinity down the spiral, initially accomplished with numerical integration. The Biot-Savart law gave the induced velocity increment caused by shed vorticity (from azimuthal change in bound circulation), but here the chordwise variation was needed. From reference 58:

“Computations of air loads is complicated by the existence of singularities in the solution. These occur as the shed wake approaches the trailing edge of the rotor and whenever the blade passes through a trailing vortex line generated by itself or another blade. The treatment of the singularities and of the nonuniform flow field presents no basic problem providing lifting surface theory is used. However, this requires the numerical evaluation of the downwash at several chordwise as well as spanwise stations and hence, usually involves a prohibitive amount of machine computation time. Approximate

methods have therefore been used to evaluate the unsteady aerodynamic effects. ...

One of the most troublesome of the singularities is that associated with a shed vortex approaching the blade. In the simplest solution for the blade air loads it is convenient to replace the blade by a single vortex line and normally the high aspect ratio of conventional rotors would suggest that this is a reasonable approach.”

The initial approach was to develop a combined analytical and numerical procedure (ref. 54):

“The rotor wake will be divided up into a “near” wake and a “far” wake, the near wake including that portion attached to the blade and extending approximately one-quarter quadrant from the blade trailing edge. ... The chordwise variations in the velocity w induced at the airfoil by the far wake will be neglected. This is equivalent to using lifting-line theory when computing the effects of the far wake on the airfoil bound circulation and lift. ... The lifting-line approximation will also be used for the near trailing wake, an approximation that is clearly justified for the high “aspect ratios” of rotors and rotor/propellers. The near shed wake will be treated using analytical techniques and lifting surface theory.”

Thus, (ref. 58) “the near wake was treated using techniques similar to classical two-dimensional theory. However, the computational sequences for such a combined analytical and digital solution are clumsy and not well suited to machine computational techniques.” In reference 56, a simpler method was developed in which the induced velocity was calculated at a single point on the airfoil chord, but only using the shed wake up to a distance $\varepsilon(c/2)$ behind the collocation point. Considering two-dimensional unsteady airfoil theory, “ ε was chosen so that the lift deficiency and phase shift predicted by the simple lifting line theory developed above would be the same as that predicted by the equivalent lifting surface theory” (ref. 58). The result was $\varepsilon \cong 0.5$ for low reduced frequency. Then the wake analysis was entirely numerical, with no analytical part.

Miller’s results included analytical work to support the assumptions and simplifications (ref. 55). A two-dimensional solution for a hovering rotor was developed to obtain Loewy’s results using a lifting line approximation for the far wake. A three-dimensional

solution for vertical flight was developed from vortex theory for an unsteady actuator disk.

Three-dimensional solutions for forward flight were obtained by numerical integration on a high-speed digital computer. In reference 55, the calculated inflow was compared with the measured airloads of Falabella and Meyer (ref. 69), interpreted as a measured downwash. In reference 58, comparisons were made with the measured airloads of Rabbott and Churchill (ref. 71), and the flight test data of Scheiman (ref. 72):

“More recent experimental data, however, have supported the prediction of these abrupt changes in downwash near the 90° and 270° azimuth positions. In particular, flight test data obtained on a four-bladed rotor by NASA [ref. 72] are compared in [fig. 17] with the loads computed in the manner described above. The abrupt change in load near the 90° azimuth is almost impulsive in nature and will have a high harmonic content. ... The computations of [ref. 54] indicated that this abrupt load change is largely dominated by the vortex generated by the immediately preceding blade.”

Professor Miller acknowledged the assistance of his student, Michael P. Scully, in preparing reference 58. Scully, who started working for Miller in September 1963, carried the research forward, dealing in reference 60 with the efficiency of the wake model:

“The original solution for the induced velocity in forward flight due to the trailing wake used numerical integration down the spiral wake [ref. 55]. This method required small interval sizes (typically 7.5° in azimuth), and hence, large amounts of computer time to get accurate results. A solution was also developed [ref. 58] where the spiral wake is replaced by a set of infinite straight line vortices (for which the induced velocity is known) placed tangent to the spiral at every point where the spiral passes under a blade during the first turn of the spiral. This solution is 20 times as fast as the numerical integration solution; however, it is less accurate. ...

Finite Straight Line (FSL): This solution replaces the spiral vortex trailing wake with a series of straight line segments [see figure 18]. Originally, it was intended to take shorter line segments in the vicinity of nearest points and longer segments elsewhere. Due to the considerable amount of

computer time involved in finding all the nearest points, however, a solution using a constant $\Delta\phi$ (change in azimuth angle) per line segment proved to be faster for equivalent accuracy.

Since FSL is approximately six times as fast as the numerical integration method for equivalent accuracy, it has been adopted as the normal method of calculating induced velocities. It is even used for distorted wake cases where the trailing wake is not a perfect spiral (skewed helix) but some more general shape.”

Thus, Scully’s attention turned to free-wake geometry calculations (refs. 61–62).

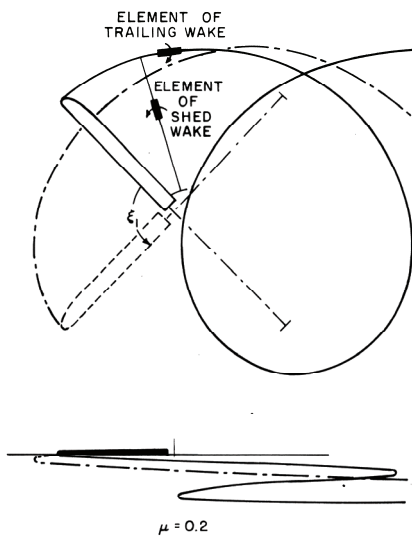


Figure 16. Wake geometry showing trailing tip vortex and element of shed wake (ref. 58).

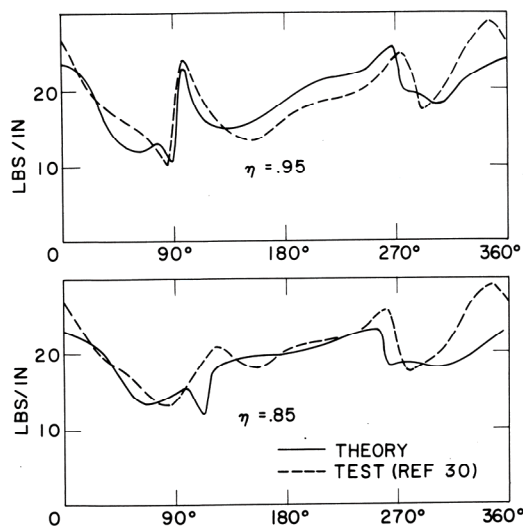


Figure 17. Comparison of computed and experimental air loads; H-34 flight test at $\mu = 0.2$ (ref. 58).

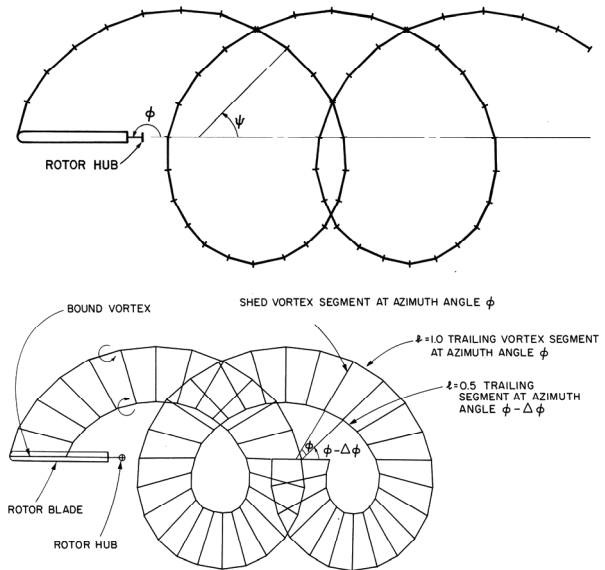


Figure 18. Finite straight-line approximation (refs. 61–62).

Piziali and DuWaldt

The work by Piziali and DuWaldt was motivated in part by flight test experience with high-oscillatory blade loads, attributed to nonuniform inflow velocities at blades (ref. 46). The CAL project was sponsored by the U.S. Army. The initial phase was conducted from September 1960 to April 1962 (ref. 63), and published as a Transportation Research Command (TCREC) report in November 1962. The work was performed largely by Raymond A. Piziali, who joined CAL in 1957. Frank DuWaldt was the group leader and Walt Targoff the division chief at the time. Targoff’s contributions were acknowledged in reference 63: “The form in which the problem was cast and the method of solution stem directly from his collaboration.” The final phase was from April 1964 to June 1965 (ref. 66). As summarized in reference 67:

“One of the most difficult problems in designing and developing a lifting rotor system is generally recognized to be the adequate prediction of the rotor performance, the blade stresses, and the pitch control settings when given only the blade and hub physical properties, the fuselage weight and aerodynamic coefficients, and the steady-state flight condition. Conceptually, the problem consists of the following three major aspects: (i) the rotor blade aerodynamic loads, (ii) the static and dynamic response of the blades, and (iii) the rotor-fuselage trim. These three aspects of the problem are closely inter-dependent and should all be included in a useful prediction method.”

References 63–65 concentrated on the aerodynamic aspect of the problem:

“Any accurate method of computing the airloads must adequately predict the wake-induced velocities at the blades because the airloads are strongly influenced by these velocities. However, because the vortical wake of the rotating wing is extremely complex and difficult to adequately represent mathematically, the practical solution of the aeroelastic problem has been delayed. Early attempts to solve this problem analytically were based on relatively drastic simplifications of the wake of the rotor to make them computationally feasible. The modern high-speed computing machines of today have made it possible to account for much more of the detail of the wake than has been possible in the past and thus permit an adequate aerodynamic representation of the blades and wake to be formulated which will enable accurate computation of the rotor airload distributions. The method of computing airloads developed in this investigation makes use of high-speed digital computation to retain much of the detail of the wake.”

Reference 67 added the blade motion solution:

“A numerical method is presented for solving the aeroelastic response problem of rotating wings in steady-state flight (hovering or translating). The method employs high-speed digital computation, is simple to use, and is relatively fast. It accounts for the shed and trailing vorticity of the wake of each blade in computing the induced velocities on the blades and satisfies the chordwise aerodynamic boundary condition for computation of the aerodynamic lift and pitching moments. The equations of motion for the blade flapping and flapwise bending degrees of freedom are included, and an iterative procedure is used which yields a simultaneous solution for the aerodynamic loads, the dynamic response and the bending moments experienced by the rotor blades.”

Reference 63 started with a vortex-lattice model of the wake (fig. 19):

“Each blade of the rotor is represented by a segmented lifting-line (bound vortex) located along the steady deflected position of the quarter-chord. ... In the wake, the shed and trailing

vorticity distributions of each blade are represented by a mesh of segmented vortex filaments; each segment is straight and of constant vortex strength. The segmented trailing vortex filaments emanate from each of the end points of the lifting-line segments. The segmented shed vortex filaments intersect the trailing filaments in a manner such that the end points of both are coincident.”

The Biot-Savart law gave the induced velocity at the collocation points (three-quarter chord) on the rotor disk. Simultaneous equations were formulated for the bound circulation at the collocation points, and an iterative solution implemented. It was observed (refs. 63 and 67) that the computed airloads were sensitive to the wake geometry: “To determine this exactly would require that the total induced velocities be computed throughout the wake for each instant of time and that the wake elements be moved according to their local induced velocities for each increment of time; such a procedure becomes computationally impractical, even on a high-speed digital computer” (ref. 65).

References 66–67 further developed the wake model (fig. 20), both for efficiency of computations and to improve the tip vortex representation:

“In the present representation, the azimuthal extent behind each blade of the grid of straight-line vortex filaments representing the shed and trailing vorticity distributions can be truncated where desired and the wake continued on as segmented rotor and/or tip trailing vortex filaments. ... This type of wake representation is believed to be a first order approximation to the actual wake which apparently rolls up very quickly into a tip vortex. ... Beyond the truncation of the wake grid, the root and/or tip trailing vortex strengths are made equal to the maximum value of the radial distribution of the bound vorticity on the blade in the azimuth position from which the elements were shed.”

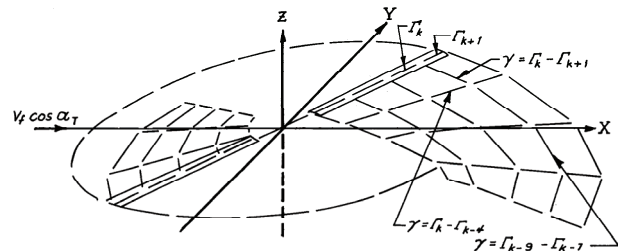


Figure 19. Pictorial example of the initial portion of the wake of a two-bladed rotor divided into four radial segments (ref. 63).

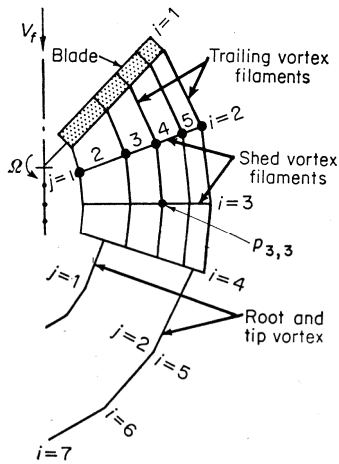


Figure 20. Example of wake configuration (ref. 67).

The early work did not deal with the issue of the near shed wake. From reference 65:

“It has been found conceptually convenient to view the aerodynamic loading aspect of the overall aeroelastic problem in the following manner: The wing and its “immediate” attached wake can be thought of as a “wing-wake system” for generating a force. ... The remainder of the wake, which is the returning wake of the wing and all the wake of the other wings in the rotor, and the motions of the wing are then thought of as providing the input to this system. ... In addition to having an adequate representation of the input source for the wing-wake system, a successful computational procedure must have an adequate representation of the wing-wake system itself. In the initial approach, the wing was represented by a single bound vortex at the quarter-chord, satisfying boundary conditions at the three-quarter-chord and the immediate wake was represented by a system of concentrated vortex filaments shed at equal increments of time. The major approximations involved in this initial approach are: (1) the boundary conditions are satisfied at only one point on the chord, and (2) the immediate wake is represented by concentrated vortices equally spaced in time from the trailing edge.”

In reference 67, “for the blade representation, the theory of two-dimensional unsteady thin airfoils has been used,” with the Biot-Savart law evaluation of wake-induced velocity along the chord, in terms of coefficients of a cosine series. The investigation dealt with the effects of discretization of the shed wake. From reference 67:

“In the wake representation of the earlier work, a segmented shed vortex was deposited in the flow at each azimuth position of the blade; thus the nearest shed vortex to the blade was behind it a distance proportional to the time it takes the blade to traverse one azimuthal increment. The adequacy of this representation of the wake shed vorticity was investigated by using it in a computational model to predict the lift and pitching moment transfer functions (for both the pitching and plunging cases) for a two-dimensional oscillating airfoil at zero mean angle of attack. The results were compared with the classical analytical solutions for this problem, and as expected, the agreement was not very good. A computational investigation of discrete shed wake representations was then conducted by use of this computational model for the two-dimensional oscillating wing problem. It was found that reasonable agreement could be obtained in the reduced frequency range of interest by using the equally spaced discrete shed vortex representation if the entire shed vortex wake were advanced, with respect to the blade producing it, a distance proportional to 70% of a time increment.”

In reference 68, Daughaday and Piziali developed a two-dimensional airfoil theory with a discretized wake model to match the Theodorsen solution, using a continuous sheet of vorticity for the shed wake directly behind the blade trailing edge. Figure 21 illustrates the two shed-wake models.

The calculated airloads were compared with data from a wind tunnel test of a NASA model rotor (ref. 71), flight test of an HU-1A helicopter (ref. 73), and flight test of an H-34 helicopter (ref. 74). Figures 22–24 illustrate the correlation. “The correlation of the computed and measured results is quite good, considering the sensitivity of the result to the blade natural frequencies and the prescribed wake configuration, and considering further that all the blade degrees of freedom and the rotor-fuselage trim constraints are not yet included” (ref. 67).

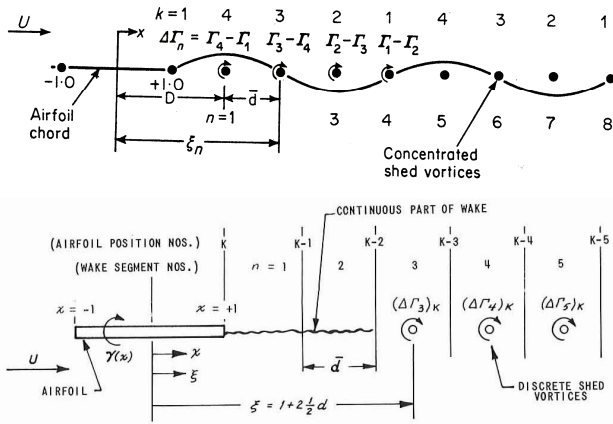


Figure 21. Near shed-wake models (refs. 67–68).

The analysis permitted important observations regarding the aerodynamic environment and performance of rotors. “It is interesting to note that the computed induced velocity distributions are always such as to oppose the retreating blade tip stall which has always been predicted on the basis of an assumed uniform inflow distribution” (ref. 63). Thus, (ref. 64):

“The calculations indicate, in general, that the effective aerodynamic angle of attack decreases with increasing radius over the outer half of the retreating blade and “tip stall” does not occur. The retreating blade tip will become stalled only when the inboard stalled region progresses outward to the tip. This is the result of the induced velocity distribution.”

Reference 64 also looked at the calculated induced drag of the blades: “Induced power calculated from the induced drag distributions was found to be more than three times that calculated on the assumption of a uniform induced velocity.”

Parallels

Miller and Piziali conducted their work largely independently, although each was aware of the other’s activities. Each described the work at the CAL/TRECOM meeting in June 1963 (refs. 57 and 65). Miller published first (ref. 54). Miller proceeded from unsteady airfoil theory and vortex theory to a discretized model of the vortex wake; Piziali took the reverse path. Both had to deal with the issue of the near shed wake. Both compared airload calculations with the recently available H-34 flight test data of Scheiman. As this research was initiated when

digital computers first became available, both Miller and Piziali had programmers to do the actual coding. Eventually, the engineers and students learned FORTRAN and took over the coding tasks. By the early 1970s, CAL was out of the helicopter research business, while Miller’s students went on to make further contributions to wake geometry and airloads modeling (refs. 62, 75, and 76).

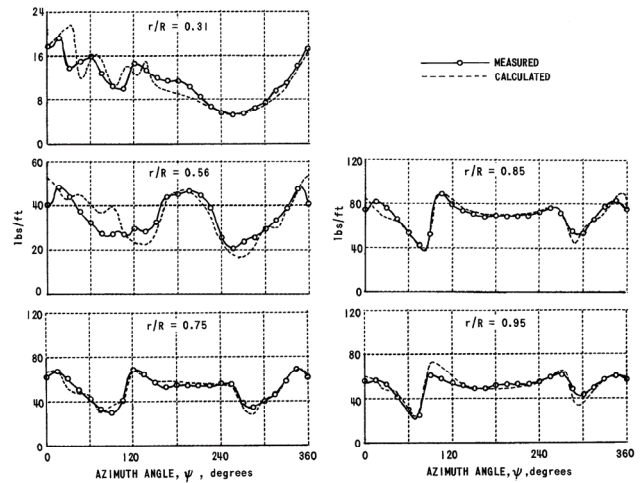


Figure 22. Azimuthal variation of airloads for NASA model rotor, $\mu = 0.15$ (ref. 64).

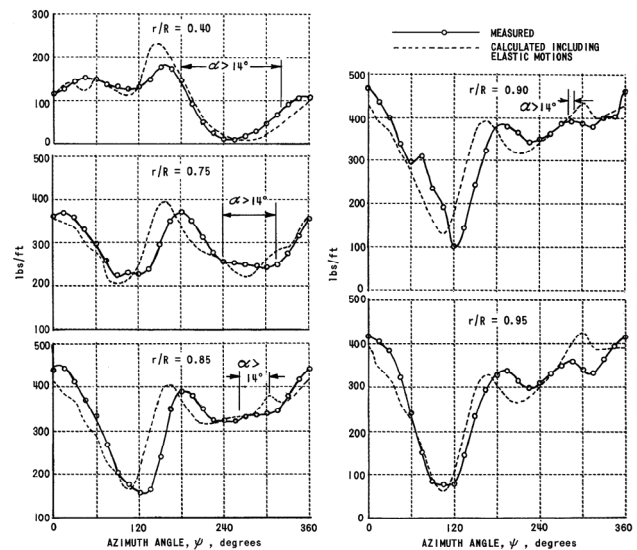


Figure 23. Azimuthal variation of airloads for HU-1A, $\mu = 0.26$ (ref. 64).

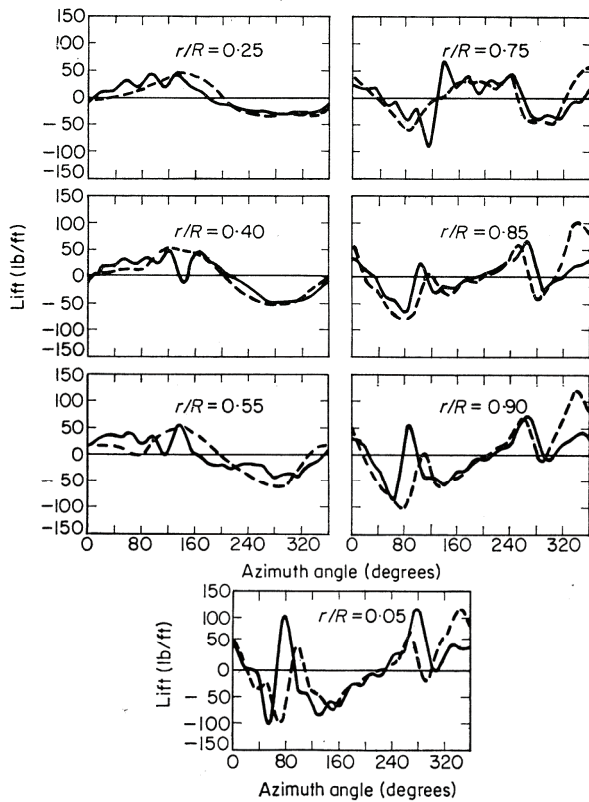


Figure 24. Measured and computed lift for H-34 at $\mu = 0.18$, mean removed; dashed line measured, solid line computed (ref. 67).

HOVER WAKE GEOMETRY

The fundamental character of the wake geometry of a hovering rotor was recognized by Robin B. Gray (refs. 77–78). Hover performance is a key to VTOL aircraft design, but theories of the time were based on simple, approximate wake models. Gray was a student of Professor Nikolsky at Princeton University, and as he recounted in his 1991 Nikolsky Lecture (ref. 79):

“Professor Nikolsky and I had tentatively agreed that my PhD research would be directed toward improving the performance prediction of a rotor in hovering flight by including blade number and wake contraction effects. ... The initial flow visualization studies were undertaken simply to determine the boundary of the rotor wake in hovering to provide some guidance in developing the analysis.”

In a report approved by A. A. Nikolsky, Gray stated (ref. 77):

“One of the major requirements which have always faced the engineer is that of predicting the blade aerodynamic loadings with some reasonable degree of accuracy. ...

It was then decided that perhaps a more vigorous application of the classical methods would yield worthwhile results even though it was expected that a great deal of numerical work would be involved. ...

A classical vortex theory was brought to bear on the problem. It is with this latter approach in conjunction with some flow visualization studies that this paper deals. ...

When it became apparent that the theoretical determination of the various constants that would appear in the analysis would be very difficult, it was decided to undertake the experimental program herein described.”

The flow visualization experiment involved high-speed photographs of the wake geometry of a model rotor. The wake was made visible by smoke (titanium tetrachloride) emanating from the blade tips. Initially, a two-bladed rotor was used (ref. 79), but Gray observed the overtaking of the tip vortex from one blade by that from the other. He attributed this behavior to differences in tip vortex strength caused by differences in blade thrust. To eliminate this interaction, a one-bladed rotor was used (ref. 79). The rotor had an untwisted, constant-chord blade, with a radius of four feet. Figure 25 is a typical photograph of the flow visualization, showing the tip vortices and inboard sheet. Forward flight tests were conducted using a truck inside the building constructed for the Princeton track facility (ref. 78).

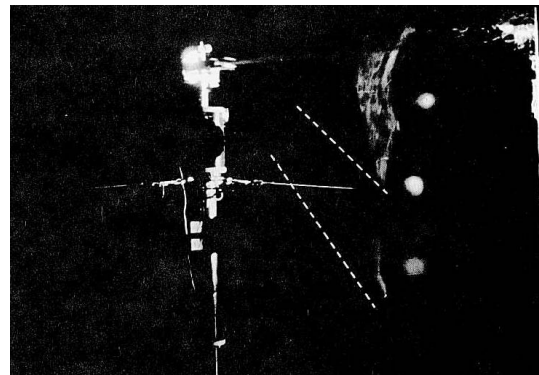


Figure 25. Fully developed wake. White dots are the tip vortex; the dashed lines show the approximate position of the vortex sheet (ref. 77).

“From these studies, the vortex model for the near wake of a single-bladed rotor was constructed” (ref. 79). Gray’s sketch of hovering rotor wake geometry (fig. 26) first appeared in reference 78. The flow visualization revealed that that tip vortex geometry could be described by an exponential contraction plus a two-stage vertical convection velocity (fig. 27). “The surprise was that the data could be fit with simple algebraic expressions involving six measured parameters” (ref. 79). The radial and axial coordinates of the tip vortex were

$$r = R(A + Be^{-\lambda_1 \psi} \sin \psi + Ce^{-\lambda_2 \psi})$$

$$Z = K_1 R \psi \quad \psi < 2\pi / b$$

$$Z = K_1 R(2\pi / b) + K_2 R(\psi - 2\pi / b) \quad \psi > 2\pi / b$$

where ψ is the wake age, and b is the number of blades. From the measured data, the variation of the parameters with rotor thrust was established.

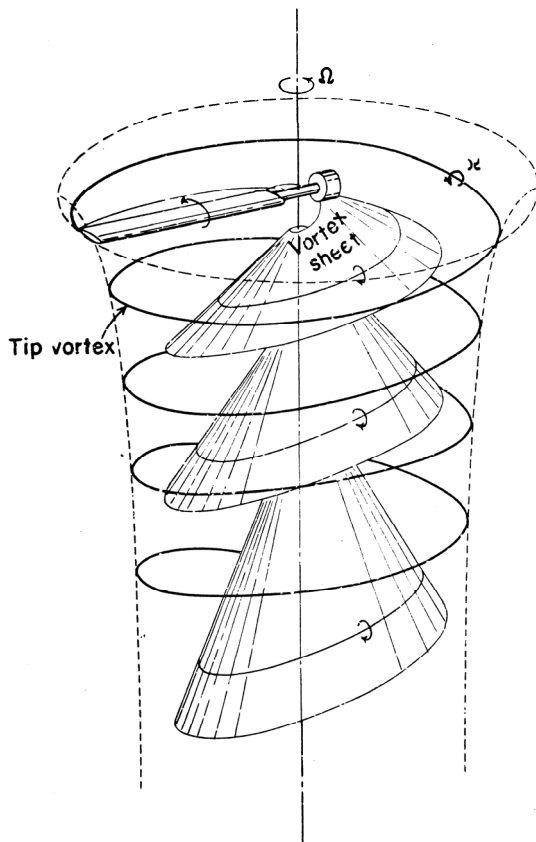


Figure 26. The vortex pattern in the wake of a single-bladed hovering helicopter rotor as obtained from smoke studies (ref. 78).

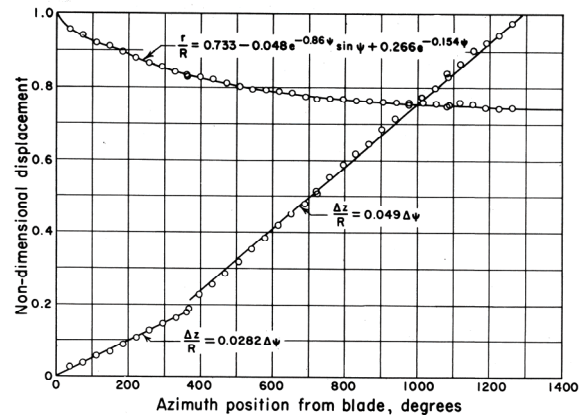


Figure 27. Nondimensional radial and vertical displacement of tip vortex as a function of azimuth position from blade (ref. 77).

Gray’s work was followed by more extensive flow visualization tests, which were used to establish prescribed wake geometry methods for hovering rotor performance calculation.

Landgrebe at United Technologies Research Center (UTRC) (refs. 80–81) conducted a flow visualization test and developed a prescribed wake geometry analysis:

“Systematic model rotor performance and wake geometry data were acquired to evaluate the influence of wake geometry on rotor hover performance.”

Figure 2 of reference 81 is Gray’s sketch of hover wake geometry. Landgrebe used externally generated smoke filaments to visualize the wake of a 2.2-foot-radius model rotor (fig. 28). The test matrix included a range of blade numbers (2 to 8), twist, blade-aspect ratio (13.6 to 18.2), and collective pitch. Landgrebe also notes the “discovery of a reduction in wake stability with increasing distance from the rotor.” Landgrebe described the structure of the wake (ref. 81):

“The wake contains two primary components. The first, and most prominent, is the strong tip vortex which arises from the rapid rolling up of the portion of the vortex sheet shed from the tip region of the blade. The second feature is the vortex sheet shed from the inboard section of the blade. The vertical or axial transport velocity near the outer end of the inboard vortex sheet is much greater than that of the tip vortex. The vertical velocity of the vortex sheet also increases with radial position, resulting in a substantially

linear cross section of the vortex sheet at any specific azimuth position. These characteristics largely result from the velocities induced by the strong tip vortex.”

From the flow visualization data, a generalized representation of the near-wake geometry was constructed. The form of the equations for contraction and convection followed Gray. Analytic expressions were developed for the variation of the wake geometry constants with C_T , C_T/σ , and twist, for the tip vortex and for the inboard and outboard edges of the wake sheet. Analyses based on this realistic wake geometry provided significantly improved prediction of rotor performance characteristics.

Kocurek and Tangler at Bell Helicopter (ref. 82) conducted a flow visualization test of a model rotor in hover, and developed a prescribed wake analysis method. The wake of a 1.0-foot-radius rotor was visualized with Schlieren techniques (fig. 29). The test matrix included a range of blade numbers (1 to 4) and blade-aspect ratio (7.1 to 18.2) beyond that of Landgrebe, specifically covering low-aspect-ratio, two-bladed rotors. The form of the equations for contraction and convection were the same as used by Landgrebe, but with different dependence on thrust and blade geometry.

Gray’s sketch of hovering rotor wake geometry remains the starting point for investigations of hovering rotor aerodynamics, and echoes of it are often seen (fig. 30). Modern flow measurement techniques confirm Gray’s description of the wake (fig. 31).

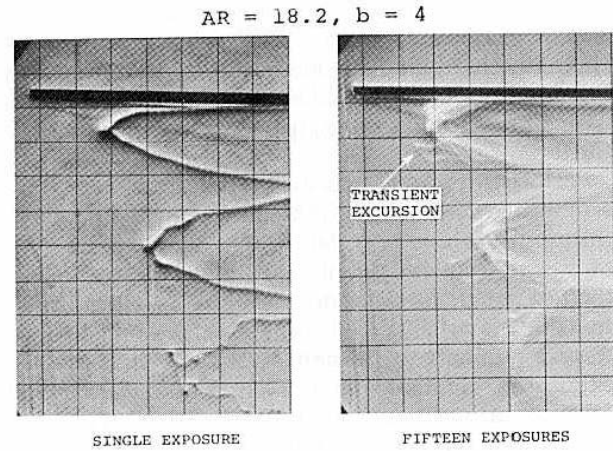


Figure 29. Kocurek and Tangler: single and multiple exposure schlieren photographs (ref. 82).

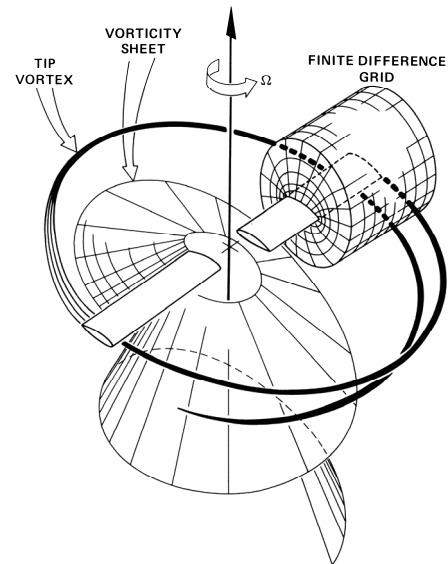


Figure 30. A rotor-wake system with an embedded finite-difference grid (ref. 83).

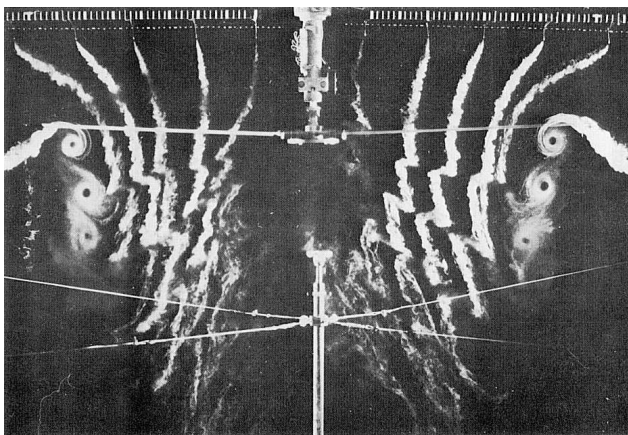


Figure 28. Landgrebe: sample flow visualization photograph (ref. 80).

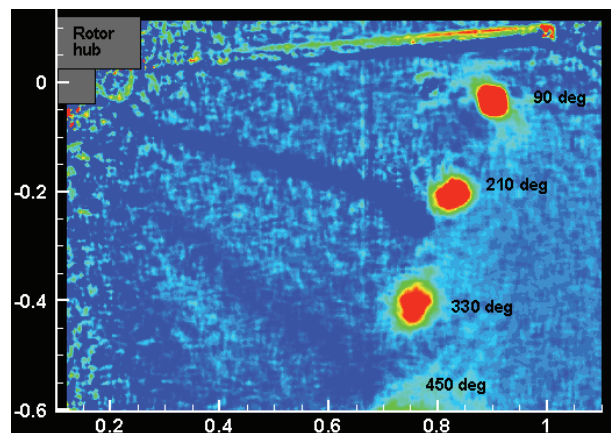


Figure 31. PIV measurement of hover wake geometry for untwisted blades (courtesy M. Ramasamy, ref. 84).

LATERAL FLAPPING

Test data for the definitive assessment of rotor wake models at low speed were obtained by Franklin D. Harris of Boeing (ref. 85). Glauert and Wheatley encountered discrepancies between calculated and measured lateral force or flapping, and attributed the difference to the simplified inflow model used. Introducing a longitudinal gradient of the inflow did improve the calculation. The capability to predict lateral flapping is needed to design the control system. Moreover, the inability to predict it implies something is seriously wrong with the analysis, as Cierva pointed out to Glauert (ref. 2).

In October 1970, as part of a wind tunnel investigation of a tandem helicopter, Frank Harris tested the aft rotor alone and measured lateral and longitudinal flapping angles for speed, thrust, and shaft angle variations at low speed. As it was a small rotor in a big wind tunnel (5.46-ft diameter in 20- by 20-ft tunnel; fig. 32), he took advantage of the opportunity to collect data on rotor behavior at very low advance ratio. He was interested in lateral flapping from previous experience trying (unsuccessfully) to predict pedal position on a tandem helicopter. There was contemporary interest because of pitch control issues on the XH-59A; because of the very stiff rotors required for the lift-offset rotor concept, longitudinal inflow gradients produce pitch moments rather than lateral flapping. Harris used the test data to assess the capability to predict lateral flapping using the wake models available at the time.

Figure 33 from reference 85 shows the lateral flapping as a function of advance ratio for fixed cyclic control, at constant thrust and shaft angle. The measured lateral flapping shows a large increase with speed, reaching a maximum value at $\mu = 0.08$, a behavior that was not predicted by simple inflow distributions, vortex theory, or rigid wake geometry models. In contrast, the longitudinal flapping angles are well predicted even with simple inflow models.

As suggested by Harris (ref. 85), a free-wake geometry analysis is required to satisfactorily calculate the lateral flapping. For example, figure 34 shows calculations obtained using Comprehensive Analytical Model of Rotorcraft Aerodynamics and Dynamics (CAMRAD) with Scully's free-wake geometry (ref. 61). Examination of the solution (ref. 86) identifies the blade-vortex interaction on the advancing and retreating sides of the rotor disk as the source of a large longitudinal inflow variation, the $1/\text{rev}$

component of which is responsible for a lateral flapping angle increment. Interaction with the rolled-up tip vortices produces large peak inflow values. The self-induced distortion of the wake moves the tip vortices close to the blades (much closer than suggested by rigid wake geometry), thereby increasing the strength of the blade-vortex interaction. Thus, a free-wake geometry calculation is needed to correctly calculate the lateral flapping as measured.

Harris's test provides a concise metric that characterizes the adequacy of a rotor wake model. Predicting his lateral flapping data requires a detailed representation of the vortex wake geometry and structure.

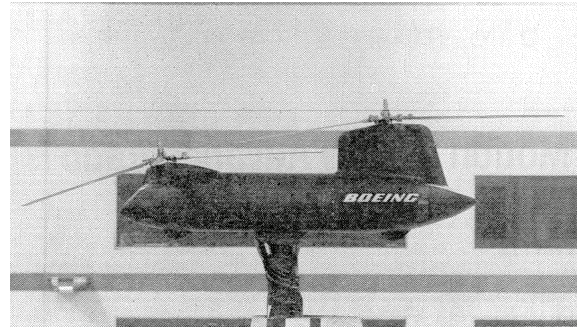


Figure 32. Vertol Division universal helicopter model (ref. 85).

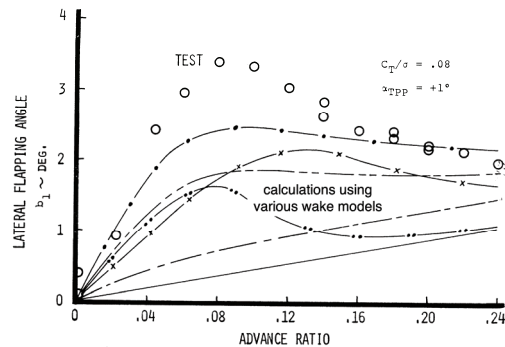


Figure 33. Measured rotor lateral flapping angle, compared with calculations using various wake models (ref. 85).

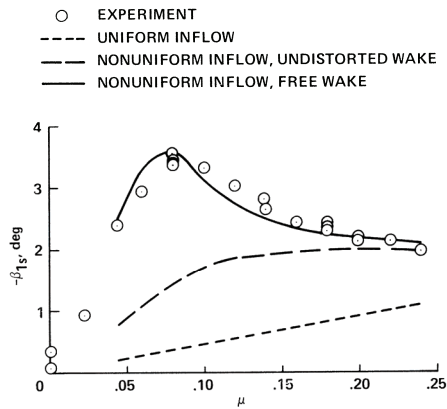


Figure 34. Calculation of lateral flapping angle using Scully’s free-wake geometry (ref. 86).

DYNAMIC INFLOW

The dynamic inflow model for the wake in unsteady rotor aerodynamics was developed by David A. Peters and Dale M. Pitt at Washington University (ref. 87). When I taught a short course on helicopters, I emphasized two crucial characteristics of rotor behavior: the blades move and wake effects are everywhere. The best representation for the wake is still a vortex model, but for stability analysis and real-time simulations a finite state model of the wake is needed. A dynamic inflow model is a set of first-order differential equations relating inflow variables and aerodynamic loading variables. The Pitt and Peters model consists of three states. The inflow variables describe the distribution of wake-induced velocity over the rotor disk: uniform (λ_0) plus linear (λ_c and λ_s). The loading variables are the integrated section lift of all blades: thrust C_T , pitch moment C_M , and roll moment C_L (aerodynamic contributions only). More than three decades of work was the foundation for reference 87.

Carpenter and Fridovich (ref. 88) examined rotor response to collective changes in hover, motivated by helicopter jump take-off maneuvers. They tested a three-bladed articulated rotor, measuring the transient thrust and flapping response. To predict the effect of a rapid blade-pitch increase, they extended momentum theory by adding a time lag:

$$T = m\dot{v} + 2\pi R^2 \rho v(v + V_v)$$

where v is the instantaneous induced velocity. Regarding the mass m :

“If the induced velocity is assumed to be uniform over the rotor disk, the initial flow field [for sudden increase in pitch angle] is exactly

analogous to the flow field produced by an impervious disk which is moved normal to its plane. The “apparent additional mass” of fluid associated with an accelerating impervious disk is given in [Munk, ref. 89] as 63.7 percent of the mass of fluid in the circumscribed sphere.”

In work originally published in 1958–1959, Rebont, Valensi, and Soulez-Lariviere (refs. 90–92) considered the response of hovering rotor thrust to collective pitch changes, making the distinction that their interest was descending flight (landing) and near autorotation, not take-off as in reference 88. They extended momentum theory “by adding an inertia term, $m\dot{X}U$ [U is the tip speed], where m represents the virtual mass associated with the disk, which may be assumed equal to that associated with a solid disk in nonuniform translation perpendicular to its plane.” (No doubt this read better in the original.) The model was verified by experiments.

Curtiss and Shupe (refs. 93–94) considered the influence of quasistatic inflow variation on hingeless rotor response, expressing the result as an effective Lock number. Essentially, this was a derivation of the static lift deficiency function, appearing in the Lock number by way of the lift-curve slope.

Ormiston and Peters (ref. 95) investigated the modeling requirements for accurate prediction of hingeless rotor response. An equivalent-hinge model of the hingeless blades was not satisfactory, instead the first two elastic flap bending modes were needed. “Simplified models of the nonuniform induced inflow were derived, using momentum and vortex theory, and found to be the most important factor in improving correlation with the data.” The inflow variables were the mean and 1/rev terms in a Fourier series, hence uniform along the blade for a given azimuth (not uniform plus linear over the disk). The three inflow variables were expressed as a linear combination of the rotor aerodynamic thrust and hub moment perturbations. For high advance ratio it was necessary to identify the inflow derivatives from the wind tunnel test data of hingeless rotor response, consisting of steady thrust and hub moment response to collective and cyclic pitch control (ref. 96). These identified derivatives exhibited anomalous behavior around $\mu = 0.8$.

Hohenemser and Crews (ref. 97) tested a two-bladed hingeless rotor in hover and at $\mu = 0.2$, measuring the blade flap response to cyclic pitch (stick stir). Crews, Hohenemser, and Ormiston (ref. 98) developed an analysis to predict this test data. Following reference 88, they introduced a time lag in the inflow model: $\lambda + \tau\dot{\lambda} = L(2\gamma/\sigma\alpha)C$, for the cosine and sine 1/rev

harmonics of the inflow (λ), in response to hub aerodynamic pitch and roll moments (C). For three-bladed rotors, the result is a lift deficiency function or effective Lock number that depends on excitation frequency. When appropriate values (dependent on collective) of τ and L were used, good prediction of the measured flap response was obtained (fig. 35). Banerjee, Crews, Hohenemser, and Yin (ref. 99) identified values of τ and L .

While the tests were conducted by measuring rotor frequency response, the analysis was no longer in the frequency domain (as with Theodorsen and Loewy), but rather finite state models in the time domain.

Peters (ref. 100) continued the investigation of modeling requirements for hingeless rotor response, using a dynamic rather than quasistatic inflow model, and comparing with frequency response as well as static measurements. Previous work was characterized: “Unfortunately, while some success has been achieved using simple models of the rotor induced flow in hover, a completely satisfactory induced flow model for forward flight has not been found, not even for the condition of steady response. In addition, neither the physical values of the induced flow time constants nor the frequency range in which they are important is known.” (The conclusions in reference 95 were less pessimistic.) The three-state dynamic inflow model was used, with inflow variables representing uniform and linear variation over the disk. Following reference 88, which obtained good agreement with transient thrust measurements, a time lag was included in the relation between inflow and loading variables. “An approximation to the apparent mass terms of a lifting rotor can be made in terms of the reaction forces (or moments) on an impermeable disk which is instantaneously accelerated (or rotated) in still air.” These apparent mass values were obtained from reference 101. The resulting nondimensional constants ($\tau = K_m / 2v$ for uniform variable, $\tau = 2K_l / v$ for linear first-harmonic variables) were $K_m = 8/3\pi$ and $K_l = 16/45\pi$; the latter agreeing with the identified τ value of reference 98. Good agreement with hingeless rotor response measurements was obtained using inflow/loading derivatives from momentum theory for hover and from the empirical model of reference 95 for forward flight. The reliance on an identified, empirical model for the derivatives was not satisfactory.

As Peters recounted in his 2008 Nikolsky Lecture (ref. 102), he “returned to Washington University in 1975 and Dale Pitt came as his second doctoral student in 1977. Peters did not want to do a literature search, but Pitt had a

better idea and discovered Prandtl, Kinner and Mangler/Squire.” Pitt’s doctoral thesis (ref. 103) appeared in 1980.

Kinner (ref. 104) used the acceleration potential approach of Prandtl to solve for the flow around a circular wing. Reference 104 begins:

“This work was intended initially as a contribution to the autogiro theory. In order to limit the scope the cross-flow of the disk was assumed to be zero, thus the disk can be replaced as a fixed wing in stationary flow.”

A footnote to this paragraph stated that the idea originated from Dr. Küssner, AVA Göttingen. The work was Kinner’s dissertation at the University of Göttingen under Professor Ludwig Prandtl. Kinner developed a separation of variables solution for a circular wing.

Mangler (refs. 105–107) used separation of variables in elliptical coordinates (fig. 36) to solve Laplace’s equation for the acceleration potential of a circular actuator disk. He had an English translation of Kinner’s paper (ref. 104) available. Mangler evaluated for hover the derivatives of uniform and linear inflow variables with thrust and hub moment loading variables. In an amazing analytical effort, he evaluated the integrals required to obtain the inflow due to thrust for the actuator disk in forward flight (a skewed cylindrical wake). Pitt and Peters (ref. 87) cite this theory as presented by Joglekar and Loewy (ref. 108).

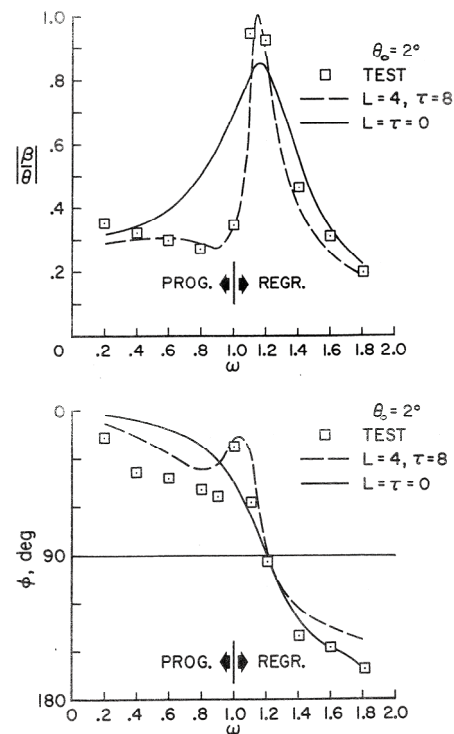


Figure 35. Flap response to cyclic stick stir, amplitude, and phase as a function of frequency ratio (ref. 98).

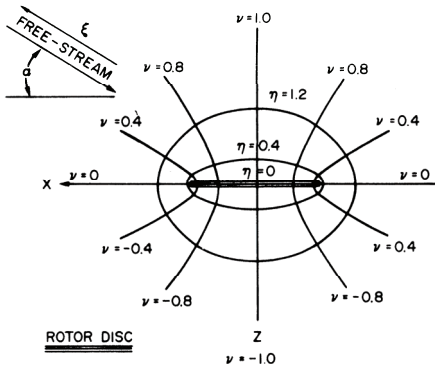


Figure 36. Ellipsoidal coordinate system (ref. 87).

Pitt and Peters (ref. 87) described the objective of the work:

“A linear, unsteady theory is developed that relates transient rotor loads (thrust, roll moment, and pitch moment) to the overall transient response of the rotor induced-flow field. The relationships are derived from an unsteady, actuator-disc theory; and some are obtained in closed form.”

and the background (reference numbers have been changed to those in the present paper):

“It has been known for some thirty years that the induced-flow field associated with a lifting rotor responds in a dynamic fashion to changes in either blade pitch (i.e. pilot inputs) or rotor flapping angles (i.e. rotor or body dynamics) [refs. 88, 109, 110]. In recent years, it has been found that dynamic inflow for steady response in hover can be treated by an equivalent (i.e. reduced) Lock number [ref. 93]. For more general conditions, such as transient motions or a rotor in forward flight, it has been determined that the induced flow can be treated by additional “degrees of freedom” of the system. Each degree of freedom represents a particular inflow distribution, and each has its own particular gain and time constant [refs. 95, 98, 100].

Although the above results have provided some impressive correlation with experimental data, there is still no general theory to predict the gains and time-constants of dynamic inflow. Values from momentum theory give excellent results in hover, but are clearly inadequate in forward flight [refs. 95, 100]. A simple vortex model [ref. 95], gives some improvement in forward flight

but is still not satisfactory. An empirical model based on the best fit of response data [refs. 95, 100], gives excellent results; but several peculiar singularities remain unexplained. Thus there is a need to determine the dynamic-flow behavior from fundamental, aerodynamic considerations.”

Representing the inflow distribution over the rotor disk by uniform plus linear terms, $\lambda = \lambda_0 + \lambda_c r \cos \psi + \lambda_s r \sin \psi$, “the dynamic inflow models of refs. 98 and 100 assume that the inflow is related to the aerodynamic loads in a linear, first-order fashion.”

$$\begin{bmatrix} M \end{bmatrix} \begin{bmatrix} \dot{\lambda}_0 \\ \dot{\lambda}_s \\ \dot{\lambda}_c \end{bmatrix} + \begin{bmatrix} L \end{bmatrix}^{-1} \begin{bmatrix} \lambda_0 \\ \lambda_s \\ \lambda_c \end{bmatrix} = \begin{bmatrix} C_T \\ C_L \\ C_M \end{bmatrix}$$

or

$$\begin{bmatrix} \tau \end{bmatrix} \begin{bmatrix} \dot{\lambda}_0 \\ \dot{\lambda}_s \\ \dot{\lambda}_c \end{bmatrix} + \begin{bmatrix} \lambda_0 \\ \lambda_s \\ \lambda_c \end{bmatrix} = \begin{bmatrix} L \end{bmatrix} \begin{bmatrix} C_T \\ C_L \\ C_M \end{bmatrix}$$

“The purpose of this research is to find the elements of $[L]$ and $[M]$ from basic aerodynamic principles and to also investigate the validity of this linear, first-order form.”

A solution was obtained for the incompressible potential flow about the rotor, which was represented by an actuator disk. The equations of mass and momentum conservation were written for small disturbances relative to the mean flow, which is a uniform free stream v at angle α relative to the rotor disk ($\alpha = 90$ degrees for axial flight). The acceleration potential (perturbation pressure) satisfies Laplace’s equation, with the boundary condition of the pressure discontinuity on the rotor disk. A separation of variables solution is possible in ellipsoidal coordinates (fig. 36), resulting in separate radial and azimuthal loading functions on the rotor disk. From reference 87:

“The actuator-disc theory that we use in this investigation is based on pressure distributions developed by Kinner [see refs. 104, 108]. Kinner discovered a family of pressure distributions that solve Laplace’s equation, and that also give a pressure discontinuity (i.e. lift) across a circular disk.”

However, this family of distributions does not encompass all solutions; in particular it does not include a uniformly loaded disk. The coefficients of the loading distribution are related to the integrated forces on the disk, with thrust and pitch and roll moments obtained only from the lowest

ROTOR AERODYNAMIC STATE

order solutions. The induced velocity is represented by a series, $\lambda = \lambda_0 + \lambda_c r \cos \psi + \lambda_s r \sin \psi$. The momentum equation is linearized in order to relate the velocity to the acceleration potential. The streamwise derivative of the velocity is obtained from the normal gradient of the acceleration potential, hence the integral of the acceleration potential from far upstream to the disk gives the normal velocity at the disk. Exact, analytical solutions are possible for axial and edgewise flow. Mangler (ref. 106) derived the Fourier series for the induced velocity (uniform and longitudinal gradient) from thrust, as analytical functions of α . This result gave the first column (C_T response) of $[L]$. Pitt numerically evaluated the roll and pitch moment response, matching the exact values for axial and edgewise flow, and from these results identified analytical functions of α for the moment terms in $[L]$. The results for the three-state dynamic inflow model were:

$$[L] = \frac{1}{v} \begin{bmatrix} \frac{1}{2} & 0 & \frac{15\pi}{64} \sqrt{\frac{1-\sin \alpha}{1+\sin \alpha}} \\ 0 & \frac{-4}{1+\sin \alpha} & 0 \\ \frac{15\pi}{64} \sqrt{\frac{1-\sin \alpha}{1+\sin \alpha}} & 0 & \frac{-4 \sin \alpha}{1+\sin \alpha} \end{bmatrix}$$

$$[M] = \begin{bmatrix} \frac{128}{75\pi} & 0 & 0 \\ 0 & \frac{-16}{45\pi} & 0 \\ 0 & 0 & \frac{-16}{45\pi} \end{bmatrix}$$

(table 4 of reference 87). In summary:

“An actuator-disc theory has been used to obtain gains and time constants (i.e. the L and M matrices) for both 3-degree-of-freedom and 5-degree-of-freedom dynamic-inflow models. ... In axial flow (e.g. hover), the gains are identical to those obtained from simple momentum theory. ... The apparent mass terms (the M matrix) for the simplest pressure distributions are identical to the apparent mass terms of an impermeable disc, but these values vary significantly with lift distribution.”

Thus, Pitt and Peters constructed the unsteady, actuator-disk theory that is the basis of dynamic inflow models of the rotor wake.

Gaonkar and Peters (refs. 111–112) summarized dynamic inflow research, and the verification of the Pitt and Peters model, by comparison of hingeless rotor response measurements (particularly the data from reference 96), both static and dynamic, in hover and in forward flight.

Experimental evidence for the existence of a rotor aerodynamic state was found by William G. Bousman of the U.S. Army in a test of the ground resonance stability of a model rotor (ref. 113). Theoretical work “had suggested ways in which aeroelastic coupling of various rotor degrees of freedom could be used to stabilize the lead-lag regressing mode and obviate the need for rotor lead-lag dampers.” The stabilizing effect of pitch-lag and flap-lag structural coupling was promising. “An experimental program was undertaken with a relatively simple, small-scale model rotor and fuselage to examine helicopter aeromechanical instabilities.” The principal objective was to explore the potential for pitch-flap coupling, flap-lag structural coupling, and matched flap and lag stiffness to stabilize the rotor regressive lag mode. In an earlier test (ref. 114), “nonlinear damping in the gimbal ball bearings prevented adequate measurements of the body mode damping.” Thus, “the gimbal frame was redesigned to replace the ball bearings with flexural pivots,” resulting in small, nearly constant, pitch and roll damping.

The model used was a 1.62-meter-diameter, three-bladed hingeless rotor, supported in a gimbal frame that allowed pitch and roll motion (fig. 37). “The rotor was designed so that most of the blade flexibility is concentrated in root flexures” (ref. 113). Five rotor configurations were tested: nonmatched stiffness rotor (configuration 1) and matched stiffness rotor (configuration 4); each with negative pitch-lag coupling; and the nonmatched stiffness with negative pitch-lag coupling and structural flap-lag coupling. Matched stiffness (equal nonrotating flap and lag stiffness) was obtained by increasing the stiffness of the flap flexure. Hence configuration 4 could generate larger hub moments, resulting in larger participation of inflow states.

The model was tested in hover, at zero collective. “A shaker was used to oscillate the model about its roll axis” in order to excite the lead-lag regressing mode — and any other low-damped modes that could be excited. “The body modes were excited by deflecting the model in either pitch or roll using a system of strings and pulleys.” From the free decay of the system, the frequency and damping of the flap, lag, and body pitch and roll modes were measured as a function of rotor rotational speed.

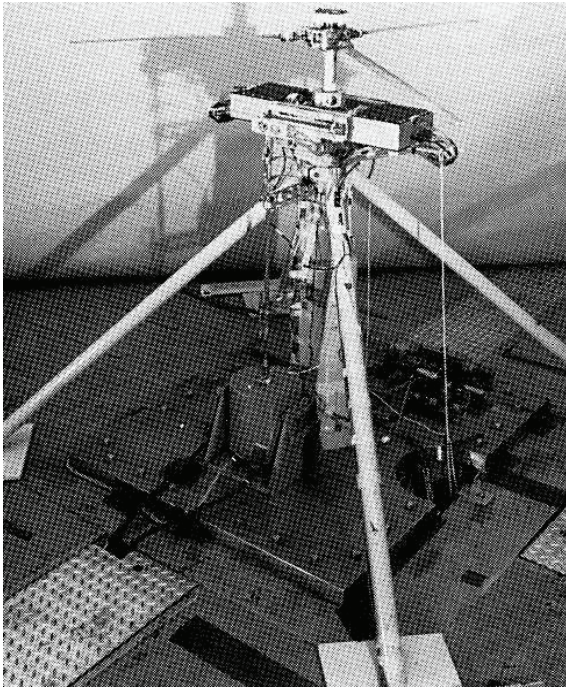


Figure 37. Overall view of model (ref. 113).

Bousman, a very careful experimentalist, found more than he was looking for. The experimental method found all modes that could be excited, not just the regressive-lag and body modes. Thus, Bousman was able to identify an aerodynamic state or inflow mode in the measured data. This constitutes unique experimental evidence that the air about the rotor (the wake) behaves as characterized by dynamic inflow states.

The experimental observation is illustrated in figure 38, which shows the measured modal frequencies for configuration 4 (matched stiffness) as a function of rotor speed, and calculations made without a dynamic inflow model. The frequency and damping of the regressive lag model (ζ_R) was accurately calculated. The three other measured modes did not correspond to the calculations at all. The damping of the roll mode (ϕ) was overestimated, the frequency of the pitch mode (θ) underestimated, and the calculated damping of the flap regressive mode (β_R) was so high that it should not have been observable in the test. For configuration 1 (lower flap stiffness), the frequencies were reasonably well predicted without a dynamic inflow model, but the pitch and roll mode damping were overestimated.

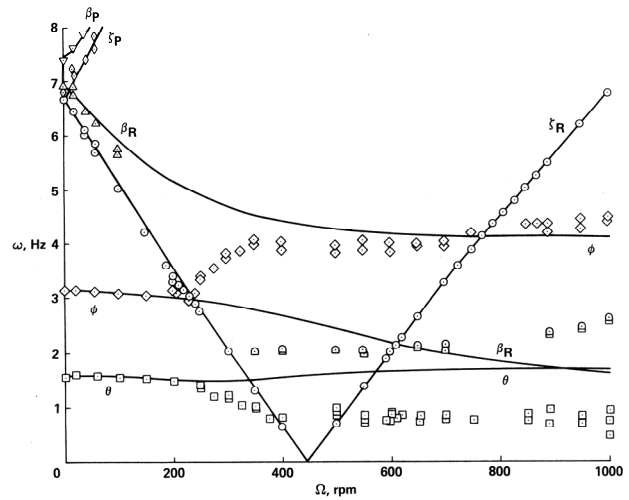


Figure 38. Modal frequencies as a function of rotor speed for configuration 4, matched stiffness: comparison of measurements (points) and CAMRAD calculations without inflow dynamics (ref. 115).

Bousman hypothesized that the differences between measured and calculated results were attributable to the influence of inflow dynamics. Reference 113 concluded that for configuration 1, “it was suggested that the deficiency in damping was due to the inflow dynamics.” For configuration 4, “correlation of theory and experiment for the body modes was poor, and it was suggested that this was due to the effect dynamic inflow had on the damping of the flap regressive mode.”

The frequency and damping for both matched and nonmatched stiffness configurations can be predicted well by including the three-state dynamic inflow model in the analysis, as illustrated in figure 39. The implication is that because of the organization of the wake, the air responds as a whole to the motion of the rotor, a response well described by the loading derivatives and time lag of simple dynamic inflow models.

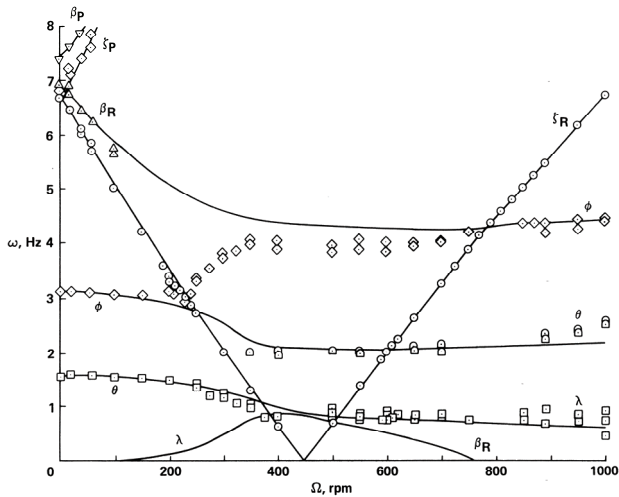


Figure 39. Modal frequencies as a function of rotor speed for configuration 4, matched stiffness: comparison of measurements (points) and CAMRAD calculations with inflow dynamics (ref. 115).

BEAM THEORY

Beam theory for elastic rotor blades was presented in first-order (linear) form by Houbolt and Brooks (ref. 116), and in second-order (nonlinear) form by Hodges and Dowell (ref. 117). An adequate structural model is essential for the prediction of loads and stability, and hence has a direct influence on the weight and design. Rotor blades almost universally have a high structural-fineness ratio and, thus, are well idealized as beams. The complexities of rotation, and now multiple load-paths and composite construction, have resulted in extensive and continuing efforts to develop appropriate beam models for the solution of rotor problems.

Preceding Houbolt and Brooks, there was notable early work on beam theory for rotor blades at Polytechnic Institute of Brooklyn (ref. 118); at Kellett Aircraft Corporation (refs. 119–120); at CAL (refs. 121–122); at NACA (refs. 123–124); and at MIT (ref. 125).

Houbolt and Brooks

John C. Houbolt and George W. Brooks of NACA brought together beam theory for bending and torsion deflection of rotor blades (ref. 116):

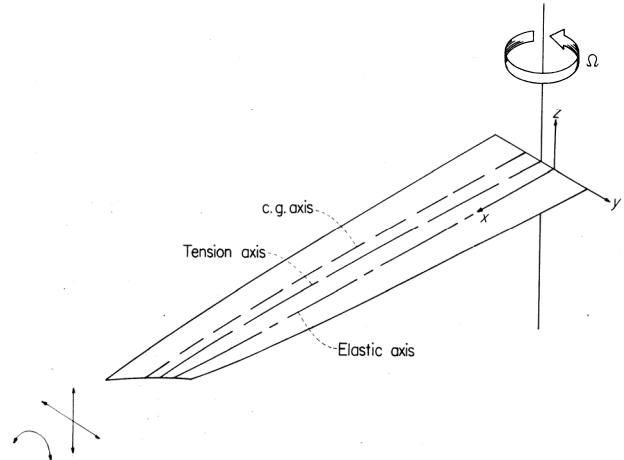


Figure 40. Case of coupled bending-torsion of twisted rotating beam (ref. 116).

“The differential equations of motion for the lateral and torsional deformations of twisted rotating beams are developed for application to helicopter rotor and propeller blades. No assumption is made regarding the coincidence of the neutral, elastic, and mass axes, and the generality is such that previous theories involving various simplifications are contained as subcases to the theory presented in this paper. ... The specific purpose of the paper is to develop the differential equation of deformation of the blade under the action of various applied loads. The development is made along the principles of “engineering” beam theory, and secondary effects, such as deformation due to shear, are not included.”

Figure 40 illustrates the model.

The principal assumptions were single load-path, permitting determination of the tension directly from the centrifugal force; isotropic material; and structural and inertial terms retained only to first order in bending and torsion deflection. The final differential equations were presented as:

$$\begin{aligned}
& - \{ [GJ + Tk_A^2 + EB_1(\beta')^2] \phi' - EB_2 \beta' (v'' \cos \beta + w'' \sin \beta) \}' + \\
& \underline{Te_A(v'' \sin \beta - w'' \cos \beta) + \Omega^2 m x e (-v' \sin \beta + w' \cos \beta) +} \\
& \underline{\Omega^2 m e \sin \beta v + \Omega^2 m [(k_{m2}^2 - k_{m1}^2) \cos 2\beta + e e_o \cos \beta] \phi + m k_m^2 \ddot{\phi} -} \\
& m e (\ddot{v} \sin \beta - \ddot{w} \cos \beta) = M + (Tk_A^2 \beta')' - \Omega^2 m [(k_{m2}^2 -} \\
& k_{m1}^2) \sin \beta \cos \beta + e e_o \sin \beta] \quad (22)
\end{aligned}$$

$$\begin{aligned}
& [(EI_1 \cos^2 \beta + EI_2 \sin^2 \beta) w'' + (EI_2 - EI_1) \sin \beta \cos \beta v'' - \\
& \underline{Te_A \phi \cos \beta - EB_2 \beta' \phi' \sin \beta}]'' - (T w')' - (\Omega^2 m x e \phi \cos \beta)' + \\
& m (\ddot{w} + e \ddot{\phi} \cos \beta) = L_z + (Te_A \sin \beta)'' + (\Omega^2 m x e \sin \beta)' \quad (23)
\end{aligned}$$

$$\begin{aligned}
& [(EI_2 - EI_1) \sin \beta \cos \beta w'' + (EI_1 \sin^2 \beta + EI_2 \cos^2 \beta) v'' + \\
& \underline{Te_A \phi \sin \beta - EB_2 \beta' \phi' \cos \beta}]'' - (T v')' + (\Omega^2 m x e \phi \sin \beta)' + \\
& \underline{\Omega^2 m e \phi \sin \beta + m (\ddot{v} - e \ddot{\phi} \sin \beta) - \Omega^2 m v} = L_y + (Te_A \cos \beta)'' + \\
& (\Omega^2 m x e \cos \beta)' + \Omega^2 m (e_o + e \cos \beta) \quad (24)
\end{aligned}$$

Thus, they started the practice of underlining terms not included in previous theories. Beginning another practice, “as a check on the derivation presented herein, the differential equations of equilibrium were derived by a completely different approach that involves energy principles.”

Later Houbolt would make a major contribution to NASA’s Apollo program by recognizing the significant weight savings possible using the lunar mission model called lunar-orbit rendezvous (LOR) instead of direct ascent or earth-orbit rendezvous, and aggressively promoting it until LOR was chosen in 1962 as the way to the moon (refs. 126–127). He received the NASA Medal for Exceptional Scientific Achievement on October 1, 1963, the citation of which reads:

“For his foresight, perseverance, and incisive theoretical analysis of the concept of Lunar Orbit Rendezvous, revealing the important engineering and economic advantages that have led to its adoption as a central element in the United States’ Manned Lunar Exploration Program.”

Houbolt was Associate Chief of the Dynamic Loads Division at NASA Langley Research Center in 1961–1962, and was still contributing to rotorcraft aeromechanics (ref. 128).

Hingeless rotors

By the end of the 1960s, the hingeless rotor was maturing rapidly (fig. 41). In the United States, the Lockheed XH-51A had undergone successful flight tests since November

1962 (ref. 129) and was even used as a basis for stopped-rotor concepts in full-scale wind tunnel tests during 1965–1966 (ref. 130). The U.S. Army was engaged with Lockheed in developing the AH-56A Cheyenne compound helicopter (ref. 131). Lockheed won the Advanced Aerial Fire Support System (AAFSS) competition in 1965, and the AH-56A first flight occurred September 1967. The Cheyenne was installed in the NASA 40- by 80-Foot Wind Tunnel at Ames Research Center in September 1969 with the objectives of investigating performance and dynamics issues. The objectives were not met because incorrect feedback to the control gyro resulted in destruction of the aircraft (ref. 132). The Messerschmitt–Bölkow–Blohm (MBB) Bo-105 was developed in Germany, with first flight in February 1967 and certification in 1970 (ref. 133). In England, the Westland Lynx first flight occurred in March 1971 (ref. 134).

As usual, invention led analysis. The Cheyenne, Bo-105, and Lynx were developed using relatively simple rotor dynamics models (refs. 132, 136, and 137). Dynamics issues with the Cheyenne demonstrated the need for analysis development (ref. 131).

There was notable work on beam theory by Mil’ (ref. 137), at CAL (refs. 138–139), at Sikorsky (ref. 140), and at Westland Helicopters (ref. 136). The development of the Bo-105 and the Lynx was accompanied by an understanding of the torsion-bending coupling arising from nonlinear structural dynamics of hingeless rotors (refs. 135–136). Bending deflections can result in a torsion moment component of trim bending moments (fig. 42), leading to effective pitch-lag and pitch-flap couplings that significantly influence blade stability and aircraft flight dynamics.

Developing even a theory of the stability of the flap and lag motion of a hingeless rotor proved difficult. Young (ref. 141) published work on nonlinear elastic flap-lag motion, concluding: “The theory predicts the possibility of unstable blade flapping motion at all flight speeds. This is a result of a nonlinear coupling of fundamental flapwise and chordwise motions in an unstable, regenerative manner.” Based on approximate stability criteria, Young predicted that high-load-factor, low-speed maneuvers would destabilize a rotor with either rigid or semi-rigid blades; and as speed and power increased, all rotor types would lose stability. The critical conditions for stability were comparable to those associated with retreating tip stall. Thus, (ref. 141):



Lockheed XH-51A helicopter



AH-56A in wind tunnel



XH-51A stopped rotor test



MBB Bo-105 helicopter



Lockheed AH-56A Cheyenne compound helicopter



Westland Lynx helicopter

Figure 41. Hingeless rotor helicopters.

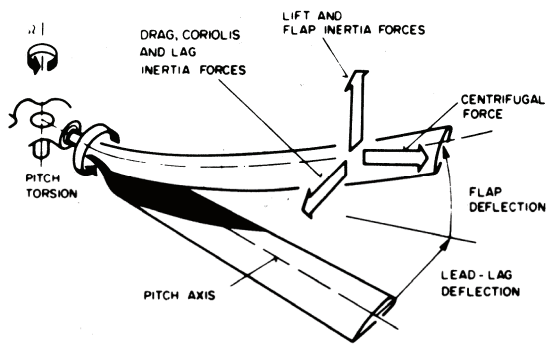


Figure 42. Flap-lag-torsion coupling on rotor blades (ref. 135).

“The important implication of the theory is that full scale rotors do not actually stall, but enter a regime of continuously unstable, but non-divergent, non-destructive limit cycle behavior. ... A second important implication of the theory is that in high speed flight, powered, partially unloaded rotors of current design practice, will be subject to violent and possibly destructive instability.”

These “implications” generated discussion. Young (ref. 142) wrote: “I believe it is worth noting at the outset that I have discussed the subject paper in correspondence and in person with numerous individuals and groups over the extended period of time since its publication.” Berman and McIntyre (ref. 142) wrote a long critique, which begins: “the author presents a theory which would, if correct, virtually preclude further development of the high speed helicopter.” They maintained that the implication regarding stall was not supported by experimental data—the flow on rotor blades does separate—and that the implication regarding instability did not agree with results from numerical integration of the equations. They found “numerous errors of analysis and interpretation in the paper completely invalidate the theory,” criticizing the approximate assessment of stability and various details of the equations. Young replied in equal length (ref. 142): “My objective was and is to provide needed visibility for substantive technical issues; I trust that with proper perspective it will be evident that their critique was ill-considered and is erroneous in all its important particulars.” The editors of the journal (Ellis and Loewy) felt it was necessary to conclude this exchange with a confirmation of the value of publishing controversial papers and providing a forum to discuss them.

No doubt most of the controversy generated by Young’s paper was over the suggestion that what had been interpreted as retreating blade stall was actually a flap-lag limit cycle instability, but attention was transferred to the question of the proper equations for the nonlinear flap and lag motion. Hohenemser (ref. 143) wrote a short note attempting to correct some of the approximations, and ended with “the writer is preparing a paper which hopefully will be free of inaccuracies such as in [ref. 141].” Young’s reply (ref. 143) was also short, but included:

“The constructive interest evidenced by Dr. Hohenemser’s letter and the paper which he is preparing on the subject of coupled blade flapping and lead-lag motion is most welcome. I look forward to the publication of this paper with keen interest. We are in agreement that the occurrence of such instabilities is a very real, rather than a remote possibility. Further, I agree that there is a need for a fresh, lucid exposition free of inaccuracies. That this is not an easy task is illustrated by the fact that I find that his present, abbreviated technical exposition overlooks several fundamental points and is also inconsistent with the results of flight tests.”

Hohenemser and Heaton (ref. 144) presented a careful derivation and an analysis of the linearized, second-order equations of flap-lag motion. A rigid blade with flap and lag flexures was used to represent a hingeless rotor. They concluded that “in a rotor without lag hinges, second order flap-lag coupling is an important issue and must be carefully evaluated in any rational dynamic rotor design.” Comparing results to those obtained by Young, they found significant differences attributed to inconsistencies in the linearization and approximations in the stability criterion. However, reference 144 had an error in the treatment of the effect of lag motion on the inplane velocity for the aerodynamic model.

It was left to Ormiston and Hodges (ref. 145) to present a really careful derivation of the flap-lag equations of motion, as well as a thorough exploration of the influence on blade stability of parameters such as thrust, flap and lag frequency, pitch-lag coupling, and structural flap-lag coupling. Regarding the original issue of hingeless rotor stability, the importance of nonlinear inertial, structural, and aerodynamic terms was clear. It was concluded that instabilities were possible, largely due to pitch-lag or pitch-flap coupling, and that flap-lag structural coupling was potentially stabilizing.

Ames Directorate, USAAMRDL

Motivated by the government and industry activities in hingeless rotor development, particularly the AH-56A Cheyenne development, the Ames Directorate of the U.S. Army Air Mobility Research and Development Laboratory (USAAMRDL) (later Aeroflightdynamics Directorate at Ames Research Center) initiated a program of theoretical and experimental research in rotor dynamics.

Robert A. Ormiston came to Ames Research Center in February 1968 after conducting PhD research on the aerodynamics of a sailwing at Princeton University, where Professor Earl Dowell read his thesis. Although his original assignment at Ames was aerodynamics, all the problems and all the questions attracted him to rotor dynamics; he was in the control room of the 40- by 80-Foot Wind Tunnel at the time of the Cheyenne accident. Dewey Hodges joined the Army laboratory in June 1970, David Peters in September 1970, and William Bousman in October 1970. I also joined the Army Laboratory in October 1970, but was at the 40- by 80-Foot Wind Tunnel branch. Ormiston, Hodges, and Peters began a systematic development of a theoretical basis for hingeless rotor blade stability and dynamics. Bousman began a series of careful experiments to provide data that would guide and substantiate the analysis.

Dewey Hodges worked at Ames as a summer student from 1970 to 1972, and part-time the rest of the year while working on his PhD at Stanford University. In their initial collaboration, Ormiston and Hodges derived the equations for rigid flap and lag motion of a blade, Ormiston using Newtonian and Hodges using Lagrangian methods. Their first efforts produced different equations, traced to different assumptions about whether the flap and lag springs rotated with collective pitch. Out of this, Ormiston developed a useful simulation of variable elastic coupling by introducing springs both inboard and outboard of the pitch rotation (ref. 145).

Ormiston asked Hodges to work on elastic flap-lag-torsion equations of a rotor blade, including effects of nonlinearity. Peters had passed on the opportunity, but later became interested in the kinematic issues (authoring the appendix of reference 117). Hodges' work became his PhD thesis (ref. 146), and the basis of further developments in 1972–1973 (refs. 147–148) on elastic bending and bending-torsion stability of rotor blades.

During 1970–1972, Ormiston sponsored work by Pin Tong at MIT on hingeless rotor dynamics. Professor Tong investigated the stability of the flap-lag equations

using perturbation methods (ref. 149), while his student Peretz P. Friedmann developed a model for bending-torsion motion of elastic blades (refs. 150–152). In 1972, Friedmann and Hodges both received their doctorates on the subject of elastic blade dynamics. Reference 152 did generate an exchange of letters with Ormiston and Hodges (ref. 153), quite professional in tone, absent the rancor that often seems to characterize exchanges between rotary-wing dynamicists.

Hodges was working full-time at Ames in 1973. Professor Earl H. Dowell of Princeton spent the summers of 1972 and 1973 at Ames, at the invitation of Ormiston. At Ormiston's suggestion, Dewey Hodges and Earl Dowell began work to develop a more rigorous derivation of the nonlinear bending-torsion equations of motion for a rotor blade. During this time there were interactions with Dave Peters regarding the kinematics. During a visit by Hodges to Princeton in 1973, they resolved issues associated with the consistent ordering within the two approaches and the basis of the equations resulting from the Newtonian derivation. The draft of reference 117 was completed in late 1973.

Hodges and Dowell

Dewey H. Hodges of the U.S. Army and Earl H. Dowell of Princeton University developed “a more complete and general nonlinear theory” of the elastic bending and torsion of rotor blades (ref. 117):

“The theory is intended for application to long, straight, slender, homogeneous, isotropic beams with moderate displacements and is accurate to second order based on the restriction that squares of bending slopes, twist, t/R , and c/R are small with respect to unity. ...

The equations of motion are derived by means of two complementary methods: the variational method based on Hamilton's principle, and the Newtonian method based on the summation of forces and moments acting on a differential blade element. Both methods used together help ensure a more accurate and consistent treatment of the nonlinear terms. The important nonlinear strain-displacement relations, required for both methods, are developed from a classical definition of strain and simplified in accordance with the premise of a long, slender beam subject to moderate displacements.”

The derivation by the variational method was largely the work of Hodges, and the derivation by the Newtonian method was largely the work of Dowell.

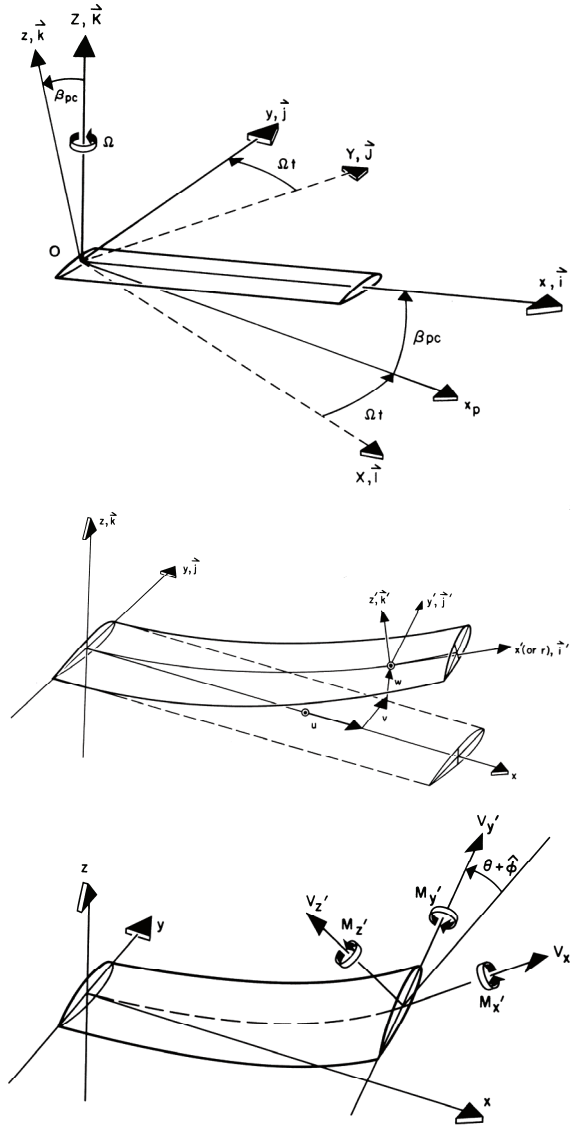


Figure 43. Undeformed coordinate systems, elastic displacements, and resultant forces and moments (ref. 117).

Reference 117 summarized the evidence regarding the importance of nonlinearities in rotor blade dynamics: inertial nonlinearities in flap-lag dynamics, based on rigid blade models (ref. 145) or elastic models (ref. 147); structural bending-torsion nonlinearities (Huber, ref. 135); and elastic bending-torsion coupling in the torsion equation (Mil², ref. 137).

Figure 43 illustrates the model. A single load-path was assumed, permitting elimination of the axial extension variable. A systematic, self-consistent approach was developed for determining which terms in the equations to retain and which to ignore. From reference 117:

“In deriving a nonlinear system of equations, it is necessary to neglect higher-order terms to avoid overcomplicating the equations of motion. When neglecting terms within a large system of equations, care must be exercised to ensure that the terms retained constitute self-adjoint structural and inertial operators. These self-adjoint operators lead to symmetric stiffness and mass matrices and an antisymmetric gyroscopic matrix in the modal equations.”

In particular, it was assumed that with bending and torsion deflections and cross-section dimensions all order ε , the extension and section warping were order ε^2 . This approach, and the assumptions made regarding order of various quantities, formed the basis for future extensions as well. The final differential equations were presented as:

$$\delta u \text{ equation: } -T' - m(\Omega^2 x + \underline{2\Omega v}) = \underline{L_u} \quad (61a)$$

$$\delta v \text{ equation: } -(\underline{Tv'})' + \left\{ -EAe_A \left(u' + \frac{v'^2 + w'^2}{2} \right) \cos(\theta + \phi) - EB_2^* \theta' \phi' \cos \theta - EC_1^* \phi'' \sin \theta + [EI_{z'} \cos^2(\theta + \phi) + EI_{y'} \sin^2(\theta + \phi)] v'' + (EI_{z'} - EI_{y'}) \cos(\theta + \phi) \sin(\theta + \phi) w'' \right\}'' + \underline{2m\Omega \dot{u}} + m\ddot{v} - me\dot{\phi} \sin \theta - 2me\Omega(\dot{v}' \cos \theta + \dot{w}' \sin \theta) - m\Omega^2[v + e \cos(\theta + \phi)] - 2m\Omega\beta_{pc}\dot{w} - \{me[\Omega^2 x \cos(\theta + \phi) + 2\Omega \dot{v} \cos \theta]\}' = \underline{L_v} \quad (61b)$$

$$\delta w \text{ equation: } -(\underline{Tw'})' + \left\{ -EAe_A \left(u' + \frac{v'^2 + w'^2}{2} \right) \sin(\theta + \phi) - EB_2^* \theta' \phi' \sin \theta + EC_1^* \phi'' \cos \theta + (EI_{z'} - EI_{y'}) \cos(\theta + \phi) \sin(\theta + \phi) v'' + [EI_{z'} \sin^2(\theta + \phi) + EI_{y'} \cos^2(\theta + \phi)] w'' \right\}'' + m\ddot{w} + me\dot{\phi} \cos \theta + 2m\Omega\beta_{pc}\dot{v} - \{me[\Omega^2 x \sin(\theta + \phi) + 2\Omega \dot{v} \sin \theta]\}' = \underline{L_w} - m\Omega^2\beta_{pc}x \quad (61c)$$

$$\delta \phi \text{ equation: } -\left[EAk_A^2(\theta + \phi)' \left(u' + \frac{v'^2 + w'^2}{2} \right) + \underline{EB_1^* \theta'^2 \phi'} - EB_2^* \theta' (v'' \cos \theta + w'' \sin \theta) \right]' - EAe_A \left(u' + \frac{v'^2 + w'^2}{2} \right) (w'' \cos \theta - v'' \sin \theta) - (GJ\phi')' + [\underline{EC_1 \phi''}] + EC_2^* (w'' \cos \theta - v'' \sin \theta)'' + \underline{(EI_{z'} - EI_{y'}) [(w''^2 - v''^2) \cos \theta \sin \theta + v'' w'' \cos 2\theta] + mk_m^2 \dot{\phi}^2 + m\Omega^2 \phi (k_{m2}^2 - k_{m1}^2) \cos 2\theta} + me[\Omega^2 x (w' \cos \theta - v' \sin \theta) - (\dot{v} - \Omega^2 v) \sin \theta + \dot{w} \cos \theta] = \underline{M_\phi} - m\Omega^2 (k_{m2}^2 - k_{m1}^2) \cos \theta \sin \theta - me\Omega^2 \beta_{pc} x \cos \theta \quad (61d)$$

where

$$T \equiv V_{x'} = EA \left\{ u' + \frac{v'^2}{2} + \frac{w'^2}{2} + k_A^2 \theta' \phi' - e_A [v'' \cos(\theta + \phi) + w'' \sin(\theta + \phi)] \right\} \quad (62)$$

with new and important terms underlined. Hodges and Dowell concluded (ref. 117):

“In the resulting system of equations, several important nonlinear terms are identified. First, the centrifugal term proportional to lead-lag velocity in the tension equation combines with the centrifugal coupling terms in the bending

equations to produce nonlinear flap-lag inertial terms. The longitudinal velocity in the lead-lag equation, a Coriolis terms, is expressed in terms of bending quantities as another nonlinear flap-lag inertial term. These terms, when linearized with respect to equilibrium, are antisymmetric gyroscopic terms and significantly influence hingeless rotor stability and forced response phenomena. Second, the nonlinear bending-torsion coupling term in the torsion equation is written in a form similar to the one identified by Mil' in [ref. 137]. The twisting moment arises from bending in two directions and is proportional to the difference in bending stiffness and the product of curvatures. The counterpart nonlinear bending-torsion coupling terms in the bending equations appear in the form of a change in elastic coupling due to elastic twist. These bending-torsion coupling terms are also important in determining the aeroelastic stability of hingeless rotors.”

Work exploring the dynamic stability and response of elastic rotor blades (refs. 154–156) followed, based on the equations of motion developed in reference 117.

After Hodges and Dowell

Subsequent to Hodges and Dowell, there were numerous investigations devoted to extending the equations of motion, either to higher order or with different ordering assumptions. Always the new terms in the equations were underlined, or double- or triple-underlined. The resulting equations grew ever more complicated. In the 1980s, beam models were developed using exact kinematics (notably refs. 157–158), and introducing implicit formulations.

Development of beam models for anisotropic or composite materials was a key step (refs. 159–162). Finite elements are needed to model the complexity of rotor structures and finite-element models were developed for rotor blade analysis in the early 1980s (refs. 163–172). Multibody dynamics technology is needed to model the mechanisms found in rotors (refs. 173–179). Finite element and multibody dynamics modeling capability, including input-driven definition of the geometry, was fully integrated into comprehensive analysis with the introduction of CAMRAD II (ref. 180) and DYMORE (ref. 181).

With the development of rotor models combining finite elements and multibody dynamics, large rigid-body motion of small individual elements can be handled with exact kinematics. Then, for most problems of rotor

dynamics, the second-order model of Hodges and Dowell is satisfactory for the motion within the element.

Finite elements

The use of finite elements in rotor blade analysis is crucial to modeling the true complexity of the mechanical and structural systems being presented by designers. The use of finite-element techniques to obtain free vibration modes of rotor blades is not uncommon (e.g., refs. 163–164). Friedmann and Straub (refs. 165–167) discretized the partial differential equations of a rotor blade using a local Galerkin method of weight residuals. While recognizing that “the finite element method is ideally suited for modeling the complicated and redundant structural system encountered in bearingless rotors” (ref. 165), they considered the equations of a single load-path rotating beam. They were particularly motivated by “the significant reduction in algebraic manipulative labor when compared to the application of the global Galerkin method” (ref. 165).

Borri, Lanz, and Mantegazza (refs. 168–169) developed an analysis with the “blade motion represented by finite elements in space-time domain,” based on Hamilton’s variational principle. The papers specifically focused on the time-finite-element development, and observed the advantage of leaving the integration problems and tedious algebraic manipulations to the computer. Hodges and Rutkowski (ref. 170) applied variable-order finite elements to blade analysis. Sivaneri and Chopra (ref. 171) analyzed the bending-torsion stability of a rotor blade using “a finite element formulation based on the principle of virtual work.” The subject was still a single load-path configuration, with the extension displacement eliminated by substitution using the centrifugal force.

Application of the finite-element method to a bearingless rotor was finally made by Sivaneri and Chopra (ref. 172). “The finite element formulation allows the multibeams of the flexure to be considered individually. The multibeams of the flexure and the single beam of the outboard are discretized into beam elements, each with fifteen nodal degrees of freedom.” With multiple load-paths, “the distribution of the centrifugal force in the multibeams of the inboard blade is not known a priori and hence the axial deflection can not be eliminated.” Cubic shape functions, hence linear moment, were used for bending; quadratic shape functions, hence linear moment, for torsion; and cubic shape functions, hence quadratic tension, for extension. Thus, the 15 nodal degrees of freedom (fig. 44) consisted of flap and lag bending displacement and slope at each end of the element, torsion at the ends and one midpoint, and extension at the ends and two midpoints.

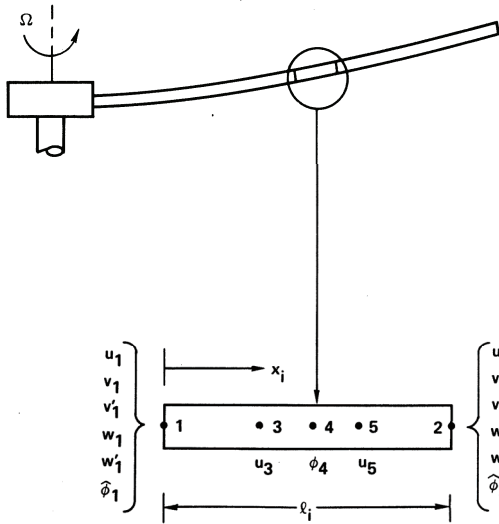


Figure 44. A finite element showing nodal degrees of freedom (ref. 172).

And multibody dynamics

Flexible and accurate modeling of the mechanisms that comprise the hub, blade root, and control system of rotors requires the technology of multibody dynamics. The combination of finite elements and multibody dynamics was brought to rotorcraft by Dewey H. Hodges and his colleagues who, in a project extending from April 1980 to September 1985, developed GRASP (General Rotorcraft Aeromechanical Stability Program). As described in reference 173:

“GRASP is a general-purpose program which treats the nonlinear static and linearized dynamic behavior of rotorcraft represented by arbitrarily connected rigid-body and beam elements. ... The basic approach which provides the foundation for large relative motion kinematics is derived from “multibody” research with an expanded emphasis on multiple levels of substructures. This is combined with the finite-element approach which provides flexible modeling through the use of libraries of elements, constraints, and nodes.”

In a series of papers in 1987, they described the methodology (ref. 174), the analysis (ref. 175), and its applications (refs. 176–177). The code “was developed to perform aeroelastic stability analysis of rotorcraft in steady, axial flight and ground contact conditions” (ref. 175) and, thus, was implemented with a limited aerodynamic model applicable only to hover and axial flow.

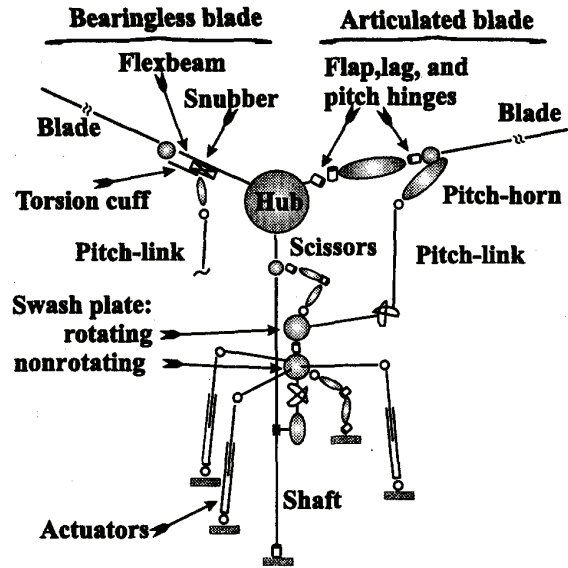


Figure 45. Detailed multibody representation of a rotor system (ref. 181).

An interesting development was the application of the general purpose multibody system analysis tool ADAMS (from Mechanical Dynamics, Inc.) to rotary-wing aeroelastic problems by Elliott and McConville (ref. 178). Bauchau and Kang (refs. 179) implemented and validated “a multibody formulation for helicopter nonlinear structural dynamic analysis” (fig. 45), focusing on the appropriate coordinates to represent the element motion and development of the corresponding constraint equations. Although no aerodynamic model was included, the method was applied to the problem of ground resonance.

MULTIBLADE COORDINATES

Multiblade coordinates (MBC) were introduced to rotor dynamics analysis by Robert P. Coleman and fully developed by Kurt H. Hohenemser. MBC are fixed-frame variables $(\beta_0, \beta_{nc}, \beta_{ns}, \beta_{N/2})$ obtained by a linear transformation of rotating frame variables $\beta^{(m)}$:

$$\begin{aligned}\beta_0 &= \frac{1}{N} \sum_{m=1}^N \beta^{(m)} \\ \beta_{nc} &= \frac{2}{N} \sum_{m=1}^N \beta^{(m)} \cos n\psi_m \\ \beta_{ns} &= \frac{2}{N} \sum_{m=1}^N \beta^{(m)} \sin n\psi_m \\ \beta_{N/2} &= \frac{1}{N} \sum_{m=1}^N \beta^{(m)} (-1)^m\end{aligned}$$

and the inverse

$$\beta^{(m)} = \beta_0 + \sum_n (\beta_{nc} \cos n\psi_m + \beta_{ns} \sin n\psi_m) + \beta_{N/2} (-1)^m$$

for N blades, equally spaced ($\Delta\psi = 2\pi/N$) around the azimuth at $\psi_m = \psi + m\Delta\psi = \Omega t + m\Delta\psi$. The blade index m ranges from 1 to N . The summation over harmonic index n goes from $n=1$ to $(N-1)/2$ for N odd, and from $n=1$ to $(N-2)/2$ for N even. The reactionless degree of freedom $\beta_{N/2}$ appears in the transformation only if N is even. This notation is from reference 11. Appropriate notation proved elusive in the development of MBC.

The use of MBC is crucial for problems involving the rotor motion coupled with the fixed frame, such as hub motion, swashplate control, or dynamic inflow. MBC are a physically relevant, nonrotating frame representation of the rotor motion; for example, coning and tip-path plane tilt for blade flapping. Consequently, introduction of MBC separates the coupling of the rotor and fixed frame into subsets and, most importantly, eliminates periodic coefficients (except for two-bladed rotors). MBC also reduce the periodicity of the equations resulting from edgewise flight aerodynamics.

In developing the equations of motion for ground resonance of a rotor with three or more blades, Coleman (ref. 27) notes “a proper choice of coordinates leads to equations with constant coefficients.” For an n -bladed rotor, each blade with lag degree of freedom β_k ($k = 0$ to $n-1$), he introduced “special linear combinations of the hinge deflections”:

$$\theta_j = \frac{bi}{n} \sum_{k=0}^{n-1} \beta_k e^{ij\alpha k}$$

$$\zeta_k = \theta_k e^{i\alpha k}$$

where b is the distance from the lag hinge to the blade center of mass, $\alpha = 2\pi/n$ is the inter-blade spacing, and ω is the rotor rotational speed. Coleman also gives the inverse transformation, from θ_j to β_k . The θ_j variables represent the hinge motion in the rotating coordinate system, while the ζ_k variables are in the fixed system. “Geometrically, θ_1 or ζ_1 is the complex vector representing the displacement due to hinge deflection of the center of mass of all the blades.” Only ζ_1 couples with the inplane shaft motion. “The physical meaning of this partial separation of variables is that a blade motion represented by ζ_1 involves a motion of the common center of mass of the blades and, thus, a coupling effect with the pylon. Blade motions in which the common center of mass does not move are represented by ζ_2, \dots, ζ_n ”. The

variables ζ_0 and ζ_1 are recognized now as the mean and first-harmonic multiblade coordinates:

$$\zeta_0 = \theta_0 = bi\beta_0$$

$$\zeta_1 = \theta_1 e^{i\alpha} = \frac{bi}{2} (\beta_{1c} + i\beta_{1s})$$

(using $\zeta_k = \theta_k e^{ij\alpha k}$ for higher harmonics). Coleman used complex combinations of the lag degrees of freedom and the shaft-motion degrees of freedom to facilitate derivation and solution of the ground resonance equations.

Thus, Coleman recognized the physical relevance of MBC, the separation of the coupling of rotor and shaft motion, and the fact that MBC lead to equations with constant coefficients. Unfortunately, the character of the MBC was obscured by the use of complex coordinates.

Miller (ref. 182) conducted an evaluation of the stability and control characteristics of several different types of helicopters, in which MBC were used for the blade flap motion. From reference 182:

“The equations of motion will be derived by considering the displacement of the helicopter and its blades relative to a system of axes fixed in space. ... x is the displacement at any time t of the rotor hub in the X direction and α_1, β_1 , the corresponding angular displacements of the helicopter and tip path plane. ... The blade flapping may be expressed as

$$\beta_\psi = \beta_0 + \beta_1 \cos\Omega t + \beta_2 \sin\Omega t$$

higher harmonics of flapping having no effect on the stability of the helicopter as a whole. β_1 and β_2 are functions of time. β_0 is constant since the thrust is constant.”

Thus, β_1 and β_2 were the longitudinal and lateral tip-path plane tilt relative to space, while $\beta_1 - \alpha_1$ and $\beta_2 - \alpha_2$ were the tip-path plane tilt relative to the hub. The rotating-frame-flap equation of motion was derived from equilibrium of inertial, aerodynamic, and hinge spring moments. Then the fixed-frame-flap equations were obtained by separately setting the coefficients of unity, $\cos\Omega t$, and $\sin\Omega t$ to zero. Citing Coleman (ref. 27), Miller also used complex combinations of variables for the airframe inplane and angular motion and the rotor flap motion, to reduce the number of equations from 6 to 3.

Grodko (ref. 183) in the ground resonance chapter of Mil’s book cited Coleman, but used MBC instead of Coleman’s variables:

“Investigations conducted by Coleman [ref. 27] and B.Ya. Zherebtsov showed that, for a rotor with a number of blades $n \geq 3$, this system of equations can be reduced to a system of linear equations with constant coefficients, if we replace [the lag variables] $\xi_k(t)$ by new variables $x_c(t)$ and $z_c(t)$ representing the coordinates of the center of gravity of the blade system.”

The coordinate transformation used was:

$$\begin{aligned}\zeta &= \sum_{k=1}^n \xi_k \cos \psi_k \\ \eta &= \sum_{k=1}^n \xi_k \sin \psi_k\end{aligned}$$

The work presented the corresponding transformation for the time derivatives of $\xi_k(t)$ and the approach for transforming the equations of motion.

Young and Lytwyn (ref. 184) used MBC in an examination of the dynamic stability of low disk loading propeller-rotors. The motion analyzed consisted of nacelle pitch and yaw degrees of freedom, plus flapping freedoms for an N -bladed rotor ($N \geq 3$). They noted that “the N blade freedoms are reduced to two quasi coordinates by observing that of all possible patterns of blade motion, only the two representing longitudinal and lateral tilting of the tip-path plane provide a possibility of an unstable coupling with the nacelle freedoms.” The quasi-coordinates and corresponding quasi-generalized forces introduced were:

$$\begin{aligned}\beta_c &= \frac{2}{N} \sum_{n=1}^N \beta_n \cos \psi_n & \beta_s &= \frac{2}{N} \sum_{n=1}^N \beta_n \sin \psi_n \\ Q_{\beta_c} &= \frac{2}{N} \sum Q_{\beta_n} \cos \psi_n & Q_{\beta_s} &= \frac{2}{N} \sum Q_{\beta_n} \sin \psi_n\end{aligned}$$

Using β_c and β_s for the first-harmonic coordinates is a start on good notation.

Johnson and Hohenemser investigated tilting moment feedback control on a hingeless rotor (ref. 185). They defined cyclic pitch as $\theta_{cyc} = -\theta_I \sin \psi_k + \theta_{II} \cos \psi_k$, and the feedback control

$$\begin{aligned}\dot{\theta}_I &= -k_{11} \sum_{k=1}^n \beta_k \cos \psi_k - k_{12} \sum_{k=1}^n \beta_k \sin \psi_k \\ \dot{\theta}_{II} &= -k_{21} \sum_{k=1}^n \beta_k \cos \psi_k - k_{22} \sum_{k=1}^n \beta_k \sin \psi_k\end{aligned}$$

where β_k is the flap degree of freedom of the k -th blade. Then it is observed (ref. 185):

“Because of the inclusion of azimuth position, a two-axis resolution of the equations of motion is necessary. For this purpose the following definitions are made.

$$\begin{aligned}\beta_I &= \sum_{k=1}^n \beta_k \cos \psi_k \\ \beta_{II} &= \sum_{k=1}^n \beta_k \sin \psi_k\end{aligned}$$

... By use of the preceding expressions, the equations of motion in terms of the re-defined variables are obtained by first multiplying the blade equations of motion by $\cos \psi_k$, summing from $k=1$ to n and then making the appropriate substitutions. The process is then repeated for $\sin \psi_k$.”

Thus, using Roman numeral subscripts “I” and “II” for the first-harmonic MBC followed from the nomenclature for cyclic control.

Hohenemser and Yin introduced the terminology “multiblade coordinates” in the title and first sentence of refs. 186–187. They cited Coleman (ref. 27) and Young and Lytwyn (ref. 184), and then generalized MBC for an N -bladed rotor:

“The multiblade coordinates represent collective flapping or coning, differential collective flapping (only for even bladed rotors), and cyclic flapping of various orders, defining tilting or warping of the rotor plane.

The flapping angle β_k of the k -th blade in terms of multiblade flapping coordinates is

$$\begin{aligned}\beta_k &= \beta_0 + \beta_d (-1)^k + \beta_I \cos \psi_k + \beta_{II} \sin \psi_k + \\ &\quad \beta_{III} \cos 2\psi_k + \beta_{IV} \sin 2\psi_k + \beta_V \cos 3\psi_k + \\ &\quad \beta_{VI} \sin 3\psi_k + \dots\end{aligned}$$

where $\psi_k = t + (2\pi/N)(k-1)$ is the azimuth angle of the k -th blade. For an N -bladed rotor only the first N terms are retained, whereby β_d occurs only in even-bladed rotors.”

Hohenemser and Yin give the inverse transformation, and describe the method for transforming the rotating frame equations of motion to the nonrotating frame. They also analyzed the periodic differential equations of flapping motion in edgewise forward flight using Floquet theory, and demonstrated the utility of the constant coefficient equations obtained by dropping periodic terms after applying the MBC transformation.

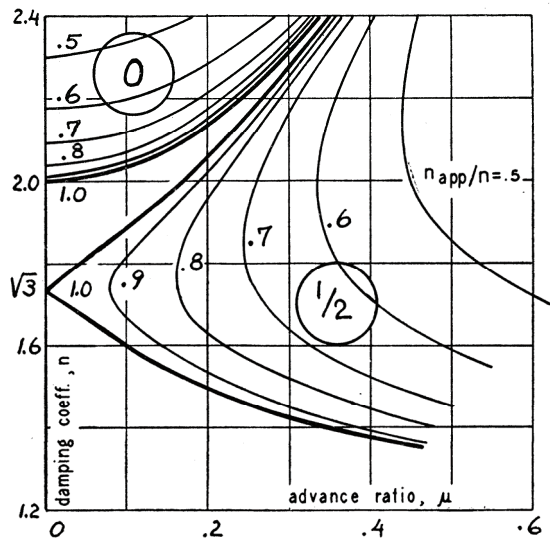


Figure 46. Rotor blade stability diagram (ref. 190).

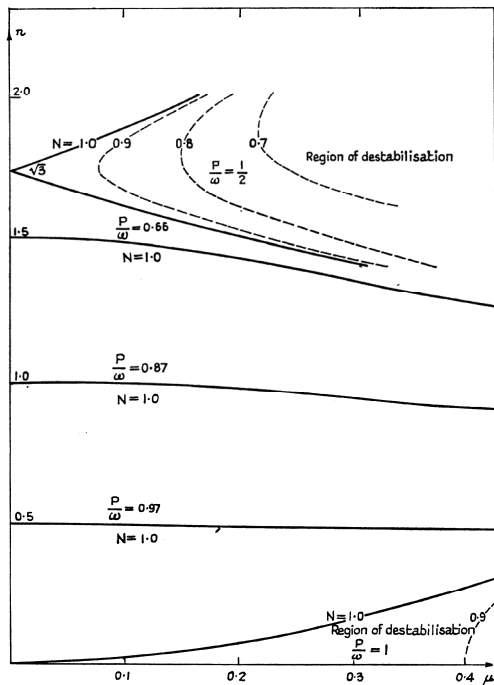


Figure 47. Regions of destabilization (ref. 194).

Floquet theory

Floquet theory is a subject that was often entwined with MBC in papers such as refs. 186–187, the connection being the periodic coefficients of rotor equations of motion, particularly with edgewise aerodynamics or two-bladed rotors. Floquet theory is a numerical method for extracting the stability of a linear, periodic dynamic system in terms of eigenvalues and periodic eigenvectors, and was described as a numerical recipe in texts on linear

systems in the 1960s (e.g., ref. 188). As a numerical solution method, Floquet theory was made practical by the digital computer, which made the study of the unique dynamic behavior of periodic systems possible.

The prototypical problem of a periodic system in rotor dynamics is the solution of the equation of blade flap motion in edgewise flight. The stability of blade flap motion has been examined by numerous investigators (refs. 189–200), beginning with Glauert. The methods used included infinite determinant, perturbation expansions and successive approximations, and numerical integration and analog computation. Horvay (ref. 190) was the first to plot the frequency and stability regions on the parameter plane of Lock number (as $n = \gamma/8$) vs. advance ratio μ (figs. 46–48). In 1970, Peters and Hohenemser (ref. 200) brought the digital computer to the task of implementing Floquet theory as an analysis tool (fig. 49). It proved to be a fast technique, although this investigation did not capture the order μ^2 behavior of the 1/rev region boundary at small μ (figure 49).

My recollection of the times is that, instead of appreciating the mathematics that describe how the world works, like physicists, we reveled in the strangeness of it all.

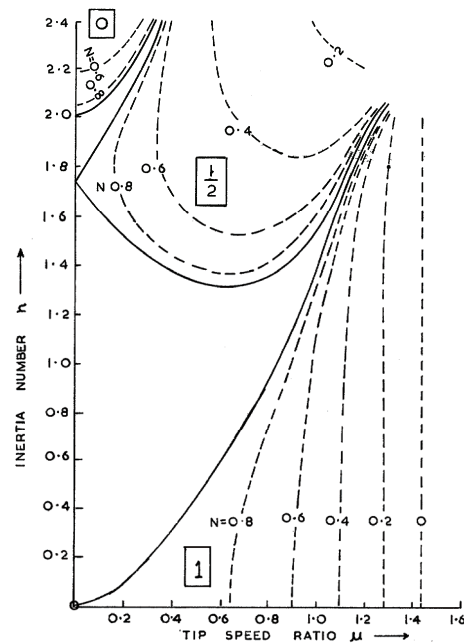


Figure 48. Rotor blade stability diagram (ref. 196).

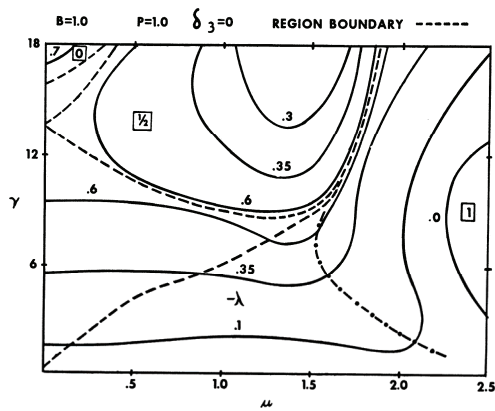


Figure 49. Damping levels of free-flapping blade (ref. 200).

COMPREHENSIVE ANALYSIS

The prototype of rotorcraft comprehensive analyses is the helicopter flight simulation computer program C81, which was developed by Bell Helicopter with major support from the U.S. Army. The complexity and multidisciplinary nature of rotorcraft aeromechanics problems demands a software tool called a comprehensive analysis: applicable to a wide range of problems (performance, loads, vibration, response, stability) and operating conditions (hover, cruise, maneuver), and a wide class of configurations (blades, hubs, rotors, aircraft), in all stages (research, conceptual design, detailed design, development) and all aspects (design, testing, evaluation) of the engineering process. The computer program C81 early on gave definition to the capabilities and expectations for such tools. The objectives as stated by Bennett in 1973 (ref. 201) were quite modern:

“The development has followed certain guidelines. First, the analysis must describe a wide variety of helicopter configurations—single rotor, compound, tandem, or side-by-side; it must also cover a broad range of flight conditions—hover, transition, cruise, or high speed. The analysis must have a uniform texture; i.e., the level of complexity of the different phases (aerodynamic, dynamic, and rotor analysis) must be uniform. The program must be applicable to diverse types of analysis—performance, stability and control, or rotor loads. The program must be user oriented in terms of preparing the input data and interpreting the results. And finally, the output format must

facilitate comparison with flight and tunnel test data.”

The early development of C81 was described in reference 202. The origin of C81 was attributed to Blankenship and Harvey (ref. 203), and Duhon, Harvey, and Blankenship (ref. 204). The prerequisite was the modern digital computer, first available at Bell Helicopter in 1959. Both of these early papers focused on the new experience of developing a computer program for engineering applications. Reference 203 devoted a paragraph to justifying the choice of a digital computer instead of an analog computer. “Based on this decision, a digital analysis for helicopter performance and rotor blade steady and oscillatory bending moments has been developed during the past three years and programmed for the IBM 7070 as a company-sponsored project.” The model was restricted to level flight and single-main-rotor configurations, but extensions were considered straightforward. Key aspects of this first code were that it modeled the entire aircraft (not just the rotor) and covered both aerodynamics and structural dynamics, earning the description “comprehensive.” Reference 204 described a computer program for the analysis of maneuver performance and handling qualities characteristics, incorporating rotor aerodynamic modeling and blade load calculation as in reference 203. The program from reference 204 was extended and used to investigate rotorcraft gust response in 1965–1967 (ref. 205). During this work the first complete documentation of the software was prepared (ref. 206). From reference 205: “A digital computer program describes the rigid-body aircraft motions in space and gives an aeroelastic representation of two rotors.” The code was applicable to single-rotor, tandem, side-by-side, and compound configurations, with articulated, semi-rigid, and rigid rotors; and calculated trim and maneuvers, subject to gusts. For reference 207, the capability to model stop-fold rotor concepts was added.

By 1967 (ref. 206), the code was called “Rotorcraft Flight Simulation Program” and designated C81. According to reference 202, “C81” doesn’t mean anything: “The C in C81 simply stood for computer program, and at the time the computing department assigned programs a number based on the order in which they were written.” For configuration control, Bell eventually adopted a different naming convention for codes, but C81 remained the common name and was considered the name of the program’s main routine.



Figure 50. U.S. Army helicopters in 1972.

In 1972, two-thirds of the more than 15,000 helicopters in the U.S. Army inventory (fig. 50) had been manufactured by Bell Helicopter (ref. 208). It is not surprising, therefore, that the Eustis Directorate of the USAAMRDL sponsored Bell Helicopter in a series of major upgrades and extensions to C81 (refs. 209–211; apparently reference 209 was never actually published). U.S. Army support of C81 development continued into 1980 (refs. 212–213).

A notable technical step was the introduction of a modal model for elastic blades. According to reference 202:

“With the 1971 release of the program, a fully time-variant aeroelastic rotor analysis was added. This feat was accomplished with the assistance of Professor N. O. Myklestad, who was a consultant to Bell Helicopter during the late 1960s. Myklestad played a pivotal role in the development of the fully coupled beam-chord-torsion aeroelastic rotor analysis. Even today the elastic rotating beam analysis used to compute rotor blade modes is simply referred to as the Myklestad program.”

Until reference 210, the codes used parametric equations to represent rotor blade section aerodynamic characteristics. Reference 210 introduced the capability to read airfoil tables, and included a built-in default table for the NACA 0012 airfoil. The C81 airfoil deck format consists of square (angle of attack and Mach number) array of data for lift, drag, and moment coefficients. The format is a fixed form designed for an IBM card: 10 columns, each 7 characters wide. The C81 airfoil deck remains a useful standard for communicating airfoil table data between organizations and between codes.

By 1973, the U.S. Army adopted C81 for rotorcraft simulation (refs. 214–215). The software was to be provided by Bell Helicopter to qualified users for design and analysis of rotary-wing aircraft (ref. 210). Reference 215 stated:

“As part of the Army’s effort to improve its capability to evaluate proposed rotary-wing aircraft and to advance helicopter technology, the Eustis Directorate has sponsored the development of computer math models to simulate all phases of helicopter flight. One such math model is the Rotorcraft Flight Simulation Program C-81, which is a generalized analysis that can encompass all of the basic rotorcraft configurations.”

Reference 214 provided a summary of the code, and reference 215 described preparations for using large, complex computer programs in the Utility Tactical Transport Aircraft System (UTTAS) evaluation, including a dry-run aircraft evaluation conducted using C81. Proposals submitted for major aircraft development programs were required to include C81 input decks, beginning with the UTTAS (1972) competition and continuing through Light Helicopter Experimental (LHX) (1988).

Several major efforts to correlate C81 calculations with test data were sponsored by the U.S. Army in the 1970s. The work covered AH-1G flight test, OLS flight test, and H-34 model data by Bell Helicopter (refs. 216–218), Bo-105 flight test data by Boeing (ref. 219), and H-53 and S-67 flight test data by Sikorsky Aircraft (ref. 220). The results were disappointing enough that the objective was stated as “to identify the strong and weak areas of C-81 prediction capability, and to establish a state-of-the-art position with regard to the global computer program concept for helicopter analysis” (ref. 220). For the H-34 model rotor correlation by Bell Helicopter (ref. 218): “Results are inconclusive due to problems related to three-dimensional and/or unsteady effects, which are especially significant for model scale rotors and which are not fully understood in the state of the art.” The assessment of the capability of C81 to model the Bo-105 hingeless rotor (ref. 219) ranged from good correlation for trim and performance, reasonable for flap bending moments, poorer correlation for rotor chord and shaft bending moments, to poor agreement for response in pull-up and pushover maneuvers. The conclusions from the application of C81 to articulated rotors (ref. 220) were very strong:

“This study did not indicate any significant increase in accuracy over other methods available for handling the disciplines covered by C81. While the ability to treat performance, stability and control, and rotor loads all within the same program has some advantages, in this case the

advantages appear to be offset by excessive running times required for performance and maneuver response problems. ... The incorporation of the C81 program as an articulated rotor helicopter design tool over existing separate helicopter performance, handling qualities, and rotor loads analyses is not recommended.”

Although partly based on modeling problems likely easily corrected (such as location of flap and lag hinges), the position against universal adoption of C81 was clear. The possibility that a comprehensive analysis developed by one helicopter company would become the standard tool throughout the industry was ill-conceived. Moreover, the C81 program “had grown difficult and unwieldy to upgrade and maintain,” and upgrades were not always successful (ref. 202).

An Advisory Group for Aerospace Research and Development (AGARD) meeting held in Milan in March 1973 (ref. 221) provided a snapshot of state-of-the-art rotor modeling, including papers from Kaman, Boeing, Aerospatiale, Sikorsky, Bell, Westland, MBB, and Lockheed. The experience of Carlson and Kerr at Lockheed (ref. 222) was to be a crucial factor in future developments, when both were leaders at the USAAMRDL.

During flight test of the AH-56A, problems with rotor stability were encountered that required the support of a fully nonlinear model called Rotor Senior, which later became REXOR (ref. 223). From reference 224: “An interdisciplinary analytical model for total vehicle simulation, revised and extended rotor (REXOR) has been developed to provide a tool for predicting the flight envelope of rotary-wing aircraft in terms of performance, dynamic stability, handling qualities, and transient load limits.” Motivated by AH-56A development, the code started as a model of the entire aircraft. From reference 222:

“An interdisciplinary analysis, which has grown out of a requirement for a nonlinear handling qualities evaluation tool, has been mechanized in a fashion which provides a capability to predict rotor loads affected by rotor/airframe interaction in steady-state and transient flight conditions.”

This mechanization was accomplished by a loads specialist modifying the nonlinear handling qualities model for rotor loads calculations. Other specialists developed their own modifications, leading to a state with inconsistent versions, unwieldy data management, and a

requirement to completely restructure the code. Recognizing the problems with this “traditional” code development approach, a new way was sought (ref. 222):

“The modeling philosophy in developing the analysis combines the capabilities of a team of analysts from several specialties to create a versatile model which provides consistent data for numerous applications.”

As described in reference 225, the new approach based on an analyst team dealt with model derivation, code structure, data management, checkout, and documentation. Reference 226 noted that Kerr recently “had the chance to implement the modeling approach outlined here by organizing an analysis team of specialists to update and restructure Lockheed’s interdisciplinary REXOR analysis.”

C81 showed what could and should be done by a rotorcraft comprehensive analysis, defining requirements by the example of its capabilities and its deficiencies. Experience with C81 and REXOR emphasized the need for a model of the complete aircraft, not just a rotor analysis. Experience sponsoring and managing rotorcraft code development showed that new approaches were needed and were possible. This was the context in which the U.S. Army embarked on the development of 2GCHAS, the Second Generation Comprehensive Helicopter Analysis System (refs. 227–228) in the late 1970s.

From there the path got complicated. The many branches of development have resulted in rotorcraft comprehensive analyses from government (2GCHAS, RCAS), helicopter industry (TECH02, COPTER, CRFM, HOST), academia (UMARC, DYMORE, MBDyn), and commercial sources (FLIGHTLAB, CHARM, CAMRAD II).

COMPUTATIONAL FLUID DYNAMICS

Advanced numerical aerodynamics today means Computational Fluid Dynamics (CFD). The quest is for an accurate first-principles solution for the flow about a helicopter rotor—three-dimensional, unsteady, vortical, compressible, viscous, and turbulent. The goal is accurate calculation of the performance, airloading, and noise of any rotor that can be built. As usual, rotation of the wing makes everything harder. In particular, modeling the returning wake demands an accurate computational domain over a volume with dimensions on the order of the rotor diameter, while also modeling flow features on the scale of the boundary layer and vortex core. I consider the

start of this quest to be the work by ONERA and the U.S. Army in 1982 on three-dimensional, unsteady analysis of lifting rotor blades (ref. 229).

The first application of CFD to the rotary wing was the paper presented by Francis X. Caradonna and Morris P. Isom in January 1972 (ref. 230). They derived the rotating-frame equation for potential flow about a rotor blade and, from it, the equation for small disturbance, transonic flow. Only hover was considered, so the equations were steady in the rotating frame. Solutions were obtained for a non-lifting rotor with rectangular blades and 6%-thick biconvex airfoil sections. The results were extended to some nonrectangular planforms in reference 231. Isom (ref. 232) extended the derivation of the small-disturbance potential equation to forward flight, using a rotating and translating coordinate system and transonic scaling as appropriate for rotor blades. The derivation of full potential and small disturbance equations was summarized in reference 233. The unsteady, three-dimensional small disturbance equations were solved for a non-lifting, rectangular planform rotor at an advance ratio of $\mu = 0.4$ (ref. 234). The difference between unsteady and quasi-steady results were significant, particularly in the decelerating flow of the second quadrant of the rotor disk.

In the early 1970s, a Memorandum of Agreement (MOA) was initiated for collaborative work in rotorcraft aeromechanics between The French Aerospace Lab, ONERA, and the U.S. Army Aeromechanics Laboratory at Ames Research Center. The first engineer from ONERA to have an extended stay at the Army Laboratory was Jean-Jacques Philippe. Experimental and numerical research on rotor aerodynamics was a major task of the MOA.

In 1975, ONERA conducted a test of an Alouette II tail rotor in the S2-Ch wind tunnel (fig. 51). The rotor and test results were described in refs. 235–237. The rotor had two blades, no twist, and symmetrical NACA sections. It was instrumented with 30 upper-surface pressure transducers at 3 tip radial stations. Rectangular planform and swept tip blades were tested with transonic tip flow at high-speed forward flight ($\mu = 0.4$ to 0.55), non-lifting. The resulting data proved to be crucial to establishing the validity of the CFD analyses being developed. Chattot and Philippe (ref. 237) showed correlation with small disturbance calculations (fig. 52), and compared results from a number of researchers with these test data.

To obtain data on a lifting rotor, ONERA tested a three-bladed rotor in the S2-Ch wind tunnel (fig. 53). The rotor and test results were described in reference 238. The blades were articulated, with -12 degrees of twist and a solidity of $\sigma = 0.137$, and straight or swept-parabolic tips. There were pressure transducers at 3 tip radial stations. The rectangular planform blade was tested in hover and forward flight, for advance ratios up to $\mu = 0.43$.

J. J. Chattot of ONERA, while on assignment at the U.S. Army Aeromechanics Laboratory, extended the method of Caradonna and Isom for solving the transonic small disturbance equation, including application to nearly arbitrary planform (ref. 239). During this period, notable work was done at NASA on quasi-static, full-potential solutions (ref. 240), and at RAE on quasi-static, small-perturbation solutions (ref. 241). Reference 238 summarized the calculations of ONERA, U.S. Army, RAE, and NASA, compared with the non-lifting ONERA data.

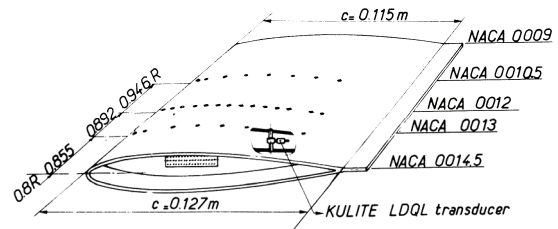
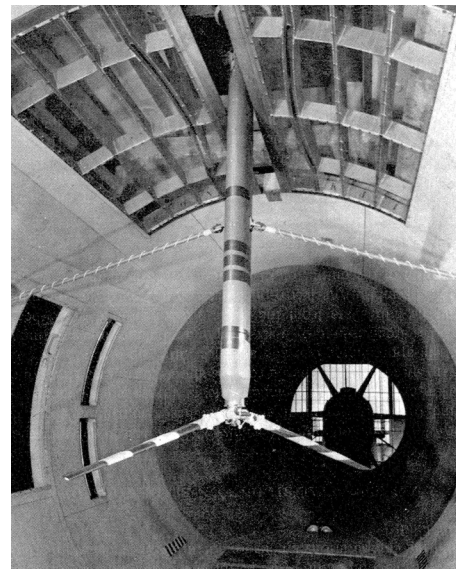


Figure 51. Rotor in S2 Chalais-ONERA wind tunnel for non-lifting tests (ref. 234).

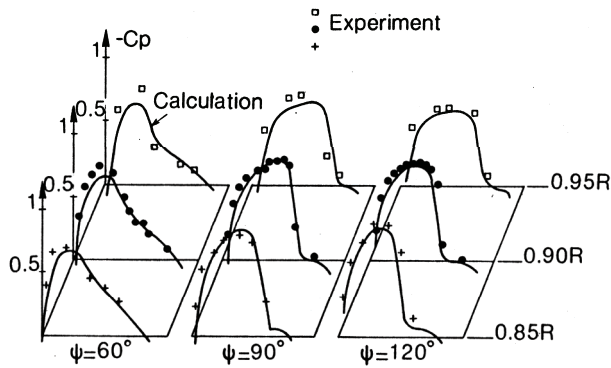


Figure 52. Comparison between calculation and experiment for straight tip, non-lifting rotor at $\mu = 0.55$ (ref. 237).

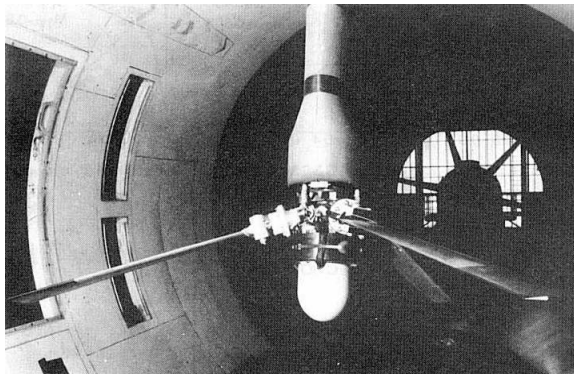


Figure 53. Three-bladed rotor in S2 Chalais-Meudon wind tunnel for lifting tests (ref. 238).

Francis X. Caradonna, Chee Tung, and Andre Desopper (ref. 229) presented calculations of the three-dimensional, unsteady, lifting flow on a rotor blade in forward flight, based on the transonic small-disturbance equations. The influence of the wake and the blade motion was accounted for by using an effective angle of attack in the blade boundary condition, calculated from a simple inflow model and the measured flapping and pitch control. The calculations were compared with the test data of reference 238 (fig. 54). Desopper (ref. 242) presented further comparisons of calculations with lifting rotor test data for both rectangular and swept-tip blades. This was the start of complete simulation of rotor flows. Reference 242 was also the start of work on including blade motion and the rotor wake effectively in the computational model, as well as extending the physics modeled by the fluid equations.

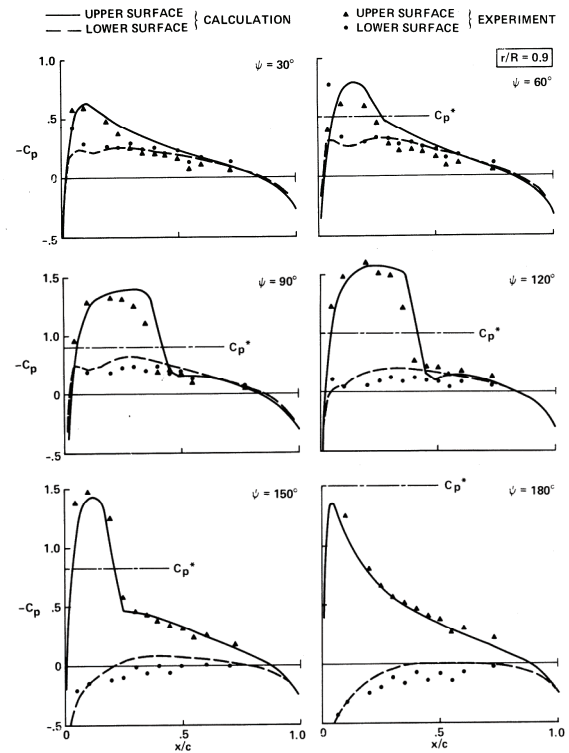


Figure 54. Comparison of measured and computed chordwise pressure distribution at different azimuth angles; $\mu = 0.39$, $C_T / \sigma = 0.0665$, $r / R = 0.90$ (ref. 229).

By the mid 1980s, solutions for rotor blade flow were published using the full potential equations (refs. 15–20) and the Euler equations (refs. 21–29). Solutions of the Navier–Stokes equations for rotors appeared in the late 1980s (refs. 30–38). Numbers of publications on rotary-wing CFD continue to grow: in my files, there are 51 papers and reports in the 1970s, 191 in the 1980s, 392 in the 1990s, and 660 in the 2000s (fig. 55). Much work is still being done on Reynolds averaged Navier–Stokes (RANS) solutions of rotor flows, particularly for wake capture, turbulence and transition, separation and dynamic stall, full aircraft models, and tight coupling with structural dynamic solutions.

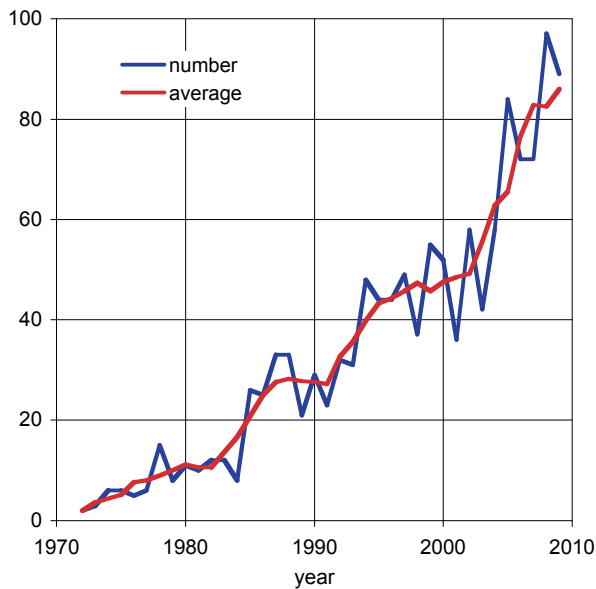


Figure 55. Publications on rotor CFD by year.

CFD/CSD LOOSE COUPLING

The interface between computational fluid dynamics (CFD) and computational structural dynamics (CSD), known as loose coupling, was developed by the author for a paper with Chee Tung and Francis X. Caradonna (ref. 243). CFD offers advances in modeling the complex aerodynamics of rotors, but for forward flight the solution must include the structural dynamic motion of the blades and trim of the aircraft. Typically, the latter tasks are handled using an existing rotorcraft comprehensive analysis (designated CSD for symmetry). The information exchanged between the CFD and CSD codes consists of integrated section aerodynamic loads and the blade section motion (or more generally, blade pressures and deformations). To combine the CFD and CSD codes requires a fluid-structure interface definition and a coupling strategy. In rotorcraft terminology, the interface methods are classified as tight coupling or loose coupling. For tight coupling, information is exchanged at every time step, often with staggered integration of the aerodynamic and structural dynamic equations, with an outer loop to handle trim. Tight coupling is required for problems involving time history solutions, such as aircraft maneuvers or aeroelastic stability assessment. Use of a time history solution method for steady-state operating conditions poses problems, particularly finding the periodic motion and the trim controls in the presence of low-damped or unstable modes, problems exacerbated by the computationally intensive nature of CFD. In loose coupling, information is exchanged for the entire revolution of periodic loads or motion, with separate time

integration in the CFD and CSD codes, and trim (adjusting controls to achieve target rotor state) is part of the comprehensive analysis (CSD) as usual.

Early in 1984, Chee Tung and Frank Caradonna of the U.S. Army were invited to contribute a paper to the aerodynamics session of the American Helicopter Society Forum. Having successfully applied CFD to rotors in hover and non-lifting forward flight, they turned their attention to the full problem of forward flight. The CFD analysis considered was the transonic small-disturbance code FDR, and the comprehensive analysis was CAMRAD. After encountering difficulties with direct application of the CFD airloads in the comprehensive analysis, they asked me to define a coupling strategy, and make the necessary modifications to CAMRAD. As described in reference 243:

“A problem arises in matching FDR to a comprehensive rotor code when a trim condition must be obtained. A trim solution typically involves computing the inflow, blade motion, and lift distribution for over 10 rotor revolutions during which the rotor controls are adjusted to achieve the desired operating state. The lift distribution so computed must not only be consistent with the inflow and blade motion, but it must also reflect the three-dimensional, unsteady, transonic flow of high-speed rotors. However, inserting a finite-difference computation in the trim loop for 10 revolutions would be prohibitively expensive. A solution to this problem is to introduce an additional outside loop, iterating between the finite-difference and integral-equation analyses. Inside the trim loop, the lift distribution is found by using the airfoil tables to find a lift *correction* to the finite-difference computed lift. That is,

$$c_{\ell}(\alpha) = c_{\ell\text{CFD}}(\alpha_{\text{old}}) + c_{\ell\text{table}}(\alpha) - c_{\ell\text{table}}(\alpha_{\text{old}})$$

where α and α_{old} are the angles of attack from the current and previous trim loops, respectively. The solution is converged when $\alpha \rightarrow \alpha_{\text{old}}$ and the lift correction vanishes—that is, when the finite-difference lift is fully consistent with the rotor inflow and motion.”

Here the section lift coefficients are $c_{\ell\text{CFD}}$ from CFD (finite-difference) and $c_{\ell\text{table}}$ from the comprehensive analysis (airfoil table). Reference 243 only considered lift coupling. The key to the coupling is to keep the comprehensive analysis aerodynamics active, responding to changes in blade motion and trim. The comprehensive analysis aerodynamics function as an estimate of the CFD

airloads due to these blade motion and trim changes. As long as this estimate is a sufficiently accurate approximation of the CFD load in the next iteration, the process will converge. This approach is also called the delta-coupling method, since the correction can be written

$$\begin{aligned}
 c_{\ell}(\alpha) &= c_{\ell_{\text{ext}}}(\alpha_{\text{old}}) + c_{\ell_{\alpha}}(\alpha - \alpha_{\text{old}}) \\
 &= c_{\ell_{\text{ext}}}(\alpha_{\text{old}}) + c_{\ell_{\text{int}}}(\alpha) - c_{\ell_{\text{old}}}(\alpha_{\text{old}}) \\
 &= c_{\ell_{\text{int}}}(\alpha) + (c_{\ell_{\text{ext}}}(\alpha_{\text{old}}) - c_{\ell_{\text{old}}}(\alpha_{\text{old}})) \\
 &= c_{\ell_{\text{int}}} + \Delta c_{\ell}
 \end{aligned}$$

where $c_{\ell_{\text{ext}}}$ is the lift obtained from the external analysis; $c_{\ell_{\text{int}}}$ is the lift calculated by the comprehensive analysis; and $c_{\ell_{\text{old}}}$ is the lift calculated by the comprehensive analysis in the previous iteration. The correction is formulated in a similar manner for drag and pitch moment, or for coefficients based on the speed of sound (M^2c), or for dimensional loads. When the iterations converge, the total load used in the comprehensive analysis equals the load calculated by CFD, which means no change of the delta load between iterations.

The CFD/CSD coupling of reference 243 was complicated by characteristics of the CFD method FDR. This small-disturbance analysis could only be applied to the outer part of the blade and only on the advancing side. The computational domain only included the wake a few chord lengths behind the blade (fig. 56). Thus, the boundary condition on the blade surface was implemented in terms of a partial angle of attack, accounting not only for the blade motion but also for the induced velocity from the wake outside the CFD domain (the partial inflow shown in fig. 56). Introducing the delta airloads in CAMRAD was a simple task; adding a calculation of the partial angle of attack required more extensive additions to the code.

The coupled solution was calculated for a 1/7-scale model of the AH-1G rotor, and compared with test data from the German-Dutch Windtunnel (DNW). Good results were obtained for the upper surface pressures on the blade (fig. 57). The CFD/CSD coupling converged in three iterations. Reference 243 concluded: "The coupling scheme is one which allows two different and independently developed codes to jointly model an entire high-speed rotor flow with few program modifications. There were no convergence problems with the iteration scheme between the differential and integral codes. ... A very limited examination of model-rotor pressure data indicates that the comparisons with the computations are not nearly of the same quality as has been achieved with non-lifting forward flight or lifting, high-speed hover model rotor data."

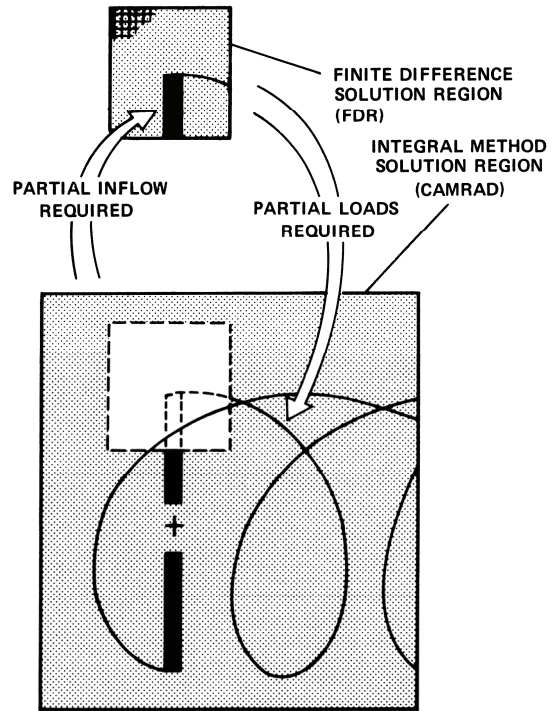


Figure 56. Matching of integral and differential rotor flow methods (ref. 243).

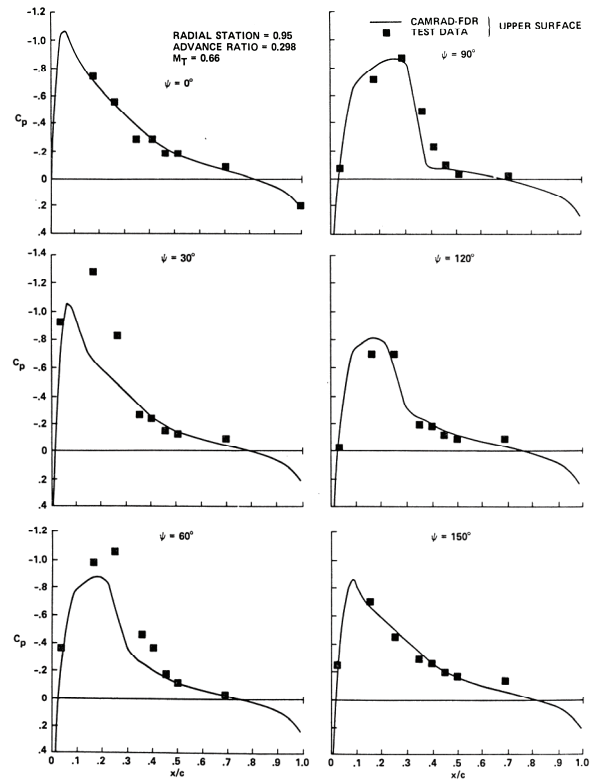


Figure 57. A comparison of computed and experimental upper surface pressures, $\mu=0.298$ and $r/R=0.95$ (ref. 243).

Results obtained in the next decade using the loose coupling method were not satisfactory, either because convergence problems were encountered or because the correlation with the experiment was not improved. Datta (ref. 244) and Tung (ref. 245) summarize the history of the loose coupling method. Moment coupling was needed, since blade torsion motion has a direct influence on the loading, yet initially moment coupling either introduced convergence problems or did not improve results.

Strawn and Tung coupled the full-potential code FPR with CAMRAD (ref. 246). The emphasis was on “including the effect of rotor wakes on the finite-difference prediction of rotor loads.” Only lift coupling was used, but for all azimuths. Results were compared with wind tunnel test data for the AH-1G model rotor, ONERA model rotor, and a blade-vortex interaction experiment. The correlation was similar to that shown in reference 243. Strawn and Tung (ref. 247) compared results from the coupled FPR and CAMRAD analysis with SA349/2 flight test data at high speed. In reference 248, FPR was coupled with CAMRAD/JA, and the airloads results compared with Puma flight test data. Again, only lift coupling was used. Because of the large cyclic pitch of the flight conditions considered, the treatment of unsteady airfoil motion in the context of the partial angle-of-attack boundary condition was an issue.

Kim, Desopper, and Chopra (ref. 249) coupled a transonic small-disturbance code TSD with UMARC, and compared the results with SA349/2 flight test data. In order to obtain convergence with both lift and pitch moment coupling, a sequential procedure was used: first only lift coupling was used, iterating until the results converged; then pitch moment coupling was introduced, but with the three-dimensional lift fixed.

Strawn and Bridgeman (ref. 250) used FPR and CAMRAD/JA, with both lift and pitch moment coupling. The calculations were compared with Puma flight test data. They found that “computed airloads show good agreement with flight-test data when lift values from the FPR code are used in the coupled calculation. However, the computed airloads from CAMRAD/JA alone also show good agreement with the experimental data.” When pitch moment coupling was used, there were convergence problems with the coupling procedure. Thus, reference 250 remarks: “It is unclear whether the current loosely-coupled iterative procedure is appropriate for introducing CFD-computed airloads into helicopter performance predictions. A more tightly-coupled procedure may be required at considerable higher computational cost.” In an investigation of tight coupling between FPX (an extended

version of the full potential code) and 2GCHAS, Lee, Saberi, and Ormiston (ref. 251) observed torsion divergence problems caused by lack of accuracy in the calculation of aerodynamic pitch moments. Reducing the time step and increasing the number of sub-iterations in the FPX calculation was necessary in order to obtain good pitch damping results.

Beaumier (ref. 252) coupled the unsteady full potential code FP3D with R85/METAR, using over-relaxation to accelerate convergence. Combined lift and pitch moment coupling converged just as well as lift coupling alone, although requiring more iterations (6 and 3 iterations respectively). Comparisons were made with data from a wind tunnel test of a the ROSOH rotor, which had soft-torsion blades. Using CFD improved the calculation of section lift, and CFD pitch moments had a significant effect on the torsion motion. The pitch moment correlation was not much better than for the comprehensive analysis results.

Servera, Beaumier, and Costes (ref. 253) coupled the Euler code WAVES with HOST, using combined lift and pitch moment coupling. Calculated results were compared with wind tunnel test data on the 7A and 7AD rotors. The use of the Euler code improved the calculation of the pitch moment at the blade tip, through the change in the 1/rev content of the blade torsion. The calculation of the lift (the CFD and comprehensive analysis results were similar) and blade torsion were not improved.

Pahlke and van der Wall (refs. 254–256) coupled the Euler/Navier–Stokes solver FLOWer with S4. Combined lift and pitch moment coupling was used, and the results compared with the 7A/7AD test data. Because of diffusion of the vorticity in the CFD calculations, the delta-airloads were filtered to retain only the harmonics up to 6/rev. The Navier–Stokes calculations improved the correlation with section lift, compared to the results using S4 alone. The improvement in pitch moment calculations was less satisfactory.

Flight test data from the UH-60A Airloads Program have provided a foundation for recent developments of advanced aerodynamic models, including CFD/CSD coupling. Correlation efforts have focused on three operating conditions (fig. 58): high speed, with negative lift on the advancing side and transonic advancing-tip flow ($\mu=0.37$, $M_{at}=0.88$, and $C_T/\sigma=0.084$); low speed, exhibiting blade-vortex interaction on advancing and retreating side ($\mu=0.15$, $M_{at}=0.74$, and $C_T/\sigma=0.076$); and high thrust, with significant dynamic stall events ($\mu=0.24$, $M_{at}=0.82$, and $C_T/\sigma=0.129$).

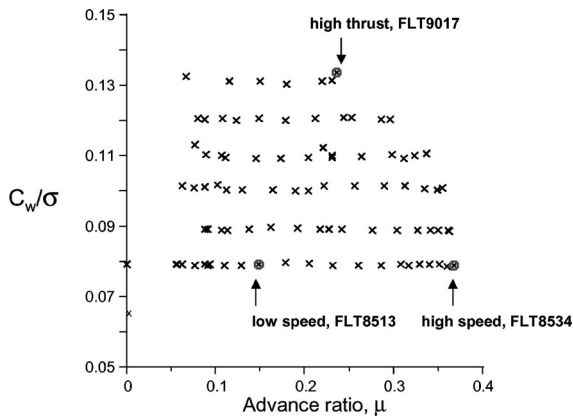


Figure 58. UH-60A Airloads Program level flight operating conditions.

Datta, Sitaraman, Baeder, and Chopra (refs. 257–258) coupled the Navier–Stokes code TURNS and UMARC. The Navier–Stokes computations were performed for the near-body domain of a single blade, with the effects of other blades included, using an induced inflow distribution (throughout the flow field) from a free-wake calculation. They compared the calculations with UH-60A Airloads Program data for the high-speed conditions. They concluded: “A 3D Navier-Stokes CFD based comprehensive analysis shows significant improvements in pitching moment predictions. Improved pitching moment predictions improve torsion-bending loads and elastic torsion deformation. Improved elastic torsion deformations improve vibratory normal force predictions at all radial stations.” Sitaraman, Datta, Baeder, and Chopra (ref. 259) coupled TURNS (using an overset mesh approach for full wake capture) and UMARC, and presented results for all three flight test conditions.

In a paper presented in 2004, Potsdam, Yeo, and Johnson (ref. 260) coupled the Navier–Stokes code OVERFLOW-D and CAMRAD II. The CFD code used high-fidelity, overset grid methodology with first-principles-based wake capturing. Loose coupling of normal force, chord force, and pitching moment was used. The three UH-60A Airloads Program flight test conditions described above were examined. The CFD calculations showed good correlation with measured lift and pitching moment for all three conditions, significantly improving upon results obtained using comprehensive analysis aerodynamic models. Reference 260 concluded:

“CFD/comprehensive analysis coupled analysis can be a significant improvement over comprehensive lifting line aerodynamics with

free wake and dynamic stall models. Normal force and pitching moment magnitudes are accurately captured in the coupled solutions. The shape of the airloads curves is usually quite accurate.

The phase of the airloads in coupled solutions when compared with test data is very good for all flight conditions. The coupled solutions resolve past problems of airloads phase prediction using comprehensive analysis.”

The blade-vortex interaction airloads were well predicted for the low-speed case, even though the far-field grid resolution (0.10 or 0.05 chord) was not sufficient to resolve tip vortex cores. Dynamic stall events were evident in the calculations, although more improvement is needed. When this work started there was some concern about the convergence of loose coupling in extreme conditions, but:

“For all cases the loose coupling methodology is shown to be stable, convergent, and robust with full coupling of normal force, pitching moment, and chord force.”

Thus, loose coupling has been confirmed as a sound and efficient method to obtain calculations of rotor loading using advanced models.

Current implementations of loose coupling (such as reference 260) use an updated delta approach:

$$\begin{aligned}
 (\Delta F)_{n+1} &= (F_{\text{ext}})_n - (F_{\text{old}})_n \\
 &= (F_{\text{ext}})_n - (F_{\text{total}} - \Delta F)_n \\
 &= (\Delta F)_n + (F_{\text{ext}} - F_{\text{total}})_n
 \end{aligned}$$

so it is not necessary to extract from the comprehensive analysis what the loading would be without the delta (F_{old}). The update of the loading increment is just the current difference between the CFD loading (F_{ext}) and the total comprehensive analysis loading (F_{total}).

The accuracy and convergence of current implementations of loose coupling owe much to the use of CFD models that simulate all the blades and all the flow field. Even if the computationally intensive Navier–Stokes calculations are limited to the blade near field, with a hybrid or approximate model of the wake, the complete aerodynamic model belongs in the CFD part of the iteration, not the comprehensive analysis. Then the interface for the CFD boundary conditions consists of just the blade motion.

HOVER AIRLOADS

Hover airloads and wake geometry measurements for correlation of rotor computational methods were obtained by Francis X. Caradonna and Chee Tung of the U.S. Army (refs. 261–262). Caradonna and Tung conducted a hover test of a stiff, two-bladed, teetering rotor with rectangular, untwisted blades and NACA 0012 airfoils (fig. 59). The simplicity of the configuration was chosen to facilitate analysis. The data were “gathered in the Army Aeromechanics Laboratory’s hover test facility, a large chamber with special ducting designed to eliminate room recirculation” (although some concern remains regarding influence of the chamber on the rotor flow). There were static pressure gages at five radial stations (three on each blade, with one radial station common between blades) and hot wire measurements of the tip vortices. Testing was conducted at several collective pitch values and a range of Mach numbers from low subsonic to transonic conditions ($M_{tip} = 0.44$ to 0.88). The pressure measurements were integrated chordwise to obtain section lift, and the rotor wake geometry was deduced from the hot wire measurements. The rotor came apart in the hover facility on the last day of testing, but all that was lost was the opportunity to take an installation photograph. Frank Caradonna still has the bent blade spar under his desk.

The test was of a lifting rotor in hover (steady) at high tip Mach numbers. The objective was stated as (refs. 261–262):

“The present study is a benchmark test to aid the development of various rotor performance codes. The study involves simultaneous blade pressure measurements and tip vortex surveys. Measurements were made for a wide range of tip Mach numbers including the transonic flow regime. ... However, there seem to be no useable data in the literature in which simultaneous blade load distribution and wake measurements were made. It is the intention of the present study to help fill this gap in the literature.”

The goal of a “benchmark test” was certainly achieved, as to date there have been more than 160 reports and papers in which the data were used to validate a computational method. For example, in reference 263 the results from full potential and small disturbance models were compared with the pressure data (fig. 60).

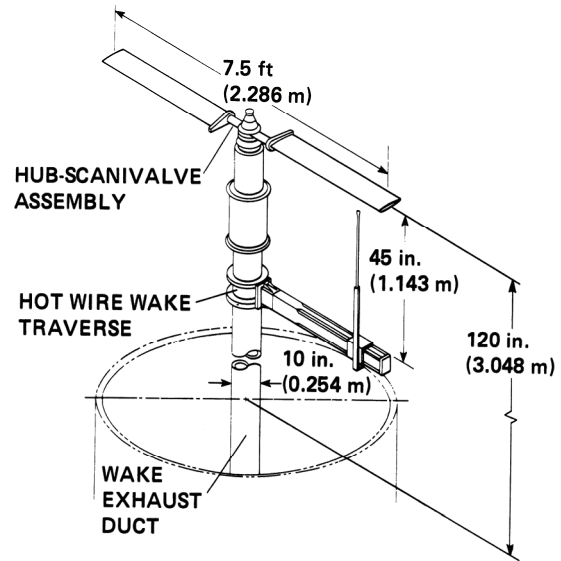


Figure 59. The model and experimental set up (ref. 261).

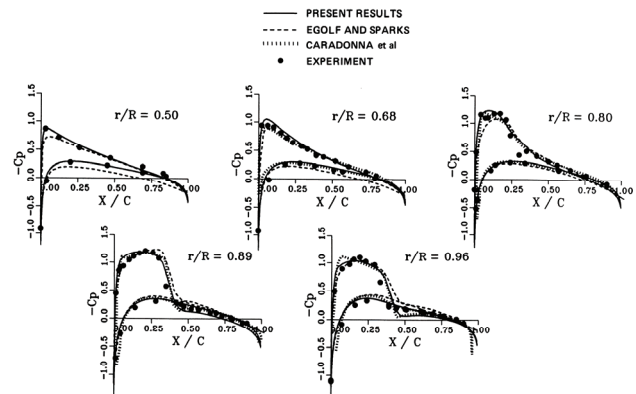


Figure 60. Comparison of measured and calculated surface pressure results for hovering rotor, $M_{tip} = 0.877$ and 8-degree collective pitch (ref. 263).

ROTOR AIRLOADS TESTS

“The knowledge of the distribution of the airloads on a rotor blade in flight is fundamental to an understanding of how a helicopter works and for the design of new and improved rotorcraft” (William G. Bousman, ref. 264). Flight test measurements of the aerodynamic pressures and structural loads on the rotating blades of a helicopter rotor are essential to developing an understanding of, and the capability to predict, the performance, loads, vibration, and noise of rotorcraft. In a survey of “all major wind tunnel and full-scale flight tests ... to examine the nature of the vibratory aerodynamic loading which causes helicopter vibration,” Hooper (ref. 265) identified 10 major airloads programs from 1956 to 1984, beginning

with Rabbott and Churchill (ref. 71). Since 1956, there have been perhaps 40 airloads test programs conducted. Of these, 3 have proven to have substantial, lasting value: the H-34 flight test and wind tunnel test (refs. 72, 74, 266–268), the UH-60A Airloads Program flight test and wind tunnel test (refs. 264 and 269), and the HART wind tunnel tests (refs. 270–271). My records show 76, 113, and 167 papers and reports based on the data from these 3 test programs, respectively.

H-34 flight test

In 1961–1962, flight tests of an H-34 helicopter were conducted at NASA (fig. 61). From reference 74:

“An extensive flight test program was conducted at the Langley Research Center to obtain helicopter rotor-blade airloads, bending moments, and blade motions. In addition, numerous flight parameters were recorded. The tabulated data presented herein are for forward speeds from 0 to 120 knots, flights in and out of ground effect, climbs, autorotations, maneuvers, and operations with forward and aft center-of-gravity locations.”

Three additional trim-level flight conditions were presented and discussed in reference 72, covering $\mu=0.18$ (blade-vortex interaction), $\mu=0.23$ (retreating blade stall), and $\mu=0.11$. The blades were instrumented with 49 differential pressure gages at 7 radial stations (fig. 62). There were 11 chordwise measurements at $r=0.85R$, 5 chordwise at the 2 inboard radial stations, and 7 chordwise at the remaining stations. Reference 74 provides a complete description of the geometric, inertial, and structural dynamic characteristics of the blades.

The instrumented rotor was mounted on a test stand and tested in the 40- by 80-Foot Wind Tunnel at NASA Ames Research Center in September 1964 (fig. 63, refs. 266–268). The NASA Project Engineer was John L. McCloud III. From reference 266: “The purpose of the present investigation was to extend the range of available aerodynamic and structural loading data to higher forward speeds.” The maximum level flight speed in the flight test was 115 knots (ref. 74), giving $\mu=0.29$. The wind tunnel test covered speeds of 110, 150, and 175 knots ($\mu=0.29$, 0.39, and 0.45) at shaft angles of $\alpha_s=-5$, 0, and 5 degrees. Seven pressure gages were added at two tip radial stations, for a total of 56 differential pressure gages (fig. 64). A difficulty with the control system was encountered in the test program (ref. 266):

“Certain modifications to the CH-34 control system were made to minimize pitch-lag

coupling and to provide for adequate strength to react the anticipated control loads which, at the high speeds and advance ratios possible in the wind tunnel, were expected to be in excess of the CH-34 design loads. The swashplate, scissors, and control horn were redesigned. ...

In anticipation of the high control loads that would be generated at high tunnel speeds, the control system was modified and strengthened as described previously. However, the modification resulted in an unusual control system kinematic coupling such that two adjacent blades had a slightly different cyclic pitch from the other two adjacent blades, which resulted in a “split” tip path plane whenever cyclic pitch was applied. The instrumented blade and the preceding blade (whose vortex system has the primary influence on the following blade) were always in plane, but the other two blades were flapped approximately one degree higher.”

Figure 65 is a sketch by McCloud of the rotating scissors change that was responsible for the difference in cyclic pitch. In order to minimize the tip-path plane split, the test was not conducted as originally planned, with zero first harmonic flapping relative to the shaft. The longitudinal flapping magnitude ranged from 0 to 1.8 degrees for the test conditions, and the lateral flapping ranged from 2.8 to 4.4 degrees.

The test data were discussed in references 74, 266, 268, and 272–274. Rabbott (ref. 275) compared small-scale and full-scale test data.

The H-34 flight test data found immediate use in developing rotor wake models (particularly the test points in reference 72), use that continues today (refs. 58, 62, 67, 276–280). Both Miller (fig. 17, ref. 58) and Piziali (fig. 24, ref. 67) compared airloads calculations with the H-34 data. Ward (ref. 274) used the flight test data to explore the aerodynamics of maneuvers. The H-34 wind tunnel data was the principal information Hooper (ref. 265) used to examine the blade vibratory aerodynamic loading. In this investigation he identified the possible influence in high speed of blade-vortex interaction with the opposite sign compared to low speed, due to the negative loading on the tip of the advancing blade. Yeo and Johnson (refs. 279–280) included both the wind tunnel data and the flight test data in a correlation of airloads and structural loads with CAMRAD II calculations.



Figure 61. H-34 flight test aircraft (ref. 74).

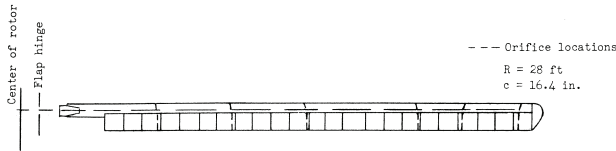


Figure 62. Blade planform and instrumentation for the H-34 flight test (ref. 74).



Figure 63. H-34 airloads rotor in the 40- by 80-Foot Wind Tunnel.

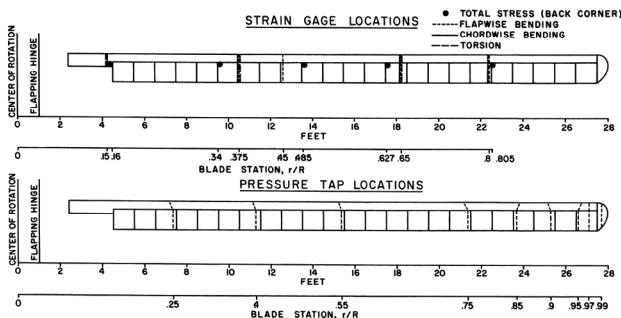


Figure 64. Blade planform and instrumentation for the H-34 wind tunnel test (ref. 268).

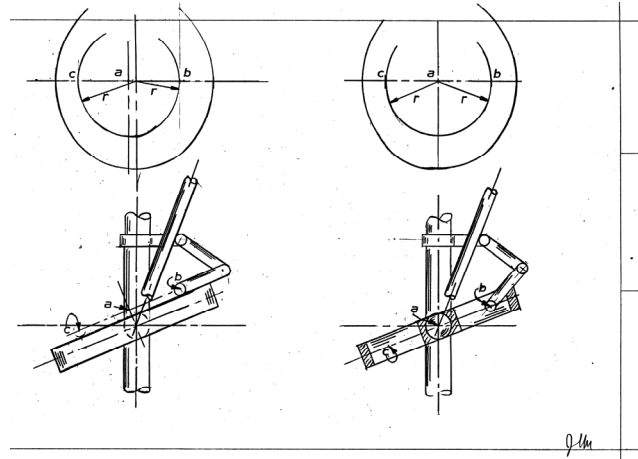


Figure 65. Rotating scissors geometry for the H-34 wind tunnel model (John L. McCloud III).

UH-60A Airloads Program

Flight tests of a UH-60A helicopter were conducted at Ames Research Center in 1993–1994 (fig. 66). The UH-60A Airloads Program “was designed to overcome weaknesses of past programs in terms of the quality and quantity of data, the bandwidth of the data, and ease of accessibility to the data” (ref. 264). Bousman (ref. 281) described the history of the program:

“The UH-60A Airloads Program was carried out by NASA Ames Research Center and the U.S. Army Aeroflightdynamics Directorate from 1984 to 1994, when flight testing was completed.

In the mid-1980s, NASA Ames Research Center devised an elaborate plan to extensively test seven or more modern rotors and develop a data base that would include flight test data, wind tunnel data, model-scale data, and fuselage shake test data for these helicopters and their rotors [ref. 282]. The first helicopter selected under this plan was the UH-60A. A contract was let with Sikorsky Aircraft in 1985 for the construction of a set of test hardware that included one blade with 242 pressure transducers and a second blade instrumented with strain gauges and accelerometers. Model-scale testing of this rotor system was accomplished under separate U.S. Army programs [refs. 283–284].

The instrumented rotor blades were delivered to NASA Ames Research Center at the end of 1988. However, the integration of the extensive suite of rotor instrumentation and the hub-mounted Rotating Data Acquisition System (RDAS) became the critical element in the test program.

Tests of early versions of the RDAS system in 1991 and 1992 were unsuccessful. The third RDAS system was demonstrated successfully at the end of 1992 and flight testing was scheduled to start in the summer of 1993.

On May 14, 1993 the UH-60A Airloads Program was cancelled by NASA Ames Research Center because of budget shortfalls. However, funding was in place to allow testing through the end of the fiscal year, September 30, 1993. Flights 82 to 85 were flown prior to the end of September, and NASA reprogrammed funds to allow testing to continue through the end of February 1994 when Flight 116 was completed.”

The test program was described in reference 264. Flight tests were conducted from August 1993 to February 1994. There were 31 research flights for a total of 57 flight hours. Over 900 different test conditions were recorded, processed, and stored in an electronic data base (ref. 269). The test conditions included hover, level flight, climbs and descents, and maneuvers. Figure 67 illustrates some of the test conditions. The blades were instrumented with 241 (ref. 269) absolute pressure gages, 221 in chordwise arrays at 9 radial stations (20 per section inboard, 30 per section near the tip) and the remainder along the leading edge (fig. 68).

The flight test data were discussed in refs. 285–290, including the maneuver data. Tung, Bousman, and Low (ref. 291) compared small-scale and full-scale test data.

The instrumented rotor was mounted on the LRTA (Large Rotor Test Apparatus) and tested in the 40- by 80-Foot Wind Tunnel in March–May 2010 (fig. 69). Reference 292 provides an overview of the wind tunnel test.

The UH-60A Airloads Program data are being used extensively to develop advanced aerodynamics models, including CFD/CSD coupling. Correlation efforts have focused on three operating conditions (fig. 58), as well as the UTTAS maneuver.



Figure 66. UH-60A Airloads aircraft over the Livermore valley (ref. 269).

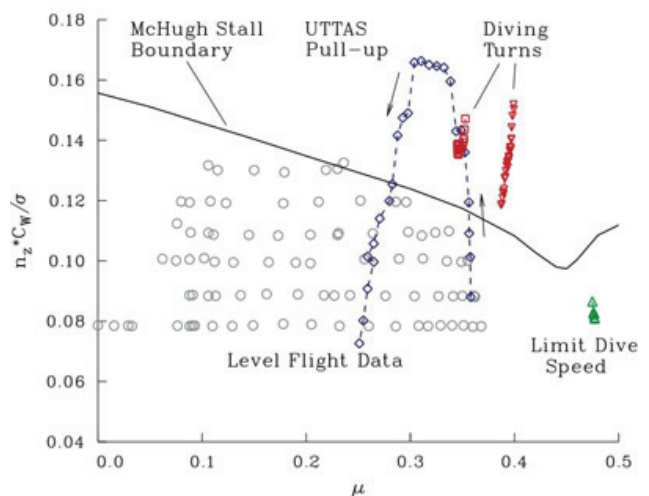


Figure 67. UH-60A Airloads Program test conditions.

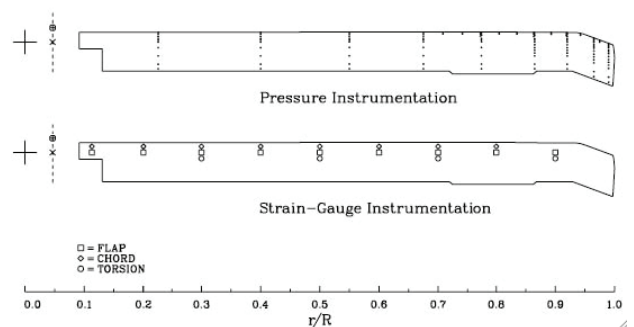


Figure 68. UH-60A blade planform and instrumentation (ref. 269).



Figure 69. UH-60A Airloads rotor in the 40- by 80-Foot Wind Tunnel.

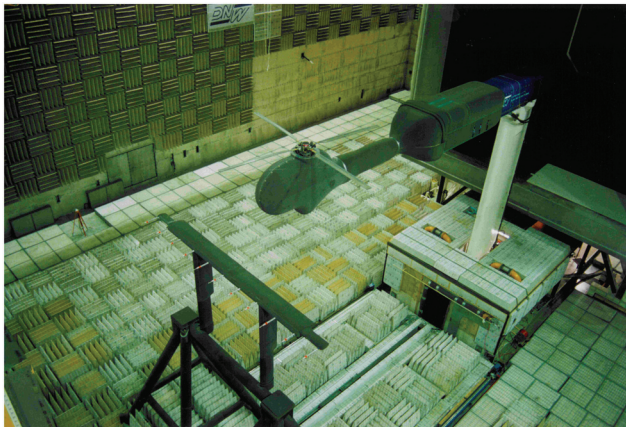


Figure 70. HART I rotor test in the DNW wind tunnel.

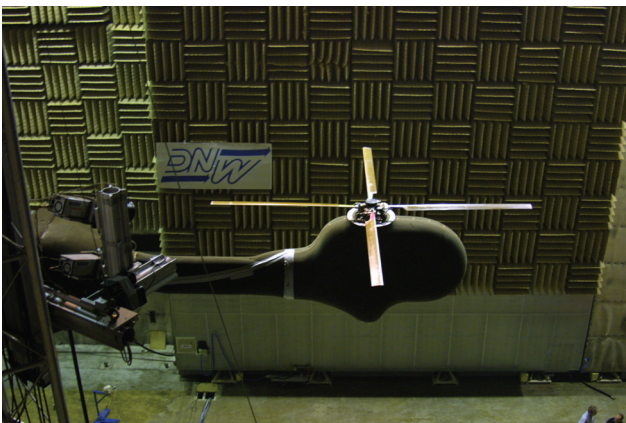


Figure 71. HART II rotor test in the DNW wind tunnel.

HART wind tunnel tests

Wind tunnel tests of a model Bo-105 rotor with higher harmonic control were conducted in June 1994 (HART I, fig. 70) and October 2001 (HART II, fig. 71). The tests are described in references 293–298. From reference 293:

“In a major cooperative program within existing US-German and US-French Memoranda of Understanding (MOUs), researchers from the German DLR, the French ONERA, NASA Langley, and the US Army Aeroflightdynamics Directorate (AFDD) conducted a comprehensive experimental program with a 40%-geometrically and aeroelastically scaled model of a BO-105 main rotor in the open-jet anechoic test section of the German-Dutch Windtunnel (DNW) in The Netherlands. The objective of the program was to improve the basic understanding and the analytical modeling of the effects of the higher harmonic pitch control technique on rotor noise and vibration reduction. Comprehensive acoustic, aerodynamic, dynamic, performance, and rotor wake data were obtained with a pressure-instrumented rotor blade. This international cooperative project carries the acronym HART (Higher-harmonic-control Aeroacoustics Rotor Test).”

The HART program started in 1990 and was concluded in 2010. The test directors were Roland Kube of DLR for HART I and Berend van der Wall of DLR for HART II. For both tests, Casey Burley of NASA led the prediction team activity as well as assisted the test directors.

The HART I blades were instrumented with 124 absolute pressure gages in 3 radial stations (fig. 72a). The chordwise arrays had 44 gages at $r = 0.75R$ and $r = 0.97R$, and 24 gages at $r = 0.87R$.

The objective of the HART II test was to obtain more extensive particle image velocimetry (PIV) measurements of the rotor wake (ref. 298); figure 73 illustrates the PIV measurement locations. The focus of HART II was on three conditions at $\mu = 0.15$: a baseline case without higher-harmonic control, and minimum noise and minimum vibration cases with 3/rev higher-harmonic control (both 0.8 degrees amplitude, different phases). From reference 297:

“Due to an accident in a preceding test the Bo105 model rotor used during the HART test of 1994 was not available. An existing uninstrumented Bo105 model rotor was thus upgraded with 51 absolute pressure transducers for the HART II

test. However, the rotor, although designed for the same fundamental frequencies in flap, lead-lag and torsion, had different behaviour in torsion due to a different design of the main spar and the location of the elastic and the center of gravity axis.”

Thus, for HART II, the blades had 51 absolute pressure gages on two blades, mainly at $r = 0.87R$ (fig. 72b).

The HART data are being used extensively to develop advanced aeroacoustics models for rotor blades. The test data are limited by the scale of the rotor, and by only consisting of pressure data at a few (three or one) radial stations near the blade tip. The HART program, however, includes higher-harmonic control, extensive acoustic and wake flow field measurements, and involves an international team of researchers.

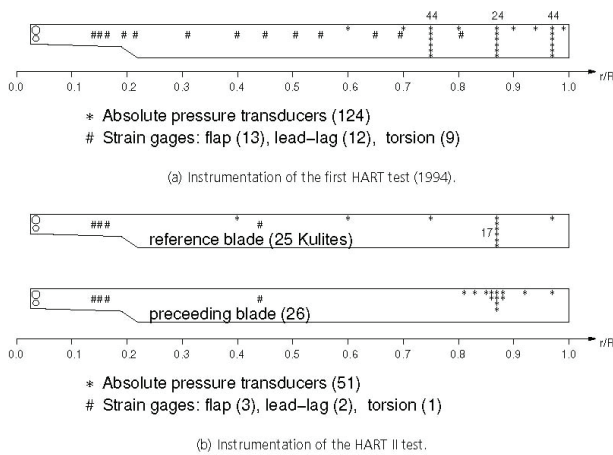


Figure 72. Blade planform and instrumentation for the HART wind tunnel tests (ref. 271).

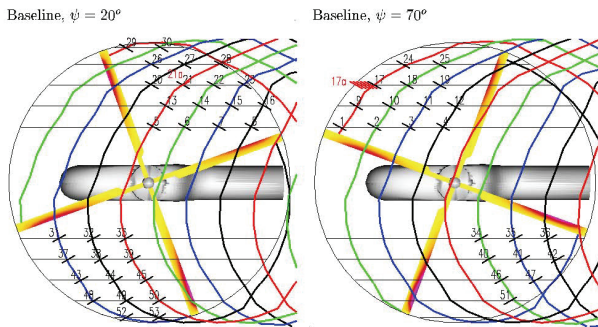


Figure 73. PIV test matrix (ref. 271).

CONCLUSION

The milestones in rotorcraft aeromechanics discussed herein are summarized in Table 1. It is a subjective list; others would no doubt make different choices. The list reflects my belief that a perspective of some years is needed to judge an event to be a critical achievement or a turning point, so we can see what made a difference.

The future will produce experiments that so define an issue that they achieve universal acceptance as essential bases for correlation, and produce theories that take the models and codes to the next level of simulation of rotary-wing aircraft. We know that there will be steady progress to advance our capability in all the disciplines of aeromechanics. Most of this progress will be achieved by many steps from numerous contributors. Sometimes there will be a critical idea or a unique insight—a new milestone—that changes the way we understand, attack, and solve a problem.

One lesson from this examination of aeromechanics is that care should be taken to compose good introductions for our papers and reports. Remember that we are writing for the historical record. It was helpful to be able to discuss the work with its authors. In some cases I discovered that the sequence of events was not as I had long believed. Several topics were dropped from consideration because I could not find a single critical event to call a milestone.

The focus on milestones was necessary to limit the scope of this history. The format allowed me to acknowledge work that I consider to be key steps in the development of the science and engineering of rotorcraft. A consequence of this approach is that now I would very much look forward to seeing a complete history of rotorcraft aeromechanics.

REFERENCES

1. Glauert, H.: A General Theory of the Autogyro. ARC R&M 1111, Nov. 1926.
2. Glauert, H.: The Theory of the Autogyro. The Journal of the Royal Aeronautical Society, vol. 31, no. 198, June 1927, pp. 483–508.
3. de la Cierva, J.: The Development of the Autogyro. The Journal of the Royal Aeronautical Society, vol. 30, no. 181, Jan. 1926, pp. 7–29.
4. Glauert, H., and Lock, C. N. H.: A Summary of the Experimental and Theoretical Investigations of the Characteristics of an Autogyro. ARC R&M 1162, Apr. 1928.
5. Lock, C. N. H.: Further Development of Autogyro Theory. ARC R&M 1127, Mar. 1927.
6. de la Cierva, J.: The Autogiro. The Journal of the Royal Aeronautical Society, vol. 34, no. 239, Nov. 1930, pp. 902–921.
7. Glauert, H.: The Elements of Aerofoil and Airscrew Theory. Cambridge: Cambridge University Press, 1926.
8. de la Cierva, J.: Engineering Theory of the Autogiro; Theory of Stresses on Autogiro Rotor Blades. J.A.J. Bennett (Ed.) c.1933.
9. Brooks, P. W.: Cierva Autogiros. Washington, D.C.: Smithsonian Institution Press, 1988.
10. de la Cierva, J.: New Developments of the Autogiro. The Journal of the Royal Aeronautical Society, vol. 39, no. 300, Dec. 1935, pp. 1125–1143.
11. Johnson, W.: Helicopter Theory. Princeton, New Jersey: Princeton University Press, 1980.
12. Lock, C. N. H.; Bateman, H.; and Townend, H. C. H.: An Extension of the Vortex Theory of Airscrews with Applications to Airscrews of Small Pitch, Including Experimental Results. ARC R&M 1014, Sep. 1925.
13. Glauert, H.: The Analysis of Experimental Results in the Windmill Brake and Vortex Ring States of an Airscrew. ARC R&M 1026, Feb. 1926.
14. Glauert, H.: Airplane Propellers. Aerodynamic Theory, Durand, W.F. (Ed.). New York: Julius Springer, 1935.
15. Hafner, R.: Rotor Systems and Control Problems in the Helicopter. Royal Aeronautical Society Anglo-American Aeronautical Conference, Sept. 1947.
16. Lock, C. N. H.: Note on the Characteristic Curve for an Airscrew or Helicopter. ARC R&M 2673, June 1947.
17. Bennett, J. A. J.: Rotary-Wing Aircraft. Aircraft Engineering, vol. 12, no. 133, Mar. 1940, pp. 131–8.
- 18) Harris, F. D.: Preliminary Study of Radial Flow Effects on Rotor Blades. Journal of the American Helicopter Society, vol. 11, no. 3, July 1966, pp. 1–21.
19. Harris, F. D.: Rotor Performance at High Advance Ratio; Theory versus Test. NASA CR–2008-215370, Oct. 2008.
20. Wheatley, J. B.: An Aerodynamic Analysis of the Autogiro Rotor with a Comparison Between Calculated and Experimental Results. NACA Report 487, 1934.
21. Sissingh, G.: Contribution to the Aerodynamics of Rotating-Wing Aircraft. NACA TM 921, Dec. 1939.
22. Bailey, F. J., Jr.: A Simplified Theoretical Method of Determining the Characteristics of a Lifting Rotor in Forward Flight. NACA Report 716, 1941.
23. Castles, W., Jr., and New, N. C.: A Blade-Element Analysis for Lifting Rotors That is Applicable for Large Inflow and Blade Angles and Any Reasonable Blade Geometry. NACA TN 2656, July 1952.
24. Gessow, A., and Crim, A. D.: An Extension of Lifting Rotor Theory to Cover Operation at Large Angles of Attack and High Inflow Conditions. NACA TN 2665, Apr. 1952.
25. Gessow, A., and Crim, A. D.: A Method for Studying the Transient Blade-Flapping Behavior of Lifting Rotors at Extreme Operating Conditions. NACA TN 3366, Jan. 1955.
26. Gessow, A.: Equations and Procedures for Numerically Calculating the Aerodynamic Characteristics of Lifting Rotors. NACA TN 3747, Oct. 1956.
27. Coleman, R. P.: Theory of Self-Excited Mechanical Oscillations of Hinged Rotor Blades. NACA ARR 3G29, July 1943.
28. Coleman, R. P., and Feingold, A. M.: Theory of Self-Excited Mechanical Oscillations of Helicopter Rotors with Hinged Blades. NACA Report 1351, 1958.
29. Feingold, A. M.: Theory of Mechanical Oscillations of Rotors With Two Hinged Blades. NACA ARR 3I13, Sept. 1943.

30. Coleman, R. P., and Feingold, A. M.: Theory of Ground Vibrations of a Two-Blade Helicopter Rotor on Anisotropic Flexible Supports. NACA TN 1184, Jan. 1947.
31. Coleman, R. P., and Feingold, A. M.: Theory of Self-Excited Mechanical Oscillations of Helicopter Rotors with Hinged Blades. NACA TN 3844, Feb. 1957.
32. Connor, R. D.: Wrecked Rotors: Understanding Rotorcraft Accidents, 1935-1945. American Helicopter Society 66th Annual Forum, Phoenix, AZ, May 2010.
33. Prewitt, R. H., and Wagner, R. A.: Frequency and Vibration Problems of Rotors. *Journal of the Aeronautical Sciences*, vol. 7, no. 10, Aug. 1940, pp. 444-450.
34. Gregory, H. F.: *The Helicopter*. Cranbury, New Jersey: A. S. Barnes and Co., Inc., 1976.
35. Gustafson, F. B.: History of NACA/NASA Rotating-Wing Aircraft Research, 1915-1970; Part II. *Vertiflite*, vol. 16, no. 7, July 1970, pp. 10-15.
36. Gustafson, F. B.: History of NACA/NASA Rotating-Wing Aircraft Research, 1915-1970; Part III. *Vertiflite*, vol. 16, no. 10, Oct. 1970, pp. 14-18.
37. Wagner, R. A.: *Vibrations Handbook for Helicopters*. Wright Air Development Center, 1954 (Vol. 7 of *Rotary Wing Aircraft Handbooks and History*, Edited by E. K. Liberatore).
38. Deutsch, M. L.: Ground Vibrations of Helicopters. *Journal of the Aeronautical Sciences*, vol. 13, no. 5, May 1946, pp. 223-234.
39. Deutsch, M. L.: Theory of Mechanical Instability of Rotors. Air Materiel Command, Engineering Division, Memorandum Report No. ENG-M-51/VF42, Add. 1, Jan. 1946.
40. Focke, H.: Fortschritte des Hubschraubers, *Schriften der Deutschen Akademie der Luftfahrt-Forschung* (Vortrag gehalten auf der 7. Wissenschaftssitzung der Ordentlichen Mitglieder am 1. Oktober 1943), no. 1070/43g, Oct. 1943, pp. 3-52; Improvements of the Helicopter, *Publications of the German Academy of Aeronautical Research* (lecture held at 7th scientific meeting of the regular members on Oct. 1, 1943).
41. Prewitt, R. H.: Report on Helicopter Developments in Germany. Society of Automotive Engineers, New York, Aug. 1945.
42. Gessow, A., and Myers, G. C., Jr.: *Aerodynamics of the Helicopter*. New York: The Macmillan Company, 1952.
43. Nikolsky, A. A.: *Helicopter Analysis*. New York: John Wiley & Sons, Inc., 1951.
44. Bennett, J. A. J.: Book Reviews, 'Aerodynamics of the Helicopter.' By Alfred Gessow and Garry C. Myers Jr. *The Journal of the Helicopter Association of Great Britain*, vol. 8, no. 4, Apr. 1955, p. 195.
45. Loewy, R. G.: A Two-Dimensional Approximation to the Unsteady Aerodynamics of Rotary Wings. *Journal of the Aeronautical Sciences*, vol. 24, no. 2, Feb. 1957, pp. 81-92.
46. Hirsch, H.: The Contribution of Higher Mode Resonance to Helicopter Rotor-Blade Bending. *Journal of the Aeronautical Sciences*, vol. 20, no. 6, June 1953, pp. 407-425.
47. Daughaday, H., and Kline, J.: An Approach to the Determination of Higher Harmonic Rotor Blade Stresses. American Helicopter Society 9th Annual National Forum, Washington, D.C., May 1953.
48. Timman, R., and van de Vooren, A. I.: Flutter of a Helicopter Rotor Rotating in Its Own Wake. *Journal of the Aeronautical Sciences*, vol. 24, no. 9, Sept. 1957, pp. 694-702.
49. Jones, J. P.: The Influence of the Wake on the Flutter and Vibration of Rotor Blades. *The Aeronautical Quarterly*, vol. 9, part 3, Aug. 1958, pp. 258-286.
50. Daughaday, H.; DuWaldt, F.; and Gates, C.: Investigation of Helicopter Rotor Flutter and Load Amplification Problems. CAL Report No. SB-862-S-4, Aug. 1956.
51. Daughaday, H.; DuWaldt, F.; and Gates, C.: Investigation of Helicopter Blade Flutter and Load Amplification Problems. *Journal of the American Helicopter Society*, vol. 2, no. 3, July 1957, pp. 27-45.
52. Ham, N. D.; Moser, H. H.; and Zvara, J.: Investigation of Rotor Response to Vibratory Aerodynamic Inputs. Part I. Experimental Results and Correlation with Theory. WADC TR 58-87, Part I, Oct. 1958.
53. Silveira, M. A., and Brooks, G. W.: Dynamic-Model Investigation of the Damping of Flapwise Bending Modes of Two-Blade Rotors in Hovering and a Comparison With Quasi-Static and Unsteady Aerodynamic Theories. NASA TN D-175, Dec. 1959.
54. Miller, R. H.: Rotor Blade Harmonic Air Loading. IAS Paper No. 62-82, Jan. 1962.

55. Miller, R. H.: Rotor Blade Harmonic Air Loading. *AIAA Journal*, vol. 2, no. 7, July 1964, pp. 1254–1269.
56. Miller, R. H.: On the Computation of Airloads Acting on Rotor Blades in Forward Flight. *Journal of the American Helicopter Society*, vol. 7, no. 2, Apr. 1962, pp. 56–66.
57. Miller, R. H.: A Discussion of Rotor Blade Harmonic Airloading. CAL/TRECOM Symposium on Dynamic Load Problems Associated with Helicopters and V/STOL Aircraft, Buffalo, NY, June 1963.
58. Miller, R. H.: Unsteady Air Loads on Helicopter Rotor Blades. *Journal of the Royal Aeronautical Society*, vol. 68, no. 640, Apr. 1964, pp. 217–229.
59. Miller, R. H.: Theoretical Determination of Rotor Blade Harmonic Airloads. MIT ASRL TR 107-2, Aug. 1964.
60. Scully, M. P.: Approximate Solutions for Computing Helicopter Harmonic Airloads. MIT ASRL TR 123-2, Dec. 1965.
61. Scully, M.P.: A Method of Computing Helicopter Vortex Wake Distortion. MIT ASRL TR 138-1, June 1967.
62. Scully, M. P.: Computation of Helicopter Rotor Wake Geometry and Its Influence on Rotor Harmonic Airloads. MIT ASRL TR 178-1, Mar. 1975.
63. Piziali, R. A., and DuWaldt, F. A.: A Method for Computing Rotary Wing Airload Distribution in Forward Flight. TCREC TR 62-44, Nov. 1962.
64. Piziali, R., and DuWaldt, F.: Computed Induced Velocity, Induced Drag, and Angle of Attack Distribution for a Two-Bladed Rotor. American Helicopter Society 19th Annual National Forum, Washington, D.C., May 1963.
65. Piziali, R. A.; Daughaday, H.; and DuWaldt, F.: Rotor Airloads. CAL/TRECOM Symposium on Dynamic Load Problems Associated with Helicopters and V/STOL Aircraft, Buffalo, NY, June 1963.
66. Piziali, R. A.: A Method for Predicting the Aerodynamic Loads and Dynamic Response of Rotor Blades. USAAVLABS TR 65-74, Jan. 1966.
67. Piziali, R. A.: Method for the Solution of the Aeroelastic Response Problem for Rotating Wings. *Journal of Sound and Vibration*, vol. 4, no. 3, 1966, pp. 445–489.
68. Daughaday, H., and Piziali, R. A.: An Improved Computational Model for Predicting the Unsteady Aerodynamic Loads of Rotor Blades. *Journal of the American Helicopter Society*, vol. 11, no. 4, Oct. 1966, pp. 3–10.
69. Falabella, G., Jr., and Meyer, J. R., Jr.: Determination of Inflow Distributions From Experimental Aerodynamic Loading and Blade-Motion Data on a Model Helicopter Rotor in Hovering and Forward Flight. NACA TN 3492, Nov. 1955.
70. Ham, N. D., and Zvara, J.: Experimental and Theoretical Analysis of Helicopter Rotor Hub Vibratory Forces. WADC TR 59-522, Oct. 1959.
71. Rabbott, J. P., Jr., and Churchill, G. B.: Experimental Investigation of the Aerodynamic Loading on a Helicopter Rotor Blade in Forward Flight. NACA RM L56I07, Oct. 1956.
72. Scheiman, J., and Ludi, L. H.: Qualitative Evaluation of Effect of Helicopter Rotor-Blade Tip Vortex on Blade Airloads. NASA TN D-1637, May 1963.
73. Burpo, F. B., and Lynn, R. R.: Measurement of Dynamic Air Loads on a Full-Scale Semirigid Rotor. TCREC TR 62-42, Dec. 1962.
74. Scheiman, J.: A Tabulation of Helicopter Rotor-Blade Differential Pressures, Stresses, and Motions as Measured in Flight. NASA TM X-952, Mar. 1964.
75. Johnson, W.: A Lifting Surface Solution for Vortex Induced Airloads and Its Application to Rotary Wing Airloads Calculations. NASA CR 192328, Apr. 1970.
76. Johnson, W.: A General Free Wake Geometry Calculation for Wings and Rotors. American Helicopter Society 51st Annual Forum, Ft. Worth, TX, May 1995.
77. Gray, R. B.: On the Motion of the Helical Vortex Shed From a Single-Bladed Hovering Model Helicopter Rotor and Its Application to the Calculation of the Spanwise Aerodynamic Loading. Princeton University, Aeronautical Engineering Department Report No. 313, Sept. 1955.
78. Gray, R. B.: An Aerodynamic Analysis of a Single-Bladed Rotor in Hovering and Low-Speed Forward Flight as Determined From Smoke Studies on the Vorticity Distribution in the Wake. Princeton University, Aeronautical Engineering Department Report No. 356, Sept. 1956.
79. Gray, R. B.: Vortex Modeling for Rotor Aerodynamics —The 1991 Alexander A. Nikolsky Lecture. *Journal of the American Helicopter Society*, vol. 37, no. 1, Jan. 1992, pp. 3–14.

80. Landgrebe, A. J.: An Analytical and Experimental Investigation of Helicopter Rotor Hover Performance and Wake Geometry Characteristics. USAAMRDL TR 71-24, June 1971.
81. Landgrebe, A. J.: The Wake Geometry of a Hovering Helicopter Rotor and Its Influence on Rotor Performance. *Journal of the American Helicopter Society*, vol 17, no. 4, Oct. 1972, pp. 3–15.
82. Kocurek, J. D., and Tangler, J. L.: A Prescribed Wake Lifting Surface Hover Performance Analysis. *Journal of the American Helicopter Society*, vol. 22, no. 1, Jan. 1977, p. 24–35.
83. Strawn, R. C., and Caradonna, F. X.: Conservative Full-Potential Model for Unsteady Transonic Rotor Flows. *AIAA Journal*, vol. 25, no. 2, Feb. 1987, pp. 193–198.
84. Ramasamy, M.; Gold, N. P.; Bhagwat, M. J.: Flowfield Measurements to Understand Effect of Wake Behavior on Rotor Performance. AIAA Paper No. 2010-4237, June 2010.
85. Harris, F. D.: Articulated Rotor Blade Flapping Motion at Low Advance Ratio. *Journal of the American Helicopter Society*, vol. 17, no. 1, Jan. 1972, pp. 41–48.
86. Johnson, W.: Comparison of Calculated and Measured Helicopter Rotor Lateral Flapping Angles. *Journal of the American Helicopter Society*, vol. 20, no. 2, Apr. 1981, pp. 46–50.
87. Pitt, D. M., and Peters, D. A.: Theoretical Prediction of Dynamic-Inflow Derivatives. *Vertica*, vol. 5, no. 1, 1981, pp. 21–34.
88. Carpenter, P. J., and Fridovich, B.: Effect of a Rapid Blade-Pitch Increase on the Thrust and Induced-Velocity Response of a Full-Scale Helicopter Rotor. NACA TN 3044, Nov. 1953.
89. Munk, M. M.: Some Tables of the Factor of Apparent Additional Mass. NACA TN 197, July 1924.
90. Rebont, J.; Soulez-Lariviere, J.; and Valensi, J.: Response of Rotor Lift to an Increase in Collective Pitch in the Case of Descending Flight, the Regime of the Rotor Being Near Autorotation. NASA TT F-18, Apr. 1960 (original paper September 1958).
91. Rebont, J.; Valensi, J.; and Soulez-Lariviere, J.: Wind-Tunnel Study of the Response in Lift of a Rotor to an Increase in Collective Pitch in the Case of Vertical Flight Near the Autorotative Regime. NASA TT F-17, Apr. 1960 (original paper September 1958).
92. Rebont, J.; Valensi, J.; and Soulez-Lariviere, J.: Response of a Helicopter Rotor to an Increase in Collective Pitch for the Case of Vertical Flight. NASA TT F-55, Jan. 1961 (original paper May–June 1959).
93. Shupe, N. K.: A Study of the Dynamic Motions of Hingeless Rotor Helicopters. USAECOM TR ECOM-3323, Aug. 1970.
94. Curtiss, H. C., Jr., and Shupe, N. K.: A Stability and Control Theory for Hingeless Rotors. American Helicopter Society 27th Annual National V/STOL Forum, Washington, D.C., May 1971.
95. Ormiston, R. A., and Peters, D. A.: Hingeless Helicopter Rotor Response with Nonuniform Inflow and Elastic Blade Bending. *Journal of Aircraft*, vol. 9, no. 10, Oct. 1972, pp. 730–736.
96. Kuczynski, W. A., and Sissingh, G. J.: Characteristics of Hingeless Rotors with Hub Moment Feedback Controls Including Experimental Rotor Frequency Response. NASA CR 114427, Jan. 1972.
97. Hohenemser, K. H., and Crews, S. T.: Model Tests on Unsteady Rotor Wake Effects. *Journal of Aircraft*, vol. 10, no. 1, Jan. 1973, pp. 58–60.
98. Crews, S. T.; Hohenemser, K. H.; and Ormiston, R. A.: An Unsteady Wake Model for a Hingeless Rotor. *Journal of Aircraft*, vol. 10, no. 12, Dec. 1973, pp. 758–760.
99. Banerjee, D.; Crews, S. T.; Hohenemser, K. H.; and Yin, S. K.: Identification of State Variables and Dynamic Inflow From Rotor Model Dynamic Tests. *Journal of the American Helicopter Society*, vol. 22, no. 2, Apr. 1977, pp. 58–60.
100. Peters, D. A.: Hingeless Rotor Frequency Response with Unsteady Inflow. American Helicopter Society Specialists' Meeting on Rotor Dynamics, Moffett Field, CA, Feb. 1974. (NASA SP-352, Feb. 1974).
101. Tuckerman, L. B.: Inertia Factors of Ellipsoids for Use in Airship Design. NACA Report 210, 1925.
102. Peters, D. A.: How Dynamic Inflow Survives in the Competitive World of Rotorcraft Aerodynamics. *Journal of the American Helicopter Society*, vol. 54, no. 1, Jan. 2009, pp. 011001-1 to 011001-15.
103. Pitt, D. M.: Rotor Dynamic Inflow Derivatives and Time Constants From Various Inflow Models. USATSARCOM TR 81-2, Dec. 1980.

104. Kinner, W.: Die Kreisförmige Tragfläche auf Potentialtheoretischer Grundlage. Ingenieur-Archiv, vol. 8, no. 1, 1937, pp. 47–80. (Theory of the Circular Wing, R.T.P. Translation No. 2345, issued by the Ministry of Aircraft Production.)
105. Mangler, K. W.: Calculation of the Induced Velocity Field of a Rotor. RAE Report No. Aero 2247, Feb. 1948.
106. Mangler, K. W.: Fourier Coefficients for Downwash at a Helicopter Rotor. RAE Tech Note Aero. 1958, May 1948.
107. Mangler, K. W., and Squire, H. B.: The Induced Velocity Field of a Rotor. ARC R&M 2642, May 1950.
108. Joglekar, M., and Loewy, R.: An Actuator-Disc Analysis of Helicopter Wake Geometry and the Corresponding Blade Response. USAAVLABS TR 69-66, Dec. 1970.
109. Amer, K. B.: Theory of Helicopter Damping in Pitch or Roll and a Comparison with Flight Measurements. NACA TN 2136, Oct. 1950.
110. Sissingh, G. J.: The Effect of Induced Velocity Variation on Helicopter Rotor Damping in Pitch or Roll. ARC CP 101, Nov. 1951.
111. Gaonkar, G. H., and Peters, D. A.: Effectiveness of Current Dynamic-Inflow Models in Hover and Forward Flight. Journal of the American Helicopter Society, vol. 31, no. 2, Apr. 1986, pp. 47–57.
112. Gaonkar, G. H., and Peters, D. A.: Review of Dynamic Inflow Modeling for Rotorcraft Flight Dynamics. Vertica, vol. 12, no. 3, 1988, pp. 213–242.
113. Bousman, W. G.: An Experimental Investigation of the Effects of Aeroelastic Couplings on Aeromechanical Stability of a Hingeless Rotor Helicopter. Journal of the American Helicopter Society, vol. 26, no. 1, Jan. 1981, pp. 46–54.
114. Bousman, W. G., and Hodges, D. H.: An Experimental Study of Coupled Rotor-Body Aeromechanical Instability of Hingeless Rotors in Hover. Vertica, vol. 3, no. 3/4, 1979, pp. 221–244.
115. Johnson, W.: Influence of Unsteady Aerodynamics on Hingeless Rotor Ground Resonance. Journal of Aircraft, vol. 19, no. 8, Aug. 1982, pp. 668–673.
116. Houbolt, J. C., and Brooks, G. W.: Differential Equations of Motion for Combined Flapwise Bending, Chordwise Bending, and Torsion of Twisted Nonuniform Rotor Blades. NACA Report 1346, 1958.
117. Hodges, D. H., and Dowell, E. H.: Nonlinear Equations of Motion for the Elastic Bending and torsion of Twisted Nonuniform Rotor Blades. NASA TN D-7818, Dec. 1974.
118. Morduchow, M.: A Theoretical Analysis of Elastic Vibrations of Fixed-End and Hinged Helicopter Blades in Hovering and Vertical Flight. NACA TN 1999, Jan. 1950.
119. Leone, P. F.: Theory of Rotor Blade Uncoupled Flap Bending Aero-Elastic Vibrations. American Helicopter Society 10th Annual Forum, Washington, D.C., 1954.
120. Leone, P. F.: Theoretical and Experimental Study of the Coupled Flap Bending and Torsion Aero-Elastic Vibrations of a Helicopter Rotor Blade. American Helicopter Society 13th Annual National Forum, Washington, D.C., May 1957.
121. Targoff, W. P.: The Bending Vibrations of a Twisted Rotating Beam. WADC TR 56-27, Dec. 1955.
122. Daughaday, H.; DuWaldt, F.; and Gates, C.: Investigation of Helicopter Blade Flutter and Load Amplification Problems. Journal of the American Helicopter Society, vol. 2, no. 3, July 1957, pp. 27–45.
123. Yntema, R. T.: Rapid Estimation of Bending Frequencies of Rotating Beams. NACA Conference on Helicopters, Langley Field, VA, May 1954.
124. Brooks, G. W.: On the Determination of the Chordwise Bending Frequencies of Rotor Blades. Journal of the American Helicopter Society, vol. 3, no. 3, July 1958, pp. 40–42.
125. Miller, R. H., and Ellis, C. W.: Helicopter Blade Vibration and Flutter. Journal of the American Helicopter Society, vol. 1, no. 3, July 1956, pp. 19–38.
126. Brooks, C. G.; Grimwood, J. M.; and Swenson, L. S., Jr.: Chariots for Apollo. A History of Manned Lunar Spacecraft. NASA SP-4205, 1979.
127. Hansen, J. R.: Enchanted Rendezvous: John C. Houbolt and the Genesis of the Lunar-Orbit Rendezvous Concept. NASA MAH-4, Dec. 1995.
128. Houbolt, J. C., and Reed, W. H., III.: Propeller-Nacelle Whirl Flutter. Journal of the Aerospace Sciences, vol. 29, no. 3, Mar. 1962, pp. 333–346.
129. Statler, W. E.; Heppe, R. R.; and Cruz, E. S.: Results of the XH-51A Rigid Rotor Research Helicopter Program. American Helicopter Society 19th Annual National Forum, Washington, D.C., May 1963.

130. Deckert, W. H., and McCloud, J. L., III.: Considerations of the Stopped Rotor V/STOL Concept. *Journal of the American Helicopter Society*, vol. 13, no. 1, Jan. 1968, pp. 27–43.
131. Johnston, J. F., and Cook, J. R.: AH-56A Vehicle Development. American Helicopter Society 27th Annual National V/STOL Forum, Washington, D.C., May 1971.
132. Donham, R. E., and Cardinale, S. V.: Flight Test and Analytical Data for Dynamics and Loads in a Hingeless Rotor. Lockheed-California Company, Report LR 26215, Dec. 1973.
133. Weiland, E. F.: Development and Test of the BO 105 Rigid Rotor Helicopter. *Journal of the American Helicopter Society*, vol. 14, no. 1, Jan. 1969, pp. 22–37.
134. Berrington, D. K.: Design and Development of the Westland Sea Lynx. *Journal of the American Helicopter Society*, vol. 19, no. 1, Jan. 1974, pp. 16–25.
135. Huber, H. B.: Effect of Torsion-Flap-Lag Coupling on Hingeless Rotor Stability. American Helicopter Society 29th Annual National Forum, Washington, D.C., May 1973.
136. Hansford, R. E., and Simons, I. A.: Torsion-Flap-Lag Coupling on Helicopter Rotor Blades. *Journal of the American Helicopter Society*, vol. 18, no. 4, Oct. 1973, pp. 2–12.
137. Mil', M. L.; Nekrasov, A. V.; Braverman, A. S.; Grodtko, L. N.; and Leykand, M. A.: Helicopter, Calculation and Design. Moscow: Izdatel'stvo Mashinostroyeniye, 1966 (Volume I: Aerodynamics, NASA TT F-494, Sept. 1967; Volume II: Vibrations and Dynamic Stability, TT F-519, May 1968).
138. Chang, T. T.: A Method for Predicting the Trim Constants and the Rotor-Blade Loadings and Responses of a Single-Rotor Helicopter. USAAVLABS TR 67-71, Nov. 1967.
139. Piziali, R. A.: An Investigation of the Structural Dynamics of Helicopter Rotors. USAAVLABS TR 70-24, 1970.
140. Arcidiacono, P. J.: Prediction of Rotor Instability at High Forward Speeds. Volume I. Steady Flight Differential Equations of Motion for a Flexible Helicopter Blade with Chordwise Mass Unbalance. USAAVLABS TR 68-18A, Feb. 1969.
141. Young, M. I.: A Theory of Rotor Blade Motion Stability in Powered Flight. *Journal of the American Helicopter Society*, vol. 9, no. 3, July 1964, pp. 12–25.
142. Berman, A., and McIntyre, H. H.: Reader's Forum and reply by author. *Journal of the American Helicopter Society*, vol. 11, no. 1, Jan. 1966, pp. 44–53.
143. Hohenemser, K.: Reader's Forum and reply by author. *Journal of the American Helicopter Society*, vol. 11, no. 4, Oct. 1966, pp. 25–26.
144. Hohenemser, K. H., and Heaton, P. W., Jr.: Aeroelastic Instability of Torsionally Rigid Helicopter Blades. *Journal of the American Helicopter Society*, vol. 12, no. 2, Apr. 1967, pp. 1–13.
145. Ormiston, R. A., and Hodges, D. H.: Linear Flap-Lag Dynamics of Hingeless Helicopter Rotor Blades in Hover. *Journal of the American Helicopter Society*, vol. 17, no. 2, Apr. 1972, pp. 2–14.
146. Hodges, D. H.: Nonlinear Bending and Torsion of Rotating Beams with Application to Linear Stability of Hingeless Helicopter Rotors. Doctor of Philosophy Thesis, Stanford University, 1972.
147. Hodges, D. H., and Ormiston, R. A.: Nonlinear Equations for Bending of Rotating Beams with Application to Linear Flap-Lag Stability of Hingeless Rotors. NASA TM X-2770, May 1973.
148. Hodges, D. H., and Ormiston, R. A.: Stability of Elastic Bending and Torsion of Uniform Cantilevered Rotor Blades in Hover. AIAA Paper No. 73-405, Mar. 1973.
149. Friedmann, P., and Tong, P.: Non-Linear Flap-Lag Dynamics of Hingeless Helicopter Blades in Hover and in Forward Flight. *Journal of Sound and Vibration*, vol. 30, no. 1, 1973, pp. 9–31.
150. Friedmann, P., and Tong, P.: Dynamic Nonlinear Elastic Stability of Helicopter Rotor Blades in Hover and in Forward Flight. NASA CR 114485, May 1972.
151. Friedmann, P.: Aeroelastic Instabilities of Hingeless Helicopter Blades. *Journal of Aircraft*, vol. 10, no. 10, Oct. 1973, pp. 623–631.
152. Friedmann, P.: Some Conclusions Regarding the Aeroelastic Stability of Hingeless Helicopter Blades in Hover and in Forward Flight. *Journal of the American Helicopter Society*, vol. 18, no. 4, Oct. 1973, pp. 13–23.
153. Ormiston, R. A., and Hodges, D. H.: Letters to the Editor and reply by author. *Journal of the American Helicopter Society*, vol. 20, no. 3, July 1975, pp. 46–48.

154. Hodges, D. H.: Nonlinear Equations of Motion for Cantilever Rotor Blades in Hover with Pitch Link Flexibility, Twist, Precone, Droop, Sweep, Torque Offset, and Blade Root Offset. NASA TM X-73112, May 1976.
155. Hodges, D. H., and Ormiston, R. A.: Stability of Elastic Bending and Torsion of Uniform Cantilever Rotor Blades in Hover With Variable Structural Coupling. NASA TN D-8192, Apr. 1976.
156. Hodges, D. H., and Ormiston, R. A.: Stability of Hingeless Rotor Blades in Hover with Pitch-Link Flexibility. *AIAA Journal*, vol. 15, no. 4, Apr. 1977, pp. 476–482.
157. Hodges, D. H.; Ormiston, R. A.; and Peters, D. A.: On the Nonlinear Deformation Geometry of Euler-Bernoulli Beams. NASA TP 1566, Apr. 1980.
158. Hodges, D. H.: Nonlinear Equations for Dynamics of Pretwisted Beams Undergoing Small Strains and Large Rotations. NASA TP 2470, May 1985.
159. Bauchau, O. A., and Hong, C. H.: Nonlinear Composite Beam Theory. *Journal of Applied Mechanics*, vol. 55, no. 1, Mar. 1988, pp. 156–163.
160. Hodges, D. H.: A Mixed Variational Formulation Based on Exact Intrinsic Equations for Dynamics of Moving Beams. *International Journal of Solids and Structures*, vol. 26, no. 11, 1990, pp. 1253–1273.
161. Yuan, K.-A.; Friedmann, P. P.; and Venkatesan, C.: Aeroelastic Behavior of Composite Rotor Blades With Swept Tips. American Helicopter Society 48th Annual Forum, Washington, D.C., June 1992.
162. Smith, E. C., and Chopra, I.: Aeroelastic Response, Loads, and Stability of a Composite Rotor in Forward Flight. *AIAA Journal*, vol. 31, no. 7, July 1993, pp. 1265–1273.
163. Bratanow, T., and Ecer, A.: Sensitivity of Rotor Blade Vibration Characteristics to Torsional Oscillations. *Journal of Aircraft*, vol. 11, no. 7, July 1974, pp. 375–381.
164. Yasue, M.: Gust Response and Its Alleviation for a Hingeless Helicopter Rotor in Cruising Flight. MIT ASRL TR 189-1, 1977.
165. Friedmann, P. P., and Straub, F.: Application of the Finite Element Method to Rotary-Wing Aeroelasticity. *Journal of the American Helicopter Society*, vol. 25, no. 1, Jan. 1980, pp. 36–44.
166. Straub, F. K., and Friedmann, P. P.: A Galerkin Type Finite Element Method for Rotary-Wing Aeroelasticity in Hover and Forward Flight. *Vertica*, vol. 5, no. 1, 1981, pp. 75–98.
167. Straub, F. K., and Friedmann, P. P.: Application of the Finite Element Method to Rotary Wing Aeroelasticity. NASA CR 165854, Feb. 1982.
168. Borri, M.; Lanz, M.; and Mantegazza, P.: A General Purpose Program for Rotor Blade Dynamics. Seventh European Rotorcraft and Powered Lift Aircraft Forum, Garmisch-Partenkirchen, Germany, 1981.
169. Borri, M.; Lanz, M.; Mantegazza, P.; Orlandi, D.; and Russo, A.: STAHR: A Program For Stability and Trim Analysis of Helicopter Rotors. Eighth European Rotorcraft Forum, Aix-en-Provence, France, Sept. 1982.
170. Hodges, D. H., and Rutkowski, M. J.: Free-Vibration Analysis of Rotating Beams by a Variable-Order Finite-Element Method. *AIAA Journal*, vol. 19, no. 11, Nov. 1981, pp. 1459–1466.
171. Sivaneri, N. T., and Chopra, I.: Dynamic Stability of a Rotor Blade Using Finite Element Analysis. *AIAA Journal*, vol. 20, no. 5, May 1982, pp. 716–723.
172. Sivaneri, N. T., and Chopra, I.: Finite Element Analysis for Bearingless Rotor Blade Aeroelasticity. *Journal of the American Helicopter Society*, vol. 29, no. 2, Apr. 1984, pp. 42–51.
173. Hodges, D. H.; Hopkins, A. S.; Kunz, D. L.; and Hinnant, H. E.: Introduction to GRASP—General Rotorcraft Aeromechanical Stability Program—A Modern Approach to Rotorcraft Modeling. *Journal of the American Helicopter Society*, vol. 32, no. 2, Apr. 1987, pp. 78–90.
174. Hopkins, A. S., and Likins, P.: Analysis of Structures with Rotating, Flexible Substructures. AIAA Paper No. 87-0951, Apr. 1987.
175. Hodges, D. H.; Hopkins, A. S.; and Kunz, D. L.: Analysis of Structures with Rotating, Flexible Substructures Applied to Rotorcraft Aeroelasticity. *AIAA Journal*, vol. 27, no. 2, Feb. 1989, pp. 192–200; originally AIAA Paper No. 87-0952, Apr. 1987.
176. Hinnant, H. E., and Hodges, D. H.: Nonlinear Analysis of a Cantilever Beam. *AIAA Journal*, vol. 26, no. 12, Dec. 1988, pp. 1521–1527; originally AIAA Paper No. 87-0953, Apr. 1987.

177. Kunz, D. L., and Hodges, D. H.: Correlation of Analytical Calculations from GRASP with Torsionally-Soft Rotor Data. American Helicopter Society 43rd Annual Forum, St. Louis, MO, May 1987.
178. Elliott, A. S., and McConville, J. B.: Application of a General-Purpose Mechanical Systems Analysis Code to Rotorcraft Dynamics Problems. American Helicopter Society National Specialists' Meeting on Rotorcraft Dynamics, Arlington, TX, Nov. 1989.
179. Bauchau, O. A., and Kang, N. K.: A Multibody Formulation for Helicopter Structural Dynamic Analysis. *Journal of the American Helicopter Society*, vol. 38, no. 2, Apr. 1993, pp. 3–14.
180. Johnson, W.: Technology Drivers in the Development of CAMRAD II. American Helicopter Society Aeromechanics Specialists Conference, San Francisco, CA, Jan. 1994.
181. Bauchau, O. A.; Bottasso, C. L.; and Nikishkov, Y. G.: Modeling Rotorcraft Dynamics with Finite Element Multibody Procedures. *Mathematical and Computer Modeling*, vol. 33, no. 10–11, May–June 2001, pp. 1113–1137.
182. Miller, R. H.: Helicopter Control and Stability in Hovering Flight. *Journal of the Aeronautical Sciences*, vol. 15, no. 8, Aug. 1948, pp. 453–472.
183. Grodtko, L. N.: Ground Resonance. In Mil', M. L., et al. *Helicopter, Calculation and Design*. Moscow: Izdatel'stvo Mashinostroyeniye, 1966. Translation Vibrations and Dynamic Stability, NASA TT F-519, May 1968.
184. Young, M. I., and Lytwyn, R. T.: The Influence of Blade Flapping Restraint on the Dynamic Stability of Low Disk Loading Propeller-Rotors. *Journal of the American Helicopter Society*, vol. 12, no. 4, Oct. 1967, pp. 38–54.
185. Johnson, R. L., and Hohenemser, K. H.: On the Dynamics of Lifting Rotors with Thrust or Tilting Moment Feedback Controls. *Journal of the American Helicopter Society*, vol. 15, no. 1, Jan. 1970, pp. 42–58.
186. Yin, S.-K., and Hohenemser, K. H.: The Method of Multiblade Coordinates in the Linear Analysis of Lifting Rotor Dynamic Stability and Gust Response at High Advance Ratio. American Helicopter Society 27th Annual National V/STOL Forum, Washington, D.C., May 1971.
187. Hohenemser, K. H., and Yin, S.-K.: Some Applications of the Method of Multiblade Coordinates. *Journal of the American Helicopter Society*, vol. 17, no. 3, July 1972, pp. 3–12.
188. DeRusso, P. M.; Roy, R. J.; and Close, C. M.: *State Variables for Engineers*. New York: John Wiley and Sons, Inc., 1965.
189. Glauert, H., and Shone, G.: The Disturbed Motion of the Blades of a Gyroplane. ARC 995, 1933.
190. Horvay, G.: Rotor Blade Flapping Motion. *Quarterly of Applied Mathematics*, vol. 5, no. 2, July 1947, pp. 149–167.
191. Horvay, G., and Yuan, S. W.: Stability of Rotor Blade Flapping Motion When the Hinges Are Tilted. Generalization of the Rectangular Ripple Method of Solution. *Journal of the Aeronautical Sciences*, vol. 14, no. 10, Oct. 1947, pp. 583–593.
192. Parkus, H.: The Disturbed Flapping Motion of Helicopter Rotor Blades. *Journal of the Aeronautical Sciences*, vol. 15, no. 2, Feb. 1948, pp. 103–106.
193. Shulman, Y.: Stability of a Flexible Helicopter Rotor Blade in Forward Flight. *Journal of the Aeronautical Sciences*, vol. 23, no. 7, July 1956, pp. 663–693.
194. Shutler, A. G., and Jones, J. P.: The Stability of Rotor Blade Flapping Motion. ARC R&M 3178, May 1958.
195. Perisho, C. H.: Analysis of the Stability of a Flexible Rotor Blade at High Advance Ratio. *Journal of the American Helicopter Society*, vol. 4, no. 2, Apr. 1959, pp. 4–18.
196. Lowis, O. J.: The Stability of Rotor Blade Flapping Motion at High Tip Speed Ratios. ARC R&M 3544, Jan. 1963.
197. Wilde, E.; Bramwell, A. R. S.; and Summerscales, R.: The Flapping Behaviour of a Helicopter Rotor at High Tip-Speed Ratios. ARC CP 877, Apr. 1965.
198. Sissingh, G. J.: Dynamics of Rotors Operating at High Advance Ratios. *Journal of the American Helicopter Society*, vol. 13, no. 3, July 1968, pp. 56–63.
199. Stammers, C. W.: The Flutter of a Helicopter Rotor Blade in Forward Flight. *The Aeronautical Quarterly*, vol. 21, no. 1, Feb. 1970, pp. 18–48.
200. Peters, D. A., and Hohenemser, K. H.: Application of the Floquet Transition Matrix to Problems of Lifting Rotor Stability. *Journal of the American Helicopter Society*, vol. 16, no. 2, Apr. 1971, pp. 25–33.
201. Bennett, R. L.: Rotor System Design and Evaluation Using a General Purpose Helicopter Flight Simulation Program. AGARD CP 122, Mar. 1973.

202. Corrigan, J. J.; Bennett, R. L.; and Hsieh, P. Y.: COPTER 2000: The QTR and Beyond. American Helicopter Society 57th Annual Forum, Washington, D.C., May 2001.
203. Blankenship, B. L., and Harvey, K. W.: A Digital Analysis for Helicopter Performance and Rotor Blade Bending Moments. *Journal of the American Helicopter Society*, vol. 7, no. 4, Oct. 1962, pp. 55–69.
204. Duhon, J. M.; Harvey, K. W.; and Blankenship, B. L.: Computer Flight Testing of Rotorcraft. *Journal of the American Helicopter Society*, vol. 10, no. 4, Oct. 1965, pp. 36–48.
205. Harvey, K. W.; Blankenship, B. L.; and Drees, J. M.: Analytical Study of Helicopter Gust Response at High Forward Speeds. USAAVLABS TR 69-1, Sept. 1969.
206. Blankenship, B. L., and Bird, B. J.: Program C81-11 Rotorcraft Flight Simulation. Bell Helicopter Company, BHC Report No. 599-068-900, Jan. 1967.
207. Livingston, C. L.; Bird, B. J.; and McLarty, T. T.: A Stability and Control Prediction Method for Helicopters and Stoppable Rotor Aircraft. AFFDL TR 69-123, Feb. 1970.
208. Military Helicopter Market, *FLIGHT International*, vol. 102, no. 3324, 23 Nov. 1972, pp. 748a–754.
209. Bennett, R. L., and Blankenship, B. L.: Rotorcraft Flight Simulation with Aeroelastic Rotor Representation. USAAMRDL TR 71-68, 1972.
210. Davis, J. M.; Bennett, R. L.; and Blankenship, B. L.: Rotorcraft Flight Simulation with Aeroelastic Rotor and Improved Aerodynamic Representation. USAAMRDL TR 74-10, June 1974.
211. McLarty, T. T.; Van Gaasbeek, J. R.; and Hsieh, P. Y.: Rotorcraft Flight Simulation with Coupled Rotor Aeroelastic Stability Analysis. USAAMRDL TR 76-41, May 1977.
212. Van Gaasbeek, J. R.; McLarty, T. T.; Sadler, S. G.; and Hsieh, P. Y.: Rotorcraft Flight Simulation, Computer Program C81. USARTL TR 77-54, Oct. 1979.
213. Van Gaasbeek, J. R., and Hsieh, P. Y.: Rotorcraft Flight Simulation Computer Program C81 with DATAMAP Interface. USAAVRADCOM TR 80-D-38, Oct. 1981.
214. Austin, E. E., and Vann, W. D.: General Description of the Rotorcraft Flight Simulation Computer Program (C-81). USAAMRDL TN 11, June 1973.
215. Vann, W. D.; Mirick, P. H.; and Austin, E. E.: Use of Computer Math Models for Aircraft Evaluation. USAAMRDL TN 12, Aug. 1973.
216. Van Gaasbeek, J. R.: An Investigation of High-G Maneuvers of the AH-1G Helicopter. USAAMRDL TR 75-18, Apr. 1975.
217. Van Gaasbeek, J. R.: Validation of the Rotorcraft Flight Simulation Program (C81) Using Operational Loads Survey Flight Test Data. USAAVRADCOM TR 80-D-4, July 1980.
218. Freeman, F. D., and Bennett, R. L.: Application of Rotorcraft Flight Simulation Program (C81) to Predict Rotor Performance and Bending Moments For a Model Four-Bladed Articulated Rotor System. USAAMRDL TR 74-70, Nov. 1974.
219. Staley, J. A.: Validation of Rotorcraft Flight Simulation Program Through Correlation with Flight Data for Soft-In-Plane Hingeless Rotors. USAAMRDL TR 75-50, Jan. 1976.
220. Briczinski, S. J.: Validation of the Rotorcraft Flight Simulation Program (C81) for Articulated Rotor Helicopters Through Correlation with Flight Data. USAAMRDL TR 76-4, May 1976.
221. Specialists Meeting on Helicopter Rotor Loads Prediction Methods. AGARD CP 122, Aug. 1973.
222. Carlson, R. M., and Kerr, A. W.: Integrated Rotor/Body Loads Prediction. AGARD CP 122, Mar. 1973.
223. Johnston, J. F., and Cook, J. R.: AH-56A Vehicle Development. American Helicopter Society 27th Annual National V/STOL Forum, Washington, D.C., May 1971.
224. Anderson, W. D.; Conner, F.; and Kerr, A. W.: Application of an Interdisciplinary Rotary-Wing Aircraft Analysis to the Prediction of Helicopter Maneuver Loads. USAAMRDL TR 73-83, Dec. 1973.
225. Kerr, A. W.; Potthast, A. J.; and Anderson, W. D.: An Interdisciplinary Approach to Integrated Rotor/Body Mathematical Modeling. American Helicopter Society Symposium on the Status of Testing and Modeling Techniques for V/STOL Aircraft, Essington, PA, Oct. 1972.
226. Kerr, A. W.: More Help for Sam. *Vertiflite*, vol. 19, no. 3, May/June 1973, pp. 4–7.

227. Kerr, A. W., and Davis, J. M.: A System For Interdisciplinary Analysis—A Key to Improved Rotorcraft Design. American Helicopter Society 35th Annual Forum, Washington, D.C., May 1979.
228. Kerr, A. W., and Stephens, W. B.: The Development of a System for Interdisciplinary Analysis of Rotorcraft Flight Characteristics. AGARD CP 334, May 1982.
229. Caradonna, F. X.; Tung, C.; and Desopper, A.: Finite Difference Modeling of Rotor Flows Including Wake Effects. *Journal of the American Helicopter Society*, vol. 29, no. 2, Apr. 1984, pp. 26–33.
230. Caradonna, F. X., and Isom, M. P.: Subsonic and Transonic Potential Flow over Helicopter Rotor Blades. *AIAA Journal*, vol. 10, no. 12, Dec. 1972, pp. 1606–1612.
231. Ballhaus, W. F., and Caradonna, F. X.: The Effect of Planform Shape on the Transonic Flow Past Rotor Tips. AGARD CP 111, Sept. 1972.
232. Isom, M. P.: Unsteady Subsonic and Transonic Potential Flow Over Helicopter Rotor Blades. NASA CR 2463, Oct. 1974.
233. Johnson, W.: Recent Developments in Rotary-Wing Aerodynamic Theory. *AIAA Journal*, vol. 24, no. 8, Aug. 1986, pp. 1219–1244.
234. Caradonna, F. X., and Isom, M. P.: Numerical Calculation of Unsteady Transonic Potential Flow over Helicopter Rotor Blades. *AIAA Journal*, vol. 14, no. 4, Apr. 1976, pp. 482–488.
235. Caradonna, F. X., and Philippe, J. J.: The Flow Over a Helicopter Blade Tip in the Transonic Regime. *Vertica*, vol. 2, no. 1, 1978, pp. 43–60.
236. Monnerie, B., and Philippe, J.-J.: Aerodynamic Problems of Helicopter Blade Tips. *Vertica*, vol. 2, no. 3/4, 1978, pp. 217–231.
237. Chattot, J.-J., and Philippe, J.-J.: Pressure Distribution Computation on a Non-Lifting Symmetrical Helicopter Blade in Forward Flight. *La Recherche Aérospatiale*, vol. 1980, no. 5, 1980, pp. 19–31.
238. Philippe, J.-J., and Chattot, J.-J.: Experimental and Theoretical Studies on Helicopter Blade Tips at ONERA. Sixth European Rotorcraft and Powered Lift Aircraft Forum, Bristol, UK, Sept. 1980.
239. Chattot, J. J.: Calculation of Three-Dimensional Unsteady Transonic Flows Past Helicopter Blades. NASA TP 1721, Oct. 1980.
240. Arieli, R., and Tauber, M. E.: Computation of Subsonic and Transonic Flow about Lifting Rotor Blades. AIAA Paper No. 79-1667, Aug. 1979.
241. Grant, J.: The Prediction of Supercritical Pressure Distributions on Blade Tips of Arbitrary Shape Over a Range of Advancing Blade Azimuth Angles. *Vertica*, vol. 3, no. 3/4, 1979, pp. 275–292.
242. Desopper, A.: Study of the Unsteady Transonic Flow on Rotor Blades With Different Tip Shapes. *Vertica*, vol. 9, no. 3, 1985, pp. 257–272.
243. Tung, C.; Caradonna, F. X.; and Johnson, W.: The Prediction of Transonic Flows on an Advancing Rotor. *Journal of the American Helicopter Society*, vol. 31, no. 3, July 1986, pp. 4–9.
244. Datta, A.; Nixon, M.; and Chopra, I.: Review of Rotor Loads Prediction With the Emergence of Rotorcraft CFD. *Journal of the American Helicopter Society*, vol. 52, no. 4, Oct. 2007, pp. 287–317.
245. Tung, C., and Ormiston, R. A.: History of Rotorcraft CFD/CSD Coupling. Rotor Korea 2009, 2nd International Forum on Rotorcraft Multidisciplinary Technology, Seoul, Korea, Oct. 2009.
246. Strawn, R. C., and Tung, C.: The Prediction of Transonic Loading on Advancing Helicopter Rotors. AGARD CP 412, Apr. 1986.
247. Strawn, R. C., and Tung, C.: Prediction of Unsteady Transonic Rotor Loads With a Full-Potential Rotor Code. American Helicopter Society 43rd Annual Forum, St. Louis, MO, May 1987.
248. Strawn, R. C.; Desopper, A.; Miller, J.; and Jones, A.: Correlation of Puma Airloads—Evaluation of CFD Prediction Methods. Fifteenth European Rotorcraft Forum, Amsterdam, The Netherlands, Sept. 1989.
249. Kim, K.-C.; Desopper, A.; and Chopra, I.: Blade Response Calculations Using Three-Dimensional Aerodynamic Modeling. *Journal of the American Helicopter Society*, vol. 36, no. 1, Jan. 1991, pp. 68–77.
250. Strawn, R. C., and Bridgeman, J. O.: An Improved Three-Dimensional Aerodynamics Model for Helicopter Airloads Prediction. AIAA Paper No. 91-0767, Jan. 1991.
251. Lee, C. S.; Saberi, H.; and Ormiston, R. A.: Aerodynamic and Numerical Issues for Coupling CFD into Comprehensive Rotorcraft Analysis. American Helicopter Society 53rd Annual Forum, Virginia Beach, VA, May 1997.

252. Beaumier, P.: A Coupling Procedure Between a Rotor Dynamics code and a 3D Unsteady Full Potential Code. American Helicopter Society Aeromechanics Specialists Conference, San Francisco, CA, Jan. 1994.
253. Servera, G.; Beaumier, P.; and Costes, M.: A Weak Coupling Method Between the Dynamics Code HOST and the 3D Unsteady Euler Code WAVES. *Aerospace Science and Technology*, vol. 5, no. 6, Sept. 2001, pp. 397–408.
254. Pahlke, K., and van der Wall, B.: Calculation of Multibladed Rotors in High-Speed Forward Flight with Weak Fluid-Structure-Coupling. Twenty-Seventh European Rotorcraft Forum, Moscow, Russia, Sept. 2001.
255. Pahlke, K., and van der Wall, B.: Progress in Weak Fluid-Structure-Coupling for Multibladed Rotors in High-Speed Forward Flight. Twenty-Eighth European Rotorcraft Forum, Bristol, UK, Sept. 2002.
256. Pahlke, K., and van der Wall, B. G.: Chimera Simulations of Multibladed Rotors in High-Speed Forward Flight with Weak Fluid-Structure-Coupling. *Aerospace Science and Technology*, vol. 9, no. 5, July 2005, pp. 379–389.
257. Datta, A.; Sitaraman, J.; Baeder, J. D.; and Chopra, I.: Analysis Refinements for Prediction of Rotor Vibratory Loads in High-Speed Forward Flight. American Helicopter Society 60th Annual Forum, Baltimore, MD, June 2004.
258. Datta, A.; Sitaraman, J.; Chopra, I.; and Baeder, J. D.: CFD/CSD Prediction of Rotor Vibratory Loads in High-Speed Flight. *Journal of Aircraft*, vol. 43, no. 6, Nov.–Dec. 2006, pp. 1698–1709.
259. Sitaraman, J.; Datta, A.; Baeder, J.; and Chopra, I.: Coupled CFD/CSD Prediction of Rotor Aerodynamic and Structural Dynamic Loads for Three Critical Flight Conditions. Thirty-First European Rotorcraft Forum, Florence, Italy, Sept. 2005.
260. Potsdam, M.; Yeo, H.; and Johnson, W.: Rotor Airloads Prediction Using Loose Aerodynamic/Structural Coupling. *Journal of Aircraft*, vol. 43, no. 3, May–June 2006, pp. 732–742.
261. Caradonna, F. X., and Tung, C.: Experimental and Analytical Studies of a Model Helicopter Rotor in Hover. *Vertica*, vol. 5, no. 2, 1981, pp. 149–161.
262. Caradonna, F. X., and Tung, C.: Experimental and Analytical Studies of a Model Helicopter Rotor in Hover. NASA TM 81232, Sept. 1981.
263. Strawn, R. C., and Caradonna, F. X.: Conservative Full-Potential Model for Unsteady Transonic Rotor Flows. *AIAA Journal*, vol. 25, no. 2, Feb. 1987, pp. 193–198.
264. Kufeld, R. M.; Balough, D. L.; Cross, J. L.; Studebaker, K. F.; Jennison, C. D.; and Bousman, W. G.: Flight Testing the UH-60A Airloads Aircraft. American Helicopter Society 50th Annual Forum, Washington, D.C., May 1994.
265. Hooper, W. E.: The Vibratory Airloading of Helicopter Rotors. *Vertica*, vol. 8, no. 2, 1984, pp. 73–92.
266. Rabbott, J. P., Jr.; Lizak, A. A.; and Paglino, V. M.: A Presentation of Measured and Calculated Full-Scale Rotor Blade Aerodynamic and Structural Loads. USAAVLABS TR 66-31, Jan. 1966.
267. Rabbott, J. P., Jr.; Lizak, A. A.; and Paglino, V. M.: Tabulated Sikorsky CH-34 Blade Surface Pressures Measured at the NASA/Ames Full Scale Wind Tunnel. Sikorsky Aircraft, SER 58399, Jan. 1966.
268. Rabbott, J. P., Jr., and Paglino, V. M.: Aerodynamic Loading of High Speed Rotors. CAL/AVLABS Symposium on Aerodynamic Problems Associated with V/STOL Aircraft, Buffalo, NY, June 1966.
269. Bousman, W. G., and Kufeld, R. M.: UH-60A Airloads Catalog. NASA TM 2005-212827, Aug. 2005.
270. Spletstoesser, W. R.; Kube, R.; Seelhorst, U.; Wagner, W.; Boutier, A.; Micheli, F.; Mercker, E.; and Pengel, K.: Higher Harmonic Control Aeroacoustic Rotor Test (HART) — Test Documentation and Representative Results. DLR Report IB 129-95/28, Dec. 1995.
271. van der Wall, B. G.: 2nd HHC Aeroacoustic Rotor Test (HART II). DLR Institute Report IB 111-2003/31, Nov. 2003.
272. Scheiman, J., and Kelley, H. L.: Comparison of Flight Measured Helicopter Rotor Blade Chordwise Pressure Distributions and Two-Dimensional Airfoil Characteristics. CAL/TRECOM Symposium on Dynamic Load Problems Associated with Helicopters and V/STOL Aircraft, Buffalo, NY, June 1963.
273. Scheiman, J., and Kelley, H. L.: Comparison of Flight-Measured Helicopter Rotor-Blade Chordwise Pressure Distributions With Static Two-Dimensional Airfoil Characteristics. NASA TN D-3936, May 1967.
274. Ward, J. F.: Helicopter Rotor Periodic Differential Pressures and Structural Response Measured in Transient and Steady-State Maneuvers. *Journal of the American Helicopter Society*, vol. 16, no. 1, Jan. 1971, pp. 16–25.

275. Rabbott, J. P., Jr.: Model vs. Full Scale Rotor Testing. CAL/AVLABS Symposium on Aerodynamics of Rotary Wing and V/STOL Aircraft, Buffalo, NY, June 1969.
276. Lowson, M. V., and Ollerhead, J. B.: A Theoretical Study of Helicopter Rotor Noise. *Journal of Sound and Vibration*, vol. 9, no. 2, 1969, pp. 197–222.
277. Johnson, W.: Application of a Lifting-Surface Theory to the Calculation of Helicopter Airloads. American Helicopter Society 27th Annual National V/STOL Forum, Washington, D.C., May 1971.
278. Quackenbush, T. R.; Bliss, D. B.; Wachspress, D. A.; Boschitsch, A. H.; and Chua, K.: Computation of Rotor Aerodynamic Loads in Forward Flight Using a Full-Span Free Wake Analysis. NASA CR 177611, Dec. 1990.
279. Yeo, H., and Johnson, W.: Assessment of Comprehensive Analysis Calculation of Airloads on Helicopter Rotors. *Journal of Aircraft*, vol. 42, no. 5, Sept.–Oct. 2005, pp. 1218–1228.
280. Yeo, H., and Johnson, W.: Prediction of Rotor Structural Loads with Comprehensive Analysis. *Journal of the American Helicopter Society*, vol. 53, no. 2, Apr. 2008, pp. 193–209.
281. Bousman, W. G.: UH-60A Airloads Program (1984–1994). UH-60A Airloads Program Occasional Note 1999-01, 1999.
282. Watts, M. E., and Cross, J. L.: The NASA Modern Technology Rotors Program. AIAA Paper No. 86-9788, Apr. 1986.
283. Lorber, P. F.: Aerodynamic Results of a Pressure-Instrumented Model Rotor Test at the DNW. *Journal of the American Helicopter Society*, vol. 36, no. 4, Oct. 1991, pp. 66–76.
284. Lorber, P. F.; Stauter, R. C.; and Landgrebe, A. J.: A Comprehensive Hover Test of the Airloads and Airflow of an Extensively Instrumented Model Helicopter Rotor. American Helicopter Society 45th Annual Forum, Boston, MA, May 1989.
285. Coleman, C. P., and Bousman, W. G.: Aerodynamic Limitations of the UH-60A Rotor. American Helicopter Society Aeromechanics Specialists Conference, San Francisco, CA, Jan. 1994.
286. Kufeld, R. M.; Cross, J. L.; and Bousman, W. G.: A Survey of Rotor Loads Distribution in Maneuvering Flight. American Helicopter Society 50th Annual Forum, Washington, D.C., May 1994.
287. Kufeld, R. M., and Bousman, W. G.: UH-60A Helicopter Rotor Airloads Measured in Flight. *The Aeronautical Journal*, vol. 101, no. 1005, May 1977, pp. 217–227.
288. Kufeld, R. M., and Bousman, W. G.: High Load Conditions Measured on a UH-60A in Maneuvering Flight. *Journal of the American Helicopter Society*, vol. 43, no. 3, July 1998, pp. 202–211.
289. Bousman, W. G.: A Qualitative Examination of Dynamic Stall from Flight Test Data. *Journal of the American Helicopter Society*, vol. 43, no. 4, Oct. 1998, pp. 279–295.
290. Bousman, W. G.: Putting the Aero Back Into Aeroelasticity. Eighth Annual ARO Workshop on Aeroelasticity of Rotorcraft Systems, University Park, PA, Oct. 1999.
291. Tung, C.; Bousman, W. G.; and Low, S.: A Comparison of Airload Data Between Model-Scale Rotor and Full-Scale Flight Test. American Helicopter Society 2nd International Aeromechanics Specialists' Conference, Bridgeport, CT, Oct. 1995.
292. Norman, T. R.; Theodore, C.; Shinoda, P.; Fuerst, D.; Arnold, U. T. P.; Makinen, S.; Lorber, P.; and O'Neill, J.: Full-Scale Wind Tunnel Test of a UH-60 Individual Blade Control System for Performance Improvement and Vibration, Loads, and Noise Control. American Helicopter Society 65th Annual Forum, Grapevine, TX, May 2009.
293. Yu, Y. H.; Gmelin, B. L.; Heller, H.; Philippe, J. J.; Mercker, E.; and Preisser, J. S.: HHC Aeroacoustics Rotor Test at the DNW — The Joint German/French/US HART Project. Twentieth European Rotorcraft Forum, Amsterdam, The Netherlands, Oct. 1994.
294. Kube, R.; Spletstoesser, W. R.; Wagner, W.; Seelhorst, U.; Yu, Y. H.; Boutier, A.; Micheli, F.; and Mercker, E.: Initial Results from the Higher Harmonic Control Aeroacoustic Rotor Tests (HART) in the German-Dutch Wind Tunnel. AGARD CP 552, Oct. 1994.
295. Spletstoesser, W. R.; Kube, R.; Wagner, W.; Seelhorst, U.; Boutier, A.; Micheli, F.; Mercker, E.; and Pengel, K.: Key Results From a Higher Harmonic Control Aeroacoustic Rotor Test (HART). *Journal of the American Helicopter Society*, vol. 42, no. 1, Jan. 1997, pp. 58–78.

296. Kube, R.; Splettstoesser, W. R.; Wagner, W.; Seelhorst, U.; Yu, Y. H.; Tung, C.; Beaumier, P.; Prieur, J.; Rahier, G.; Spiegel, P.; Boutier, A.; Brooks, T. F.; Burley, C. L.; Boyd, D. D., Jr.; Mercker, E.; and Pengel, K.: HHC Aeroacoustic Rotor Tests in the German-Dutch Wind Tunnel: Improving Physical Understanding and Prediction Codes. *Aerospace Science and Technology*, vol. 2, no. 3, Mar. 1998, pp. 177–190.

297. van der Wall, B. G.; Junker, B.; Burley, C. L.; Brooks, T. F.; Yu, Y.; Tung, C.; Raffel, M.; Richard, H.; Wagner, W.; Mercker, E.; Pengel, K.; Holthusen, H.; Beaumier, P.; and Delrieux, Y.: The HART II Test in the LLF of the DNW — A Major Step Towards Rotor Wake Understanding. *Twenty-Eighth European Rotorcraft Forum*, Bristol, UK, Sept. 2002.

298. Yu, Y. H.; Tung, C.; van der Wall, B.; Pausder, H.-J.; Burley, C.; Brooks, T.; Beaumier, P.; Delrieux, Y.; Mercker, E.; and Pengel, K.: The HART-II Test: Rotor Wakes and Aeroacoustics with Higher-Harmonic Pitch Control (HHC) Inputs—The Joint German /French/Dutch /US Project. *American Helicopter Society 58th Annual Forum*, Montreal, Canada, June 2002.